UNIVERSIDADE DA BEIRA INTERIOR
Engenharia

Mechanical and hydraulic long-term behavior for an experimental compacted liner embankment

Leonardo Perelló Marchiori

Dissertação para obtenção do grau de mestre em

Engenharia Civil

(2º ciclo de estudos)

Orientador: Victor Manuel Pissarra Cavaleiro

Covilhã, Outubro de 2022

DECLARAÇÃO DE INTEGRIDADE

Eu, Leonardo Perelló Marchiori, estudante com número de aluno M11119 do curso de Engenharia Civil – Geotecnia e Ambiente da Faculdade de Engenharia, declaro ter desenvolvido o presente trabalho e elaborado o prexente texto em total consonância com o Código de Integridades da Universidade da Beira Interior.

Mais concretamente afirmo não ter incorrido em qualquer das variedaddes de Fraude Académica, e que aqui declaro conhecer, que em particular atendi à exigida referenciação de frases, extratos, imagens e outras formas de trabalho intelectual, e assumindo assim na íntegra as responsabilidades da autoria.

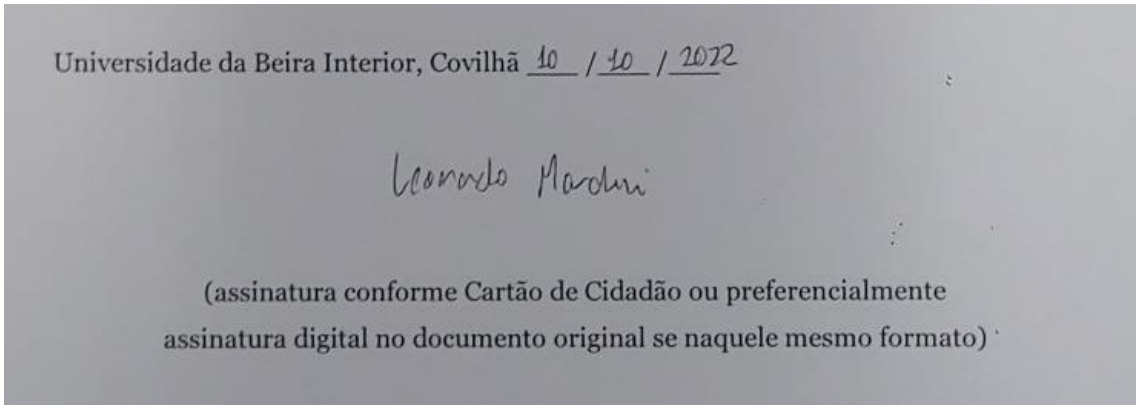

Dedicatory

To my family.

Acknowledgment

First, I would like to thank my parents - Sergio and Sandra – for everything. To my brother, Felipe, to all my friends - and more than friends - for always be there for me. They know how it has been, and yet they were always there.

To my supervisor Professor Dr. Victor Manuel Pissarra Cavaleiro, and Professor Dr. António Albuquerque, for all the dedication, guidance, disponibility, and friendship.

I'm grateful to the Foundation for Science and Technology (FCT - Portugal) for financial support by national funds through the projects UIDB/00195/2020 – FibEnTech - and UIDB/04035/2020 – Geobiotec. I would like to acknowledge Dra. Ana Gomes, from UBI's Optical Center, Dr. Pedro Gabriel Almeida from Civil Engineering and Architecture Department, Dr. Abílio Silva, from Electromechanical Engineering Department, Dr. Fernando Rocha, Eng. Cristina Sequeira and Eng. Denise Terroso from Geoscience Department of University of Aveiro for the disponibility and help with equipments and analyzis.

And, of course, the PhD's colleagues, friends and more.

Thank you all.

Resumo

Desempenho mecânico e hidráulico, como compactação, consolidação e permeabilidade, desempenham um papel importante no projeto e construção de terraplenagem. Um mau dimensionamento dessa magnitude pode levar a grandes desastres, inviabilizando estruturas, perdendo recursos e até mesmo vidas. Este trabalho procura correlacionar testes rápidos de mecânica dos solos com parâmetros de difícil obtenção - in loco e de laboratório -, seja por falta de recursos ou pelo acesso em algumas áreas inexploradas.

Um aterro experimental localizado em Penalobo, Guarda (Portugal) foi escolhido para a realização de ensaios in situ e amostragem para ensaios laboratoriais. Os ensaios de caracterização geotécnica – gravidade específica, limites de Atterberg, distribuição granulométrica, compactação Normal Proctor, medidor de densidade do solo e densímetro gama -, comportamento mecânico – expansibilidade livre, consolidação edométrica unidimensional, cisalhamento triaxial consolidado não drenado, ensaio de carga em placa, penetração dinâmica leve e pesada, e teste de penetração de cone -, composição química - difraturas de raios X, fluorescência, imagens microscópicas de energia de varredura, capacidade de troca catiônica e pH -, e condutividade hidráulica através do permeâmetro de cabeça descendente permitiram correlacionar diversos parâmetros.

Os resultados caracterizam o solo como um típico solo granítico, uma areia bem graduada sem plasticidade classificada como A-1-b segundo AASHTO, gravidade específica de 2,55, com compactação ótima seguindo w = 14,0% e ρd = 1,86 g/cm3. Composto principalmente por quartzo, caulinita e muscovita, juntamente com altas quantidades de SiO2 e Al2O3, além de menores porcentagens de NaO2 e Fe2O3, também apresentou pH = 6,0 e capacidade de troca catiônica = 17,0 meq/100g. O solo possui alta expansibilidade livre, porém baixa compressibilidade edométrica quando compactado, o ângulo de atrito interno efetivo é em torno de 35º e não possui coesão.

Várias rodadas de testes foram feitas para esta avaliação e, como o local é estudado há mais de dez anos, foi realizada outra análise em prol do comportamento de longo prazo da estrutura. Análises de comportamento de longo prazo e correlações de parâmetros foram desenvolvidas em torno das características de compactação dentro do Normal Proctor, medidor de densidade do solo e resultados do gammadensímetro; condutividade hidráulica direta e indireta através de ensaios laboratoriais oedômetros

e permeâmetros; relação de testes de perfuração entre leve e pesado de penetração dinâmica, teste de penetração padrão e testes de penetração de cone; além de oedômetro laboratorial e teste de carga em placa in-situ, a consolidação do revestimento do aterro.

Palavras-chave:

Aterro ; Liner; Compactação; Consolidação; Permeabilidade; Resistência

Abstract

Mechanical and hydraulic performance, as compaction, consolidation, and permeability, play an important role in the design and construction of earthworks. A bad dimensioning of this magnitude can lead to major disasters, making structures unfeasible, losing resources and even lives. This work looks to correlate quick tests of soil mechanics with parameters that are difficult to obtain - in situ and laboratory tests -, either because of lack of resources or the access in some unexplored areas.

An experimental embankment located in Penalobo, Guarda (Portugal) was chosen to perform in situ tests and sampling for laboratorial tests. The tests for geotechnical characterization – specific gravity, Atterberg limits, particle size distribution, Normal Proctor compaction, soil density gauge, and gamma densimeter -, mechanical behavior – free expansibility, one-dimensional oedometric consolidation, consolidated undrained triaxial shearing, plate load test, dynamic penetration lightweight, and heavyweight, and cone penetration test -, chemical composition – x-ray diffractures, fluorescence, scanning energy microscopic images, cation exchange capacity, and pH -, and hydraulic conductivity through falling head permeameter permitted to correlate several parameters.

Results characterize the soil as a typical granitic soil, a well-graded sand without plasticity classified as A-1-b according to AASHTO, specific gravity of 2.55, with optimal compaction following w = 14.0% and ρ_d = 1.86 g/cm^3. Mainly composed by quartz, kaolinite, and muscovite, along with high amounts of SiO_2 and Al_2O_3, besides lower percentages of NaO_2 and Fe_2O_3, also showed pH = 6.0 and cation exchange capacity = 17.0 meq/100g. The soil has high free expansibility, although low oedometric compressibility when compacted, effective internal friction angle is around 35º and has no cohesion.

Several rounds of tests were made for this evaluation, and since the site is studied for over ten years, another analysis on behalf of long-term behavior of the structure was carried out. Long-term behavior analysis and parameters correlations were developed around compaction characteristics within Normal Proctor, soil density gauge and gammadensimeter results; direct and indirect hydraulic conductivity through oedometer and permeameter laboratorial tests; drilling tests relationship among dynamic penetration lightweight, and heavyweight, standard penetration test,

and cone penetration tests; in addition to laboratorial oedometer and in-situ plate load test analysis the consolidation of the embankment liner.

Keywords

Embankment; Liner; Compaction; Consolidation; Permeability; Resistance

Figure List

Table List

Graphic List

Summary

Chapter 1 – Introduction

1. Scoping and justification

The main geotechnical aspects of an embankment involve the control of its base and top to minimize soil movement and infiltrations while maximize mechanical resistance. In addition, it is needed to secure the best places and materials to construct earthworks. It's generally made by controlled compacted layers of 30-50 cm, besides analysing the subsoil as a foundation. Mechanical and hydraulic performance, as compaction and permeability parameters, play a major role in the design and implementation of various earthworks. A bad dimensioning of this magnitude can lead to major disasters, making structures unfeasible, losing resources and even lives.

This work is based on the need to correlate quick tests of soil mechanics, in situ or laboratory, with parameters that are difficult to obtain, either because of the lack of resources or the difficulty of access in some unexplored areas. Several tests were selected to make this evaluation, and since the site is studied for over ten years, another analysis on behalf of long-term behavior of the structure will be carried out, also looking to prevent disasters and unuseful structures.

The chosen location for all soil testing, both in the laboratory and *in situ*, is Penalobo, at the municipality of Sabugal, Portugal. Tests were done in many points of the embankment for a complete understanding of the structure. An aerial image of the site is shown in Figure 1 and Figure 2, according to Google Earth data, the embankment is in the coordinates 40º23'27.2''N; 7º13'20.7''W, with approximately 150 m^2, near Portugal-Spain border.

The region is referred by [1] that despite the region being a slump basin, its originality lies in the fact that its subsoil is almost completely rocky, however there is a small phenomenon of alteration of the granitic rocks, yet to be analysed during the time. Embankment is understood as a work built predominantly by earth – earthwork -, intended to cover or level a land mass, or create a platform for some essential activity in civil construction, such as, for example, foundations, hydraulic embankments such as canals, sanitary landfills, embankments for dams and dikes, terrain modeling, among others. Controlled landfills are intended to provide an adequate degree of security for their service and use.

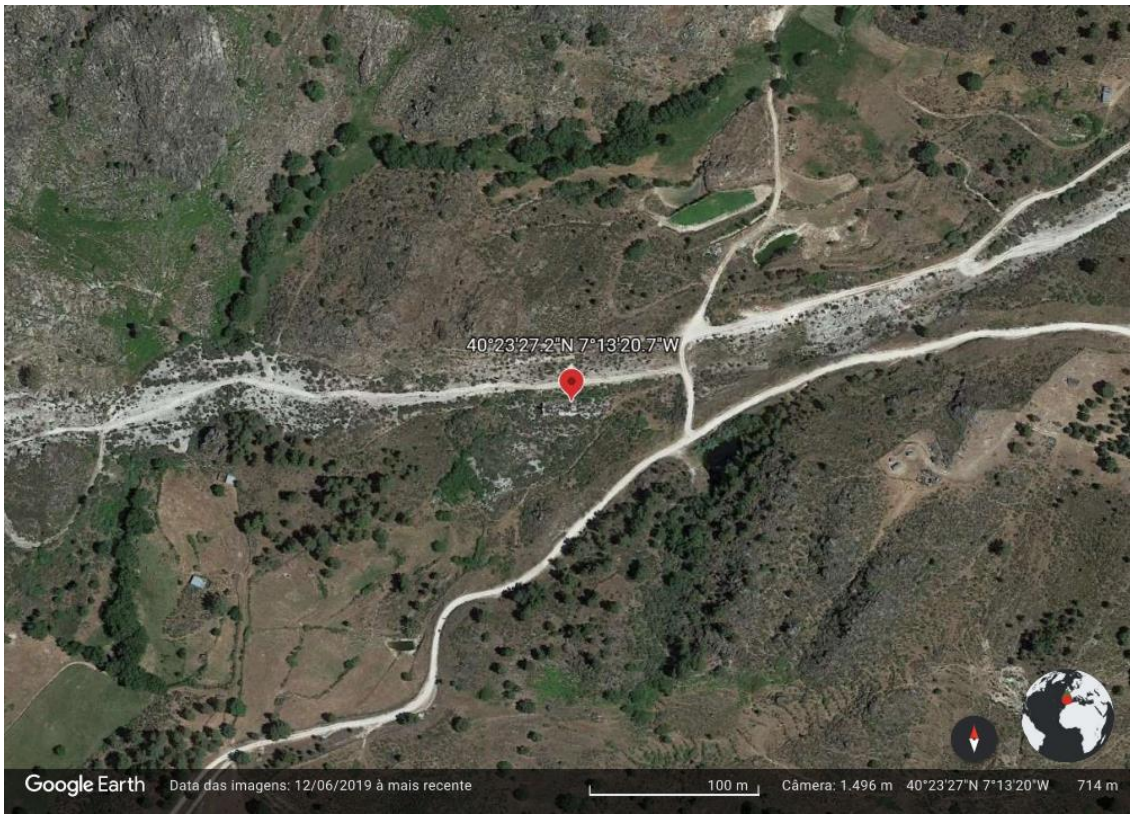

Figure 1. Embankment location

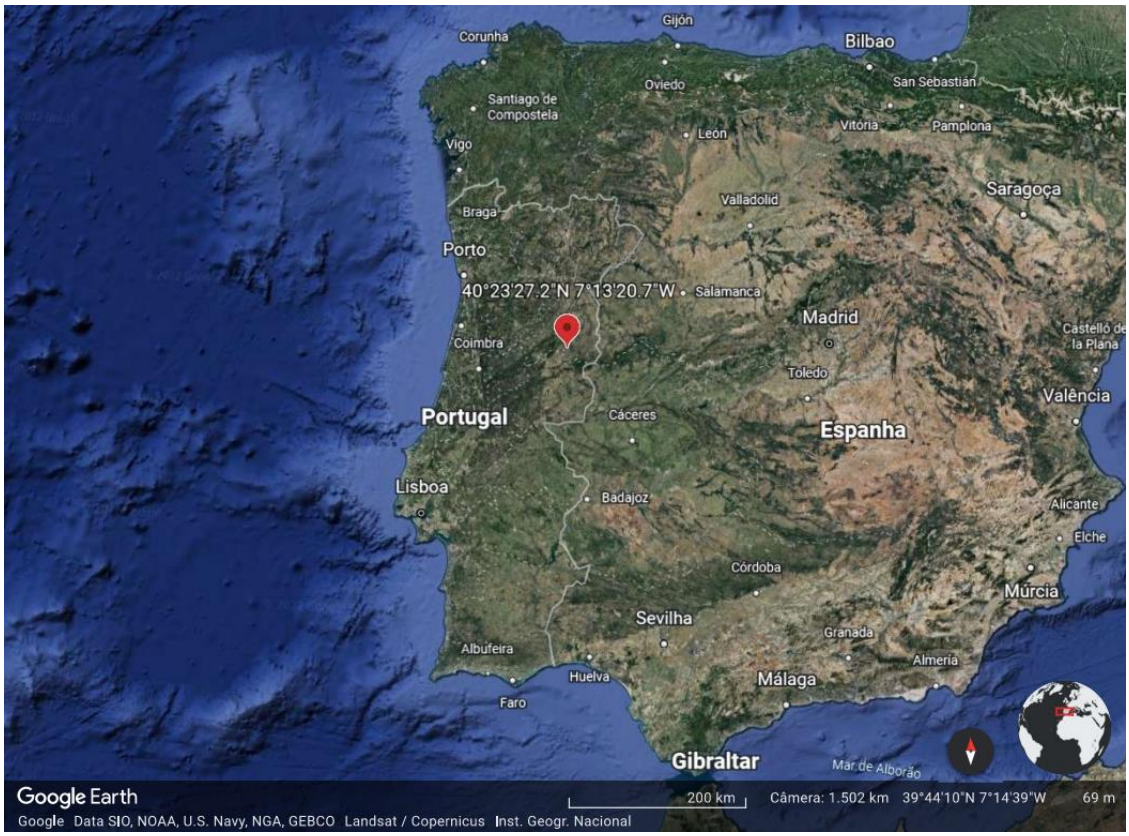

Figure 2. Embankment in the world

Thus, the testing program evaluate different aspects of the behavior of earth massifs, physical, chemical, mechanical, and hydraulical ones, exposed in Table 1.

Table 1. Testing program

Geotechnical	**Mechanical**	**Chemical**	**Hydraulic**
Index Properties	Expansibility	X-Ray Diffractures	Falling Head Permeability
Specific Gravity	Oedometric Consolidation	X-Ray Fluorescence	
Atterberg Limits	Triaxial Shear	Scanning Energy Microscopic	
Granulometry Distribution	Plate Load Test	Cation Exchange Capacity	
Normal Proctor	Dinamic Penetration Lightweight	pH	
Troxler	Standard Penetration Test		
Soil Density Gauge	Cone Penetration Test		

2. Objectives

The main objectives are:

- Develop correlations over several geotechnical parameters for the analyzed soil, around mechanical and hydraulic properties, namely

    1. Proctor versus Troxler versus SDG200
    2. Indirect and Direct Hydraulic Conductivity through Consolidation and Permeability
    3. DPL versus DPSH and SPT versus CPT
    4. Oedometer versus Plate Load Test

- Evaluated long-term behavior of the earthwork due to mechanical and hydraulical parameters which were specified through years.

3. Thesis Structure (Preamble)

Chapter 1 – Introduction

A brief introduction around the theme, its importance for civil and geotechnical engineering, the objectives that this work aims to achieve, the data collected, and the studied site presentation.

Chapter 2 – State-of-art

Presentation of past studies like what is done in this work, also a state-of-art around compaction and permeability for soils, and possible predictions for the objectives.

Chapter 3 – Methodology

Detailed description of laboratorial and in situ tests performed for this work and in past works in the same studied site, referencing them and the standards used.

Chapter 4 – Results and Discussion

Expose all results for the carried tests, along with an analysis over those parameters.

Chapter 5 – Conclusions and Proposals

Where it shows the main conclusions, limitations of the study and suggestions for future ones, such as all the references that supported theoretically this study. And, in sequence, there are the appendices.

Chapter 2 – State-of-art

1. Soils

1.1. Introduction

Geotechnical engineering is divided in two emphases, first is soil mechanics, around properties and mechanical behaviour, and second, foundation engineering, applying soil mechanics, geology, and structural engineering in foundations for earthworks. Mineral formation of the soils is related to which parent rock they derived, igneous rocks are from cooling process of magma, occur at various depths below surface; sedimentary rocks are by layers due to settlement of large masses into water; metamorphic ones are product of high temperatures or pressures changing the previous types. Soils are derived by weathering of rocks, to exemplify the causes, can be cited many physical processes, as temperature variation, wet-dry cycles, freeze-thaw cycles, animal and vegetation actions, and chemical ones, like oxidation, carbonation, hydration.

According to formation processes, soils can be divided between primary or residuals, primary, when they occur in the place where they are formed from the mother rock (magmatic, metamorphic, or sedimentary) or secondary or sedimentary or transported, when in a higher distance from the local of formation of a parent rock [2]. Residual soils are considered autochthonous materials, resulting from meteorization processes of igneous rocks (granite and gabbro), metamorphic (gneiss and shale) and sedimentary (limestone and marl). They are more frequent and involve broader and deeper horizons, reaching depths of hundreds of meters in regions characterized by high temperatures and rainfall [3]. Sedimentary soils are formed with the accumulation in one location or deposit of mineral particles resulting from decomposition and disintegration of rocks from another location. The transport of particles to such a sedimentary deposit is carried out by gravity, wind, and water, in liquid and solid form, ice [4], the deposits formed after transport by water are usually called alluviums and the ones formed in the valleys resulting from the transport of particles through the water and by gravity along slopes are called colluviums.

Furthermore, geological deposits of soil are divided into residual soils, disintegrated, or decomposed of bed rock in the same place; transported soils, by the action of water and/or wind; and glacial soils; with a mention for special soils as expansive soils,

collapsing soils, limestone, quick clays, and organic soils. The studied soil is residual soil, its characteristics vary according to environmental conditions, and the degree of weathering changes with the depth, joint and shear zones in the rock help this process. A typical residual soil profile is exposed:

Nomenclature	Profile	Description
Topsoil	Vegetation	Dark, highly organic
Residual Soil	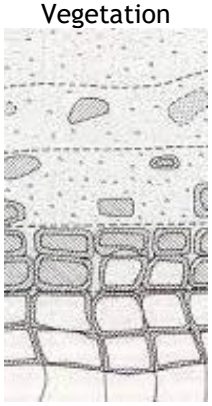	All rock material transformed to soil
Completely Weathered		All rock material disintegrated and/or decomposed
Highly Weathered		More than 35% of rock material decomposed
Moderately Weathered		Less than 35% of rock material decomposed
Slightly Weathered		Discoloration indicates weathering
Bedrock		No visible weathering

Graphic 1. Typical residual soil profile [5].

Granite is a rock which weathering results in granitic soils. Granite can be from igneous rock (granite) or resuls of metamorphic rocks (granite gneiss), and the mineral composition of it is mainly orthoclase microcline, 30-45%, and quartz, around 30-35%, with minor portions of plagioclase, mica, and kaolin, for granite gneiss mica can reach 20%. Granitic soils have variation of granulometry among boldes, cobbles, gravels, silty sand, clayey sand, silt, clays, and solutions, which are produced following the chart flow adapted from [5].

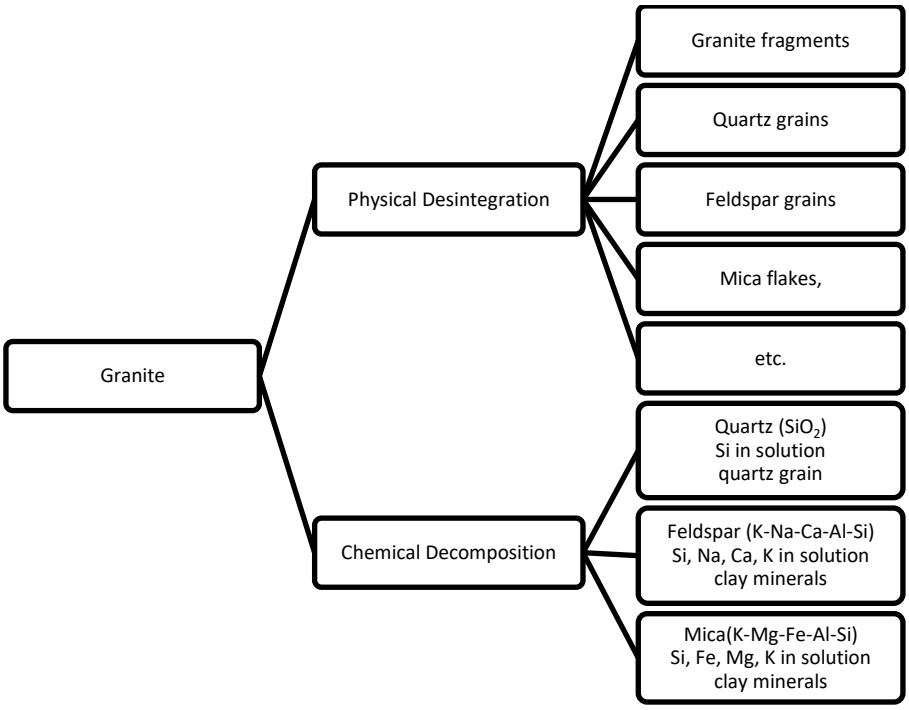

Graphic 2. Granitic soils formation (author)

Clayey minerals are mainly from feldspar and micas chemical weathering, they habe small particle sizes and high surface area per mass unit, or specific surface (SS), which surface have negative residual charge and when in contact with water present plastic behavior. Kaolinite consists in mineral particles connected by strong hydrogen bonds between layers forming stable stacks.

Compaction characteristics have directed influence in several geotechnical parameters; therefore, soil composition characteristics should be studied. Soils can be composed of two or three phases, for completely dry case, they have solid phase and air in the pores, while a fully saturated soil has solid and liquid phase in the pores, however the most found in nature are partially saturated soils composed of all three phases, solid, liquid and air, these components are represented by a phase diagram shown in Figure 3.

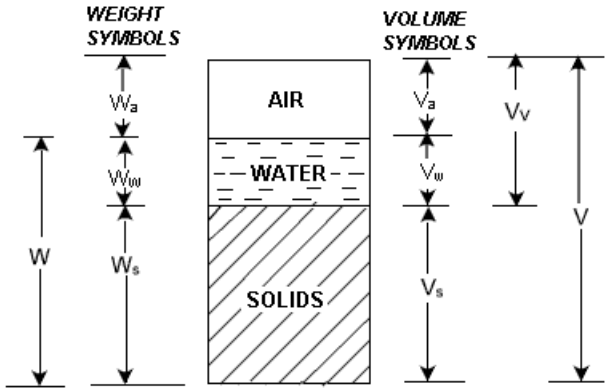

Figure 3. Soil's phase diagram

Water occurs into soils in three different ways showed in Graphic 3, pore water - inside the pores, free and oriented which affect the primary behavior of soils -, adsorbed water – adsorbed by clays and retained between crystalline structure layers -, and hydration water – present in clay mineral crystal, it cannot be removed by oven drier. Water is inside void's soil, and its movement lead to seepage and permeability, water has no shear strength, it is almost incompressible, although transmits water pressure, pore pressure for saturated samples, through the soil mass.

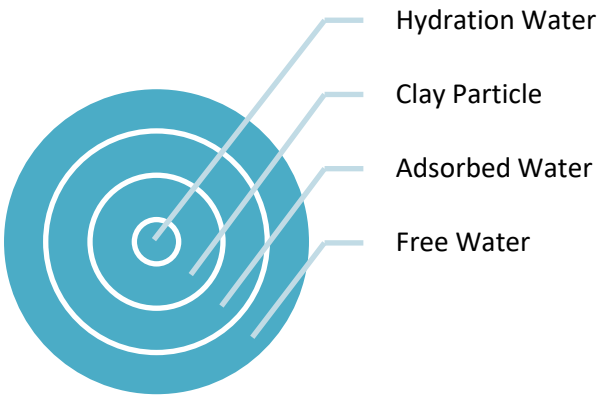

Graphic 3. Water into clays (author)

Capillarity is the behavior associated with fluid's surface tension, for soils it happens between the solid and water content of the structure, this tension is a result of the difference between water attraction forces and the soil ones. This phenom plays an important role due to its influence in soils mechanical and hydraulic behavior, mostly for clayey and silty soils, some authors can predict the capillarity yield rise (h_c) according to the granulometry distribution with the D_{10} parameter, therefore the accurance is questionable, it follows:

$$h_c = \frac{1.50}{D_{10}}$$

Equation 1

Among geotechnical engineering problems the most common are seepage and water flow related, volume change and settlement, stability of soil masses, and load transfer in accordance with bearing capacity. Those hydraulic and mechanicals problems will be discussed in further topics.

1.2. Soil Behavior

Own weight and structural loads tensions are imposed on a soil mass, it presents deformation and volume changes, for cohesionless soils those changes are less perceptives. Firdtly, Terzaghi introduced the concept of effective stress for geotechnics. The self-weight of a deposit stresses is known as geostatic stresses, the vertical stress (σ_v) of a horizontal surface at a given depth (z), considering more than one type of material present with different depths (h) is determined by:

$$\sigma_v = \sum_{1}^{n} \gamma_n \cdot h_w$$

Equation 2

When groundwater is present, then neutral pressure (u_0) due static head of water is:

$$u_0 = \gamma_w \cdot h_w$$

Equation 3

According to Terzaghi, when load is applied to a soil, the total stresses increase, then it developed stresses within the pore spaces called pore pressure (u) and effective stresses (σ') are the difference between total stresses (σ) and pore pressure, given by:

$$\sigma' = \sigma - u$$

Equation 4

Some hypotheses are defined when analysing soil's stresses, as:

- Homogeneity of soil mass
- Obeys Hooke's law and linear elasticity behavior
- Isotropic, same properties in all directions

Those are difficul to respect when working on practical problems, firstly, for a controlled layer it is possible to be homogeneous, although very rare to found in the nature; then soils have ineslastics behaviour; and they are mainly anisotropic due to formation's processes. The stresses within a soil mass can be exposed as compressive stresses as positive, and tension stresses as negatives in a coordinate system, two-dimension representation is in Figure 4 following isotropic properties in the plain x-y.

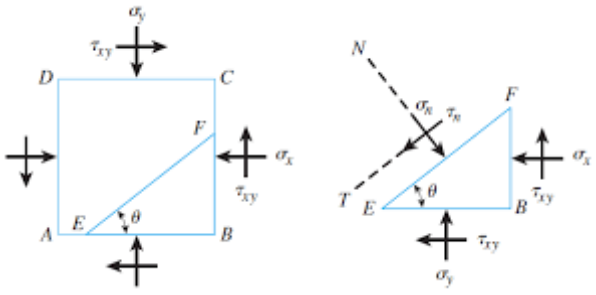

Figure 4. Stresses within soil

Looking to solve and understand this force diagram, Mohr developed the Mohr circle (Figure 5) in terms of compressive stress (σ), ans shear stress (τ) which describes the stresses within a soil mass using a circle equation with radius (r), and center as:

$$(\sigma;\tau) = \left(\frac{\sigma_y + \sigma_x}{2}; 0\right)$$

Equation 5

$$r = \sqrt{\left(\frac{\sigma_y - \sigma_x}{2}\right)^2 + \tau_{xy}^2}$$

Equation 6

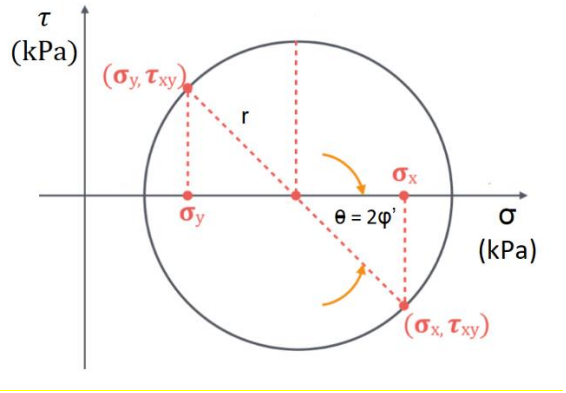

Figure 5. Mohr circle

Stress due to a vertical embankment load in Figure 6 can be determined integrating Boussinesq equation, and the solution for a vertical infinite embankment within an elastic, homogeneous, isotropic half space follows:

$$\Delta\sigma_z = \frac{q}{\pi}\left[\alpha_2 + \frac{x\alpha_1}{B_2} + \frac{z}{R_3^2}(B_2 + B_1 - x)\right]$$

$$\Delta\sigma_x = \frac{q}{\pi}\left[\alpha_2 + \frac{x\alpha_1}{B_2} + \frac{z}{R_3^2}(x - B_2 - B_1) + \frac{2z}{B_1} ln\frac{R_2}{R_0}\right]$$

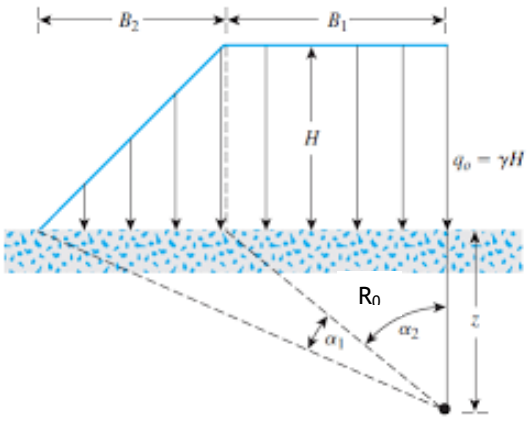

Figure 6. Embankment loading

The limit value to evaluate deformations or stain due to loadings is the shear strength, it can be defined as the support ability of the soil while receiving distorcions or even due failure. Laboratory tests methods used to measure it are many, commonly the direct shear, unconfined compression, and/or triaxial test, those tests are design to analyse the pore pressure due to while allowing deformations. The abovementioned stresses and tensions can be analyzed as the capacity of the embankment to support different loads and pressures. A well compacted layer increases shear resistance. Coulomb and Mohr strength theory express shear strength (τ_θ) in terms of cohesion (c') and friction angle (φ') and utilizing Terzaghi concept of effective stress, parameters c' and φ' can be determined from triaxial tests.

Triaxial tests consist in a cylindrical specimen enclosed in flexible membranes between a cap and a pedestal for drainage and axial load, this conjunction is put in a pressure chamber filled with water. The load is applied in two stages, in the first, the water in the chamber confines the specimen and the second is applied axial load from a constant rate press, for consolidated undrained (CU) triaxial, usually to simulate liner conditions, the first stage is saturation and consolidation, where the specimen drain or consolidate at confining pressure (σ_c') and in the second stage, drainage is not permitted but pore pressure may be measured. Different pressures are applied called deviator stress (σ_d), at least three, to generate a Mohr-Coulomb line or determine the effective stress path due parameterizations with σ_3'= σ_c' and σ_1'= σ_c'+ σ_d, following:

$$s' = \frac{\sigma'_1 + \sigma'_3}{2}$$

Equation 7

$$t = t' = \frac{\sigma'_1 - \sigma'_3}{2}$$

Equation 8

Two or more Mohr circles define Mohr failure envelope with a slope of φ' angle. The value of the effective angle of shearing resistance (φ') using the slope angle of the failure line to the horizontal s' axis (a'), and cohesion (c') based on the intersection with vertical t' axis (α') are following:

$$\sin \varphi' = \tan \alpha'$$

Equation 9

$$c' = \frac{a'}{\cos \varphi'}$$

Equation 10

Changes in pore pressure when loaded can cause deformations, Skempton introduced the pore pressure coefficient (B), which B=0 for a dry soil, and B=1 for a fully saturated soil, partially saturated are in between those values, B value are determined through:

$$B = \frac{\Delta u}{\Delta \sigma}$$

Equation 11

Stresses and strains within a soil mass are directly related with the water content and water pressure in the voids, the pressure can be applied in two different situations, drained one, which the water from the voids is released when under pressure, having no excess of pore pressure, and the undrained, when the water remains confined within the pores. Undrained conditions are used when studying liners, the pore pressure of a saturated consolidated sample will increase, and the ratio of increasing Δu/Δσ, resulting in another parameter, A, like B although due to the pore pressure increase. This pore pressure coefficient A will be positive for low stains, then it will become negative, the stress-strain relation depends on the degree of saturation and the energy of compaction of the sample.

Load placement into soil results in a decrease of void ration, once fulfilled by air, gases, or water, those materials are removed during loads above it, mainly while occurring three phenoms, one is the compression of the solid matter, then compressing and expelling water and air, and through drainage of water and air from the void. This gradual adjustment of the voids in soil's skeleton due to load is called consolidation.

Usually, with higher compaction degree, lower is the soil's compressibility. Fine grained soils are supposed to have three components of settlement, namely, initial

settlement (δi) during immediately load, consolidation settlement (δc) determinate from one-dimensional consolidation theory assuming that the soil is saturated and homogeneous for a constant load increment, and the secondary compression settlement (δs) after primary consolidation. Primary settlement within safety factor must consider the permanent load plus the short-term load, to analyses permissible load capacity against rupture by shear and for repression considerations.

Consolidation process can be explained by the spring analogy, the spring, being the soil skeleton, inside of a cylinder fulfilled with water, representing pore water, measuring the water pressure at the the beginning (u_0), and a drainage valve closed, and an overburden pressure (σ) over the assembly – this is the initial equilibrium. While drainage valve is released, the water is expelled from the voids, the initial pressure varies (Δσ), along with pore pressure (Δu), resulting in a settlement at certain time. When the variation of water pressure is toward to zero with Δσ, it is called a consolidated material. If the loaded surface is release, some expansion will occur, although it will not recover the initial shape

For liner considerations, it is very important to analyze the hydraulic conductivity of a layer, meanwhile the permeability decreases when the soil is well compacted. Hydraulic conductivity can be determined by field and/or laboratory mainly utilizing distilled water, to determine leachate effect on the permeability of a soil, the hydraulic conductivity can be obtained with $CaSO_4$ or with tap water, due their representative salt concentration. According to [6], the factor that affect k values are the nature of permeameter, its density, viscosity and temperature, and soil's properties – finer grains composition, well compaction at optimum wet and saturated soils which permits the permeant to flow are characteristics which decrease k values.

1.3. Soil Design

Geotechnical structures are divided by the type of interaction, the ones which work with surrounded soils are foundations, retaineing wall, tunnels, buried pipes, and underground constructions; and the ones that do not have these loads, like earthfills, earthdams, pavements, backfills, and embankments. Soil and subsoil exploration is made due to borings, and design specification will determine the depth, number, and spacing; sampling for testing, and its types along with time intervals; geological and/seismical occurrences; and hydrological conditions. Site exploration is mainly investigated with drilling process evaluating the resistance and getting field samples for laboratory tests.

Even though it is not the objective of this work, it is important to have an addendum regarding the dimensioning of this type of structure, according to EC7, the design requirements are calculated through ultimate limit state (ULS), associated with structural failure, and/or through serviceability limit state (SLS), with the corresponded service requirement. For both, it should avoid the limit states, mainly by calculation, verifying model tests or full-scale tests, dimensioning calculus, prescriptive measures, observational methods, among others. The design flow chart described for directives follows a criterious process, firstly, stablishing preliminary geotechnical parameters for the type of construction, then there is an investigation over the ground and design characteristics, the next step is the abovementioned dimensioning. After, a constant laboratorial and field supervision when executing the work is done, the design should consider the structure degradation to evaluate the work's durability, the monitoring can be evaluated observing deformations on the ground, non considered actions, forces or displacements on the structure, contact pressure, and pore pressure.

Before the design theories application, two independent phases are undertaken, physical properties of the soil must be predicted or determined by testing, and it is necessary to provide a soil profile of the construction site, mainly by sondage equipments. The calculation for geotechnical design is divided by the understanding and analysis of geotechnical actions and resistance, involving loads and displacements, soil's properties, limits for deformations, vibrations and crackings, verifying that limit states are respected. The calculation model can be analytical, numerical - example finite element method - or semi-empirical, and the selection of geotechnical paramentes can use statistical methods.

Design's reliability is always dependent of the geotechnical, ground and field investigations, information around the site, laboratory testing and geological investigation, and field investigations. Geotechnical parameters quantified soil and rock properties for design calculation, directly or within correlations, theorically or empirically, and its obtainance are mainly through standards over plasticity, deformation, stresses, resistance, pressures, among other relevant for the investigation. These data must have treatment applying calibration and correction factors, factors that must convert the test values in field parameters which represent the behavior of the soil when used for a specific application. Other important phase is when there is a need of new material, fill, dewatered, improved, or reinforced, it must satisfy the same design requirements for the site ground.

1.4. Soil Problematic

Usual techniques are used to improve soil properties, and consequently solving soil problems around reducing compressibility, increasing strength, and reducing permeability, for foundations, pavements, and dams, respectively. Techniques available are mainly compaction, densification expelling air from voids, preloading/consolidation, expelling water from voids, and dewatering, removing again the water.

A very common problematic is soils' volume change and settlement when on loads, it occurs particularly in sites not very desired for construction and need fill material from other sites, increasing loads on lower soils, for example a layer of clayey soil between sandy material. The problem is to evaluate the consolidation of the clay, on a loose situation, the volume change is low and immediately after the load, although the low permeability of the clay will take the consolidation for a long time, make difficult to predict the behavior. Slope stability is another geotechnical issue, the slope tends to move downward or outward helped by gravity, thus the failure surface is dependent of shearing resistance, inclinometers can be used to control the stability of a slope. It is important to analyse the soil to make it feasible for foundations, which main purpose is to hold the load from constructions, in this case, the bearing or support capacity is the parameter to search and test, the type of the foundation is dependent on the type of subsoil.

Hydraulic failure occurs by uplift, heave, internal corrosion, and/or piping, the main actions that must be considered to avoid failure are hydraulic gradients, pore pressures and seepage forces. Investigation should comprehend the soil's permeability variation in time and space, water and groundwater levels variation changing the pore pressure action, and possible geometry modifications. The failure by uplift is verified by comparing the sum of water pressure under the structure and all the upwards forces considered in design criteria, water pressure can be permanent, water level, and variable ones, level changes due to capillarity. This configuration is dealed when checking the stability of submerged structures and satability against uplift of impermeable layers in excavations. Liners are used as geological impermeable layers, in this case the design value of water pressure acting in the interface between layers must be lower than the total weight of soil above the layer.

Failure by heave happens while upward seepage acting is equal or higher than soil's weight above, reducing vertical effective stress to none, this verification must consider

pore pressure and total stress, or seepage forces and submerged weight. A simple and thin layer of impermeable soil change drastically the pore pressure distribution on soil masses, being reasonable to pay a sever attention over it.

Internal corrosion can be evaluated around the geometry of the grain and voids preventing finer particle being transported through seepage, it can be done within filter and hydraulic criterias, checking the filter satisfied the soil itself or in layers interface. Mainly internal corrosion occurs when soil and water are transported in excess, more than 3% of soil, inside the construction, this transport need an evaluation to prevent failure through corrosion. A particular case of internal corrosion is failure by piping, where the transport begins at the ground surface generating a flow into soil mass connecting the soil and the foundation until pipe-shaped tunnel happens. Verification over when the worst hydraulic condition if hydraulic heave occurs or not, and if the top layer of the surface has sufficient level or preventions against internal corrosion as filters layers.

When moving on to the construction phase, it is not known what compaction energy the available equipment can transmit to the soil, as well as the soil characteristics themselves, there are still other aspects to be defined as a priority for the execution of the landfill, such as the thickness of the layers, number of equipment passes. Therefore, for these definitions, experimental landfills are often performed before the definitive ones, in order to test these possibilities. Experimental embankments should be over two or more layers of identical embankment to approximate reality, as the base may exhibit absorption or reflection of compaction energy.

A methodology for experimental embankment was referred by [7], following:

- Deposit and spread the soil
- Compact the soil by layers from 30 to 60cm with plain roller passing from 6 to 12 times
- Layer by layer, perform a minimum of 3 test in different sites, for the parameters:
  - Density by sand bottle and/or gammadensimeter and/or soil density gauge
  - Water content by Speedy method and gammadensimeter and/or soil density gauge
  - Granulometry by sieves
- After compaction, collect samples in a minimum of 3 different sites for:
  - Dry unit weight and water content relation within Normal Proctor

- Atterberg limits

In addition to the references used in this topic, it is important to cite [2], [3], [15], [32]–[84].

2. Compaction

2.1. Introduction

Densification through soil compaction improves soil's strength and bearing capacity and reduces compressibility and permeability. Civil engineering earthworks usually use compaction of soils, this is a major in geotechnical activities as transport industry, embankments, landfills, and foundations. Although, excessed compaction can display behaviors such as plastic deformation, when under wetting condition, swelling and collapse compression, and cracking under drying, also changes in density due to wet/dry and freeze/thaw cycles [4], [8]. Extended compaction is the capacity of increasing shear strength and reducing permeability coefficient, it can be recommended for structures such as building or road subgrade and final cover of a landfill [9].

In embankments and dams' constructions, loose soil is placed in layers with thicknesses that can vary from 75-450mm, and each layer is compacted following the project specifications, using roller, vibrators, or sockets compactors. In general, the greater the compaction degree (CD), the higher shear strength and the lower compressibility of the soil have. The CD is determined in terms of dry density (γ_d) [2]. Embankment dams have been incorporating various types of soils with different granulometries, from clays for the watertightness of the dam body, to sand and gravel in the transition layers, filters, and drains, in addition to rockfill in massive stabilizers, drains and protection.

Soil compaction can be differentiated for cohesive and non-cohesive soils. Cohesive soils have smaller granulometry, clayey minerals, with predominance of surface forces due to chemical reactions favored by the aluminosilicate minerals present. Due to these negative ions on the surface, the salt molecules Na^+, K^+, Ca^+, and Al^+ are easily attracted because the water molecules are interconnected by Van der Waals forces, weak bonds. For high moisture contents, equilibrium is established with a large distance between the particles, due to the attraction of water and consequent repulsion by the peripheral soil particles, resulting in a soil with a high void index and low consistency. If, on the other hand, the soil is a low moisture content, this

equilibrium is only partially achieved, resulting in soils with lower void rates, greater compactness, and large interparticle forces generating high consistency.

Non-cohesive soils are not as sensitive to the effects of water as cohesive ones, both because of their structure and their higher permeability, also their specific surface is much lower than cohesive soils, reducing the need for lubrication of their grains. Consequently, the compaction curves do not present peaks as well defined as in cohesive soils, so intermediate and variable values are obtained. From this, it is common to present compaction characteristics by the compaction index (I_D) of non-cohesive soils, preferably to compaction curves, the higher the compaction index, the lower soil's compressibility.

Several authors have tried to understand theoretically the explanation of when compacted soils increase in density with the increase of water for the dry branch and decrease in density with the increase of water in the wet branch. This task is extremely complex due to phenoms involved in compaction, such as physicochemicals involving three-phase system, and overlapping effects by capillarity, osmotic pressures, shear resistance, deformations, permeability, among others.

2.2. Field Compaction

Compaction in earthworks is not only carried out with effective soil compaction equipments, but several others are also used to perform this process. Trucks are used to transport the soil, excavators to remove the soil from one place to another, usually with the presence of rippers to disaggregate the excavated material, chisel equipment to prepare the surface to be compacted, irrigation machines, essential to obtain the humidity of desired compaction, soil mixing equipments, among others important, although not specified in this work.

For adequate field compaction, a minimum number of passes must be made with the equipment chosen to achieve the required dry density, usually between 3-12 passes, in general, for thicker layers to be compacted, heavier equipment is required [2]. Field compaction involves studies around the area, depth, and volume to be compacted, working and material costs, characteristics and types of soils, equipments and existing structure availability, quality, engineering, and construction safety factors application. Therefore, economics will determine the technique to be used [5].

Historically, the beginning of roller compaction started in 1830 in France, rollers drawn by horses, in 1860 steamrollers were invented, and sheep foot rollers around 1910 in

the United States, ranging from 3-4.5 tons [8]. Roller compaction is done by different roller types, the simplest plain, pneumatic ones, ram compactors, and harrow rollers.

Dynamic Compaction

Compaction by pressure is made from the load transmitted by the vehicle with consecutive passes on the ground. It is used for clayey soils, aggregating the particles, but not reaching high depths.

Plain rollers consist of hollow steel drums whose mass can be increased by ballasts of water or sand, they are suitable for most soils, except for uniform sands and silty sands, a smooth surface is produced in the compacted layer, favoring the flow of rainwater, the landfill will tend to be laminated. Such rollers can be towed or self-propelled. They are in some disuse due to the use of vibrating plain rollers, as they reach thicker layers.

Pneumatic rollers follow the same pattern, but with tires instead of steel drums, such tires are wide preventing the soil from being displaced laterally and transmitting a kneading action to the soil. As well as plain rollers, they are not being used much due to the limitation in the thickness of the compacted layer.

Sheep foot rollers have steel drums but with multiple tapered or club-shaped feet protruding from surfaces, such foot allow high pressure to be exerted in a small area. These rollers are more suitable for fine soils or for coarse soils with more than 20% of fines, the action of the foot homogenizes the soil, breaking harder materials [4]. The successive passage of the roller will increase the resistant capacity of the lower areas of the layer, thus having a compaction from bottom to top, reaching deeper layers.

Vibratory Compaction

Vibratory compaction became very prominent after the Second World War as a very effective in producing compacted layers [8]. They are divided in rollers and plates, they follow the same methodology of roller but with an addition of a motorized vibration mechanism, are mainly used when the moisture content is slightly higher than the optimum, particularly effective for coarse soils [2], usually limited to 1-2m depth. Dynamic deep compaction has been used for loose sands, weak soils, collapsible soil, mining ponds, and sanitary landfills compaction, for cohesive soils, the water is expelled because of the impact.

Vibrating plates, essentially plates connected to a motor that vibrates at certain rotations, are the smallest compaction elements of a work, they are mainly used for access in certain areas that it is not possible to use larger equipment.

Vibroreplacement is another technique which involves placing stone columns into the soil through a supended equipment and vibrate permitig the particles to rearrange, and with water accompanion causes local liquefaction. It is used for cohesive soils or cohesionless with at least 20% of fines.

Table 2 summarized which compaction equipment should be used in accordance with the soil type, along with max weight, depth, and uniformity of the equipments.

Table 2. Dynamic compaction equipments characteristics

Roller	**Max Weight (ton)**	**Max Depth (cm)**	**Layer Uniformity**	**Soil**
Static Sheep Foot	20	40	Good	Silts and Clays
Vibratory Sheep Foot	30	40	Good	Silty or Clayey Sands
Light Pneumatic	15	15	Good	Silty or Clayey Sands
Heavy Pneumatic	35	35	Very Good	All
Vibratory Roller	30	30	Very Good	Sand and coarsed
Plain Roller	20	20	Regular	Coarse-grained
Grid Roller	20	20	Good	Coarse-grained

Impact Compaction

Impact impact can be divided between free fall and explosions, they are very specific methods that depend on a previous investigation of the terrain for their feasibility. Compaction is achieved by waves generated by the impact of a body. The free-fall consists of dropping objects of a certain size and weight onto the area to be compacted, in order to speed up the compaction process. Compaction by explosives was once utilized, rarerly, although it is useful form an economic standpoint, limited to remote areas, sands with less than 15% of fines. Boring tests like standard penetration test (SPT) or cone penetration test (CPT) can verify the success of this application, along with legal and nuisance investigation.

Intelligent Compaction

More recent technologies insert several devices into the compaction equipment to monitor and control the quality of the compaction, it is called intelligent compaction.

In addition, sensors can be installed on the cylinders to obtain parameters in real time and making corrections and adaptations in a short period of time. [7] summarizes the main advantages of intelligent compaction such as greater efficiency and productivity due to automatic processes, optimization of the number of passes, and greater adaptability to any type of soil layer.

2.3. Laboratory Compaction

A study by California Highway Department between 1920s and 1930s showed the degree of compaction the main reason for roads failures, addressing this practice, two important developments occurred, the Proctor compaction curves for compaction specification and California Bearing Ratio (CBR) for pavement design [8], [10].

The CBR test uses a cylindrical mold to undertake loading tests on the soil surface using a plunger. Based on the load-displacement curves obtained, the CBR value is the percentage ratio of the standardized load measured at designated displacements. Since the loads are referenced to specific displacements, the CBR is a measure of the relative stiffness of the compacted soil under monotonic loading [1].

Compaction is a process where energy load is applied over soil increasing density or weight of the specimen causing a volume decrease of samples. It can be affected due several reasons - type and nature of the soil as its granulometry, density and plasticity, the water content at compaction, weather, layer thickness and type of machine used in field compaction. An equation to calculate the compaction energy follows:

$$Compaction\ Energy = \frac{(N°Blows) \cdot (N°Layers) \cdot (Weight\ Hammer) \cdot (Height\ Hammer\ Drop)}{Volume\ of\ Mold}$$

Equation 12

The Normal Proctor, design by Proctor, have a gross energy input of 600 kN.m/m^3 = 12400 ft.lbf/ft^3, some-times referred to as 1Ec. Later, the test was modified to simulate heavier compaction equipment in the field using higher gross energy of 2700 kN.m/m^3 = 56250 ft.lbf/ft^3 and referred as 4.5Ec, standardized as the modified Proctor test.

Compaction quality and methods influence in several aspects of a liner, when well compacted, it increases density and strength and decreases permeability, showing their importance for this type of earthwork. The moisture content and compaction method affect hydraulic conductivity and shear strength. Design field density and

compaction moisture content are based on laboratory tests, which use standard or modified compaction, standard is the most common for basic design since it yields an optimum moisture higher than modified one, compaction curves are essential for practical and trustworthy analysis for filed compaction quality [11].

The laboratory objective is to relate the dry density (γ_d) or void ratio (e) and moisture content (w), plotted in Figure 7, this relationship generates a typical compaction curve with an inverted parabolic shape and the identified maximum point of the parabolic gives the optimum dry density ($\gamma_{d,opt}$) and the optimum moisture content (w_{opt}). Low values of humidity tend to present a rigid and difficult compaction, with the increase of humidity, the soil becomes more malleable, facilitating the compaction process, being able to obtain the maximum value of dry density. However, with the increasing addition of water, the dry density decreases while an increasing portion of the soil volume is being occupied by water, a material lighter than soils [2]. The traditional theory of soil compaction states that the maximum points of the curves, also known as the line of optimums (LOO) have a course sensitively parallel to the 100% saturation curve (Sr = 1), exposed in Figure 7.

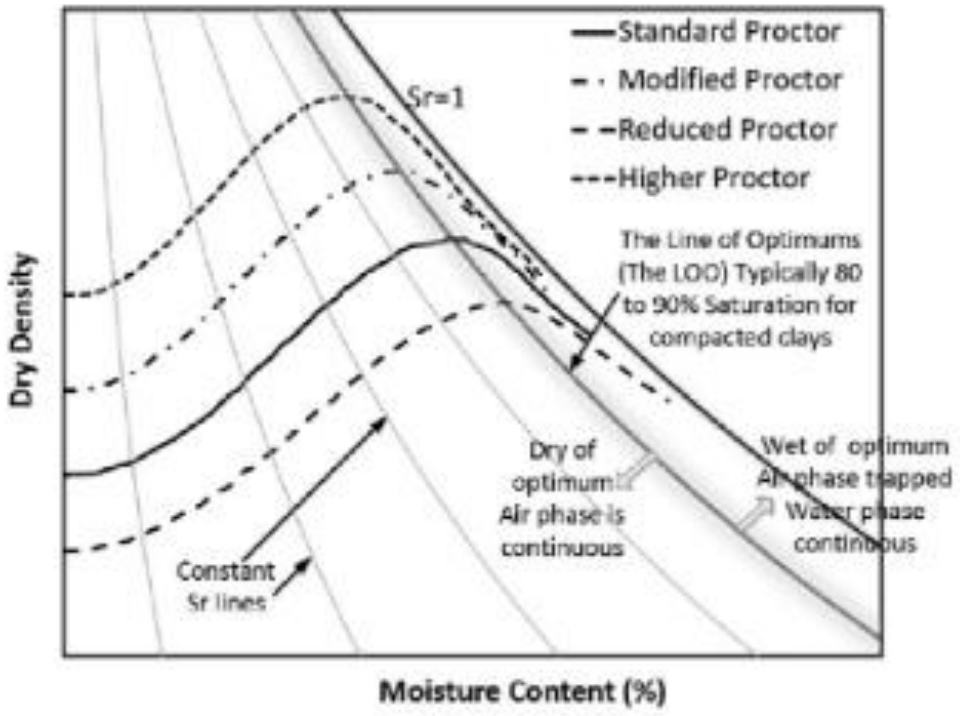

Figure 7. Proctor curves [1].

Proctor justified this shape due water dual effect of capillarity (suction) and lubrication, with high capillarity, dry density is lower for dry soils, and along with

water addition, particle interaction gets lubricated, and capillarity is reduced, rising dry density to the optimum point. Since void ratio is a fundamental state parameter for modelling and interpretations in deformation and swelling-collapse occasions, a relationship to present a simple transformation between γ_d and e is showed below:

$$\gamma_d = \frac{G_S \cdot \gamma_w}{1 + e}$$

Equation 13

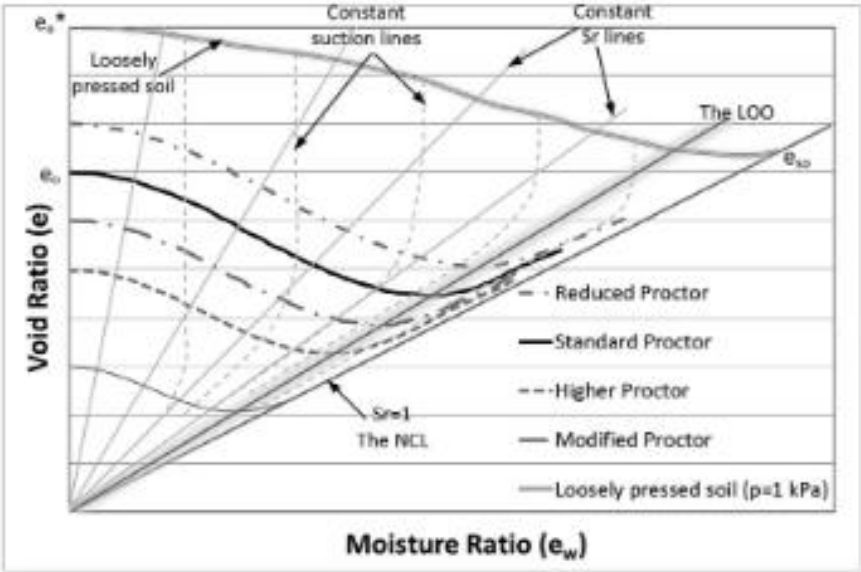

Figure 8. Proctor's void ratio analysis [1].

Figure 9 presents compaction curves using Normal and Modified Proctor for different types of soils along with the related zero void air curve (ZVAC) or saturation line (S,100%), which is only useful when the estimated point of intersection is a solid, while several materials behave as a non-Newtonian fluid, mostly liquid, ZVAC use this equation:

$$\gamma_{ZAV} = \frac{\gamma_w}{w + \frac{1}{G_s}} = S, 100\%$$

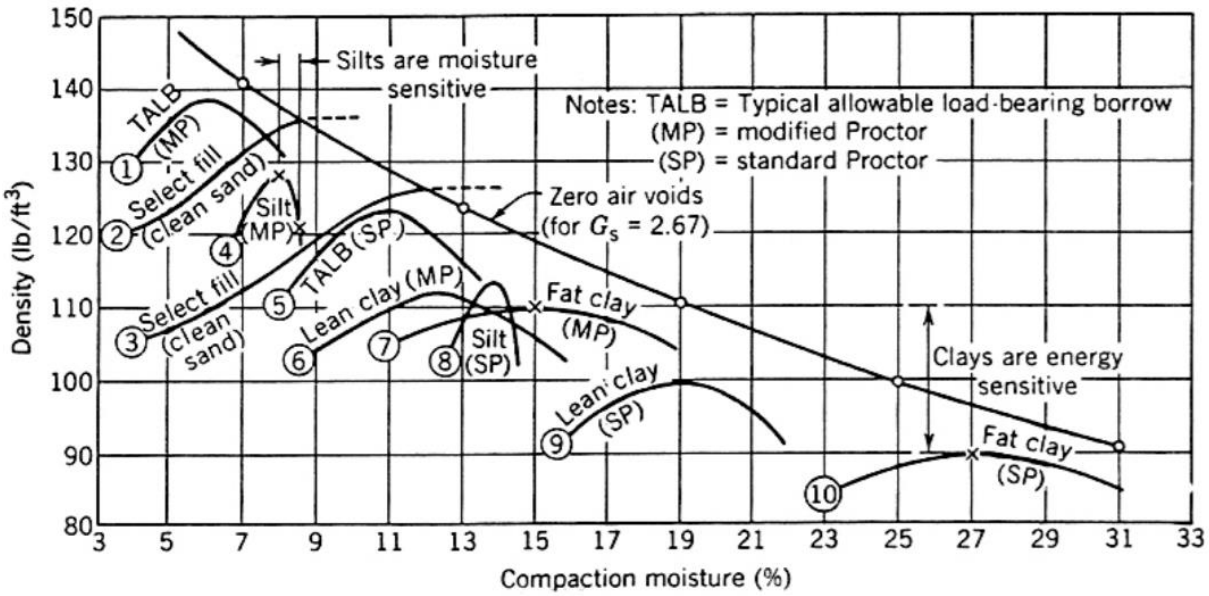

Figure 9. Compaction curves for different soils [1].

[8] summarized compacted fills properties considering dry and wet sides of optimums behavior:

- Stiffness and shear and tensile strengths tend to be higher on the dry side of optimum, due suction reduction when moisture content is lower
- Saturated soil's permeability tends to be higher on the dry side of optimum, due aggregated structure with higher void ratio
- Shrinkage and swelling tend to be higher on the dry side of optimums
- When compacted in wet side, soils behave more anisitropically, more compressive, more permeable, and less resistant to loads
- For the dry side, the opposite behaviour of the abovementioned, and a higher expansibility

2.4. Compaction Control

Several specifications must be included when controlling compaction and dimensioning embankments, for example soil preparation requirements, minimum density to be achieved, moisture range, degree of saturation limits, layer thickness ranges, roller types and characteristics, and other specific features regarding the shape of the landfill. Intelligent compaction is highly adopted with a view to increase compaction homogeneity due premature failure issue, although the subject needs more investigation [8].

Compaction control can be performed with many equipments and tests, namely the Sand Bottle, Densimeter Baloon, Gamadensimeter (Troxler), Soil Density Gauge (SDG), all of them calculating soil's density, their methodology will be described in Chapter

3. Compaction degree can exceed 100% in some cases, when it applied compaction energy in the field higher than the applied in laboratory. In place soil density determination is used for compaction control. Laboratorial tests evaluate the dry density ($\gamma_{d,l}$) relation for different water contents for remolded soils, then the field dry unit weight ($\gamma_{d,f}$) must be specified, normally ranging between 95-98% of optimum laboratory parameters, this parameter is called compaction degree (CD) expressed in percentage, and following:

$$CD = \frac{\gamma_{d,f}}{\gamma_{d,,l}}$$

Equation 14

Besides the references in the text, others like [8], [22]–[31] were used in this topic.

3. Permeability

3.1. Introduction

All soils are permeable materials and the water pressure in the pores is called neutral pressure or pore pressure. Permeability is the capacity of water to flow through soil voids. There are some forms of water flow through soils, the first one is linked to geology and occurs in large land masses, while in small volumes of soil it is linked to soil mechanics, and there are also capillary flows, when a liquid, in this case water, is introduced into a very thin tube and open at its ends, there is a rise in the liquid due to surface tension forces according to physical laws. Capillarity can maintain water in soil's voids with negative pressure [4], [5]. Soils are not monolithic solids, they are composed by the junction of their particles, it leaves interstitial voids, in which can contain air and/or water. The interstitial water is electrically charged explained by the water chemical equation below:

$$H_2O \rightarrow H^+ + OH^-$$

Equation 15

Charged ions generate an attraction of the soil grains with the H+ proton. This water can be in solid phase - adsorbed, heavily subjected to this attraction force -, viscous - medium attracted -, or liquid - free, percolates naturally through voids. The finer the soil is, higher the adsorption. Unconfined water movement in soils can be explained by flow networks in Figure 10.

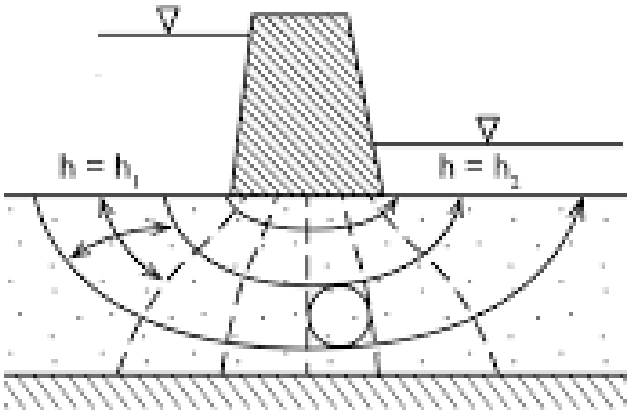

Figure 10. Flow network [1].

For permeability evaluation, some hypotheses are defined [5], [12]:

- water is incompressible
- in a saturated sample, the volume of water that enters is equal to the volume that leaves, so there is no water accumulation
- water has a certain viscosity, and it changes according to its temperature
- Terzaghi's equation: $\sigma = \sigma' + u$ is valid.

Applying Bernoulli's Theorem to pore pressure and due percolation velocities are normally very low, the kinetic load produced can be neglected, result in hydraulic head (h) as a function of pore pressure (u), specific weight of water (γ_w), and the height (z) between a point in the measured water and a reference point, for geotechnical application follows:

$$h = \frac{u}{\gamma_w} + z$$

Equation 16

Darcy studied the hydraulic conductivity (k) through a cross section area (A) perpendicular to the direction flow and showed that for laminar flow with average percolation speed (v), the rate of flow (q) was proportional to the hydraulic gradient (i), this one being the defined by the total head loss (pressure plus elevation head) divided by the distance (L) in which head loss occurs, and the relation is:

$$q = -k \cdot i \cdot A = -v \cdot A = -k.\frac{h}{L} \cdot A$$

Equation 17

Hydraulic conductivity can be determined by field and/or laboratory measurements mainly utilizing distilled water, [6] explained that to determine leachate effect on the

permeability of a soil, the hydraulic conductivity should be obtained with CaSO4 or with tap water, due their representative salt concentration. According to [4]–[6], the factor that affect k values are the nature of permeameter, its density, viscosity and temperature, and soil's properties – finer grains composition, well compaction at optimum wet and saturated soils which permits the permeant to flow are characteristics which decrease k values. Generally, gravel and sand k range from 1 cm/s to 1 x 10^{-2} cm/s, sand and silt mixtures range from 1 x 10^{-2} cm/s to 1 x 10^{-6}, and clays range from 1 x 10^{-6} cm/s to 1 x 10^{-8} cm/s.

3.2. Laboratory Permeability

The permeability coefficient depends mainly on the average pore size, which is related to the particle size distribution, the shape of the particles and the structure of the soil, some empirical relationships were developed from this, as for sands, Hazen determined around the effective size (D_{10}) in mm, a typical k value in m/s, following:

$$k = D_{10}^2 \cdot 10^{-2}$$

Equation 18

Even though being limited, Taylor offered a relationship between k of two soils and their void indexes (e), using constants (C_1 and C_2), which for sandy soils do not have a significant change ($C_1 = C_2$), following:

$$k_1 : k_2 = \frac{C_1 e_1^3}{1 + e_1} : \frac{C_2 e_2^3}{1 + e_2}$$

For laboratorial tests, the dry unit weight is not significantly changed by normal laboratory's temperature, among 15-25°C, however the viscosity (η) of water have influence in k measurement, and can be calculated according to the correction and values below:

$$k_{20} = \frac{\eta_T}{\eta_{20}} k_T$$

Equation 19

Table 3. Water viscosity for temperatures

T (°C)	η (-)
15	1.140
16	1.110
17	1.082
18	1.056
19	1.029
20	1.004
21	0.980

22	0.957
23	0.936
24	0.925
25	0.895

Common values for permeability, the main soil, and usual k determination are summarized:

Table 4. Permeability values for soils, drainage, and k determination

k (m/s)	**1**	**10^{-1}**	**10^{-2}**	**10^{-3}**	**10^{-4}**	**10^{-5}**	**10^{-6}**	**10^{-7}**	**$<10^{-7}$**
Drainage	Good					Poor		Impervious	
Soil Types	Clean gravels			Clean sands		Very fine sands, organic and inorganic soils, silt, clays, among others			Homogeneous clays below weathering
Direct k Determination	Pumping tests								
	Constant head permeameter								
Indirect k Determination	Computational from grain size					Computational from consolidation			
	Falling head permeameter								

The methodology for permeability analysis in laboratory is very simple, although differs according to the soil to be studied, falling head permeameter is used for low permeability soils such as clays, and constant head permeameter for high permeability soils, like sands.

Falling Head Permeameter

Falling head permeability can be measure from upward or downward through the soil, however, downward flow can transport fines and occurring clogging of the sample. The sample to be studied is inserted into a measured cylinder with a cross section (A) and specimen height (L), this cylinder is connected through tubes to another graduated cylinder with a cross section (a) that contains water to a certain level. At a certain initial moment (t_1), there is a certain hydraulic load according to the height (h_1), at another moment (t_2) there is another hydraulic load (h_2), presented in Figure 11.

Hydraulic conductivity (k) is calculated through:

$$k = \frac{a \cdot L}{A \cdot \Delta t} \cdot ln\left(\frac{h_1}{h_2}\right)$$

Equation 20

Or

$$k = \frac{2.3 \cdot L}{A \cdot \Delta t} \cdot log\,(\frac{h_1}{h_2})$$

Equation 21

Constant Head Permeameter

The sample to be studied is inserted into a measured cylinder with a cross section (A) and specimen height (L) like falling head, but connected to a constant level (h) water recipient, it is measured for a certain time (t) the volume of water which percolated through the soil (Q) in Figure 12, explained in Equation 22.

Hydraulic conductivity (k) is calculated through:

$$k = \frac{Q \cdot L}{A \cdot h \cdot t}$$

Equation 22

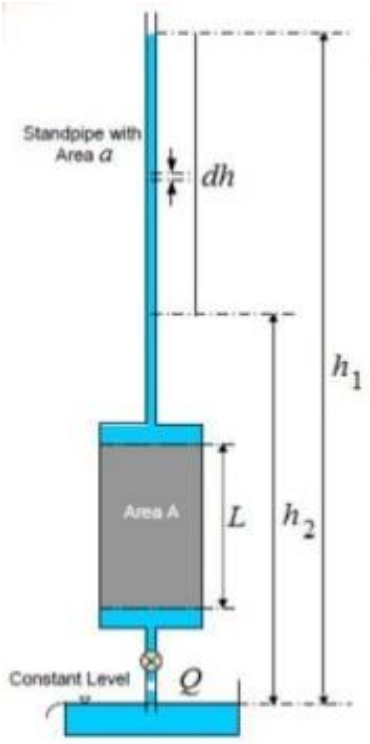

Figure 11. Falling head permeameter

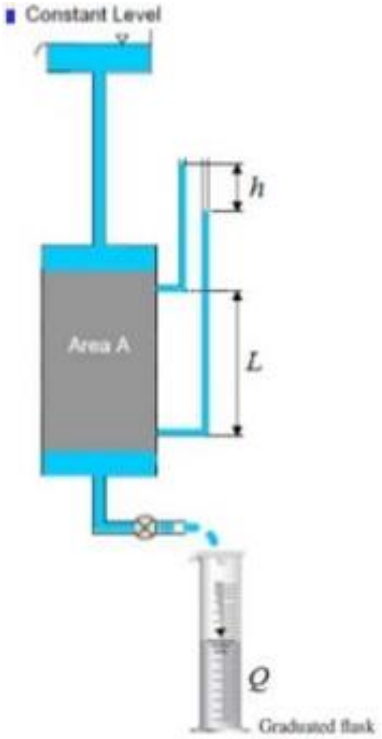

Figure 12. Constant head permeameter

Hydraulic conductivity can also be obtained indirectly by other laboratory tests, one example is using oedometer cells for consolidation evaluation for each load stage calculating the compressibility coefficient (a_v), the change in void ratio per unit of pressure change as a result of consolidation, the consolidation coefficient (c_v), the relation of pore pressure changing in time, to the amount of water drained due consolidation, calculated using Casagrande method following the expressions below:

$$k = c_v \cdot m_v \cdot \gamma_w \cdot g$$

Equation 23

$$m_v = \frac{a_v}{1+e} = -\left(\frac{1}{1+e}\right) \cdot \frac{\delta e}{\delta p}$$

Equation 24

3.3. Field Permeability

Laboratory permeability tests not always can achieve applicable results, mainly for the sample that is extracted and have different conditions from real field ones. Thus, in situ tests are more reliable than laboratories. Field permeability tests are many, therefore the principle is very similar measuring for a variation of time a volume of water correspondent.

Pumping Test

The auger hole method is a quick test and can be easily performed in the field when the water table is shallow, also the soil profile can be identified during the test, disturbed and undisturbed soil samples can be collected while drilling the holes, and several other geotechnical tests can be performed simultaneously. This method requires monitoring wells to be drilled that extend below the groundwater table, since the observation well is completed and the water table inside the well reaches equilibrium, the test starts by removing the water in the hole, then the groundwater seeps into the hole, returning to the original level, the time required to reach equilibrium is measured. The are the hole dimensions (radius r, depth h + H), the location of the water table in the hole (h), and the location of the impermeable layer below the hole (S) explained in Figure 13, and following the equation below [12].

$$k = \frac{4000}{(\frac{H}{r} + 20) \cdot (2 - \frac{y}{H})} \cdot \frac{r}{y} \cdot \frac{\Delta y}{\Delta t}$$

Equation 25

Guelf Permeameter

The Guelph permeameter (Figure 14) method is an in situ constant head test that measures unsaturated soils' saturated permeability using a Mariotte siphon reservoir. Interpretation of the test results can be made with one, but preferably two points of measurements. Two-point measurements provide a better estimate of α* - the ratio of saturated hydraulic conductivity to matric flux potential (Φm), measurements of one

steady flow rate with a single ponded head, in which k can be obtained with the steady intake rate of water (Q), the well height (H) and radius (r), such as dimensionless shape factor (C), according to the equations below:

$$k = \frac{C \cdot Q}{(2\pi H^2 + \pi r^2 C + \frac{2\pi H}{\alpha^*}}$$

Equation 26

$$C = \left[\frac{\frac{H}{r}}{2.074 + 0.093\frac{H}{r}}\right]^{0.754}$$

Equation 27

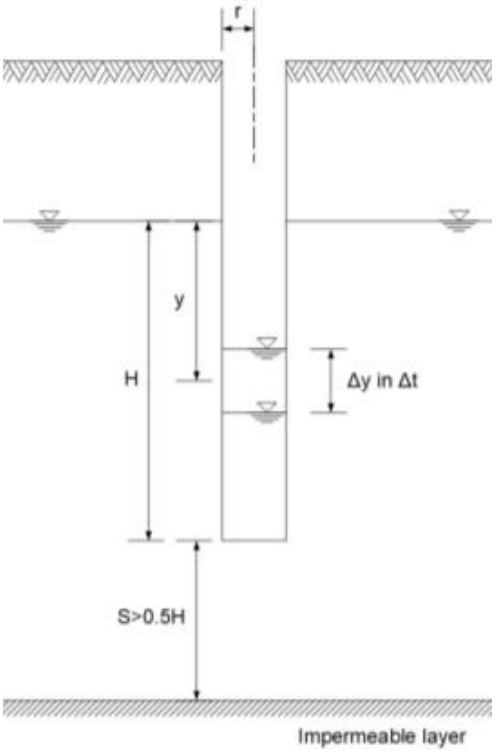

Figure 13. Auger hole method

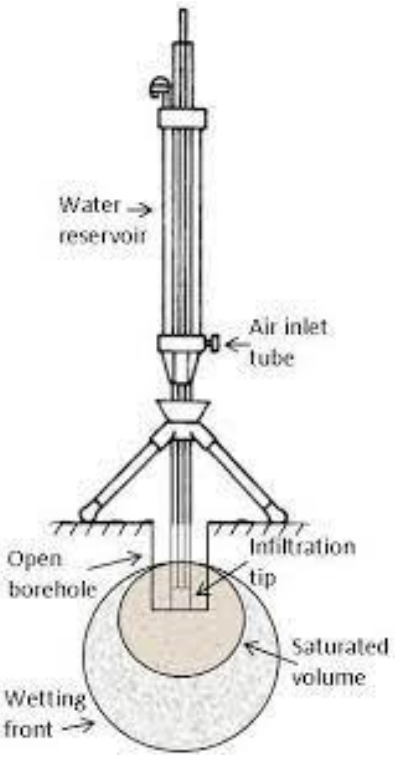

Figure 14. Guelf permeameter

Seepage Velocity

An indirect method can be measured for k, mainly for coarse grained soils,measuring the average velocity (ve) of seepage for two points, several method can be applied for flow determination, electrolytes, galvanometers, radioactive charges, Geiger counters, and placing fluorescein color into the first hole and chronometer the time

until it appears in the second can be used to define the time of flow, and calculate through porosity (n) and hydraulic gradient (i):

$$k = \frac{v_e n}{i}$$

Equation 28

For this topic, were also utilized the references around liners like [32], [33], [35], [38], [46], [48], [50], [63], [68], [70], [73], [77], [79], [82], [85]–[155].

Chapter 3 – Methodology

1. Sampling

The sampling procedure was conducted as follows based on [13] Theory of Sampling:

1. samples of approximately 50 kg were collected and stored in plastic boxes tagged with a soil code, the collection date, and the site's coordinates.

2. transport from collection place to the Soil Mechanics Laboratory of the Civil Engineering and Architecture Department, Universidade da Beira Interior (DECA-UBI), Covilhã.

3. approximately 50% of the total sample was storaged as replacement material, also used in mixtures, and the other 50% was dehydrated and determined the water content based on EN ISO 17892-1

4. the dehydrated portion of the sample was divided for laboratory tests according to each standard and amounts as stated in Table 5.

Table 5. Sample's amounts and granulometry

Laboratory Test	Sample Amount	Max Diameter
Water Content	3x 100g	4.000 mm
X-ray Diffraction	3x 10g	0.075 mm
X-ray Fluorescence	3x 10g	0.075 mm
Scanning Eletron Microscope	3x 10g	0.075 mm
Cation Exchange Capacity	3x 500g	0.075 mm
Specific Gravity	3x 50g	0.400 mm
Atterberg Limits	3x 500g	0.400 mm
Normal Proctor Compaction	6x 2500g	4.000 mm
Oedometer Consolidation	1x 2500g	4.000 mm
Triaxial Test	3x 1500g	4.000 mm
Permeability	1x 2500g	4.000 mm

2. Geotechnical Characterization

2.1. Index Properties

Soils are a very complex system consisting of different mineral particles, sizes, and shapes, with voids filled with gases and/or liquids [4], [6], relationships used to express the state of a soil are described in **Error! Reference source not found.**, according to volume (V) and weight (W), and among them. Some of the the values are estimated in the field while others determinated in laboratory.

Porosity (n) and void ratio (e) are important to evaluate capilarity, concept that explains the percolation of water or liquid and solid pollutants while reacting with the soil, hydrodynamic characteristics associated with run-off, such as advection, molecular diffusion, and dispersion, are also influenced by the variation in porosity [14].

Water content (w) is the percentage of water in a dry sample determinated through EN ISO 17892-1. Free, capillary, and weakly bonded water are lost on heating up to 150°C, from 150-400°C, strongly held water in crystalline structure evaporates, and only heating 400°C or higher that chemically bonded water in hydroxides form evaporates. For soils, mainly w is under 100%, although for marine and organic soils it can reach up to 300%, w is directly dependent to size, shape and arrangement of the particles, its plasticity and adsorption properties.

2.2. Specific Gravity

Inorganic soils usually have specific gravity (Gs) values ranging of 2.6-2.8, commonly assumed 2.65 for sandy soils and 2.7 for clayey. The most common method is using pycnometer throught EN ISO 17892-3, a method by fluid displacement was applied for particle size under 4mm, the test consists in measure the difference of the same volume inside a calibrated pycnometer of distilled water and distilled water with a certain amount of soil, knowing wet and dry weigth characteristics. Dry unit weight (γd) was determinated from extractors from Cavaleiro (2001).

From Table 6, several parameters were obtained from the abovementioned tests.

Table 6. Index properties

Properties	Formula
Porosity (n)	$n = \frac{V_V}{V}$
Void Ratio (e)	$e = \frac{V_V}{V_S}$
Degree of Saturation (S)	$S = \frac{V_W}{V_V}$
Water Content (w)	$w = \frac{W_W}{W_S}$
Solid content (s)	$s\ (\%) = \frac{1}{1+w}$
Unit Weight of Water (γ_w)	$\gamma_w = \frac{W_W}{V_W}$
Unit Weight of Solids (γ_s)	$\gamma_S = \frac{W_S}{V_S}$

Specific Gravity (G_S)	$G_S = \frac{\gamma_S}{\gamma_w}$
Total Unit Weigh (γ)	$\gamma = \frac{W}{V} = \gamma_w \cdot \frac{(G_S + S \cdot e)}{(1+e)}$
Dry Unit Weight (γ_d)	$\gamma_d = \frac{W_s}{V} = \gamma_w \cdot \frac{G_S}{(1+e)} = \frac{\gamma}{(1+w)}$
Specific Gravity - Saturation	$G_S \cdot w = S \cdot e$

Other index properties which can be obtained are compactness index (I_d), consistency index (I_C), plasticity index (PI), and clay activity (A_C), following:

$$I_d = \frac{e_{max} - e}{e_{max} - e_{min}}$$

Equation 29

$$I_C = \frac{w_L - w}{w_L - w_P}$$

Equation 30

$$A_C = \frac{I_P}{Clay\%}$$

Equation 31

Table 7. Physical indexes

I_d (%)	Classification	I_C (%)	Classification	A_C (%)	Classification
<15	Very loose	<25	Very soft	<50	Inactive
15-35	Loose	25-50	Soft	50-75	Low active
35-65	Regular Compated	50-75	Regular	75-125	Regular active
65-85	Dense	75-100	Strength	125-200	Active
>85	Very dense	>1	Very strength	>200	Very active

2.3. Consistency Limits

Atterberg proposed limits which the action of water content can be compared and distinguished through consistency and sensitivity, they are upper limit of viscous flow; liquid limit; sticky limit; cohesion limit; plastic limit; and shrinkage limit, currently perspective, soils may be in a liquid, plastic, semi-solid or solid state [6] according to its water contents, soil can be in liquid, plastic, semi-solid and solid state, the upper and lower limits of moisture content values in which the soil exhibits plastic and liquid behavior are defined as the liquidity limit (w_L) and plasticity limit (w_P), respectively, and the plasticity index (PI), a parameter correlated with strength, given by:

$$\mathrm{PI} = w_L - w_P$$

Equation 32

Skempton also defined the clay activity (A_C) in accordance with PI and the ratio of fine particles less than 0.002 mm to the soil sample – clay portion (P_C), and inactive soils have $A_C < 0.75$, normal soils $0.75 < A_C < 1.25$, and active soils with $A_C > 0.75$, following:

Shrinkage or expansibility is the volumetric variation that certain soils present when their water content varies, causing an increase in volume due to the absorption of water, and by drying the opposite phenomenon occurs, observing retractions. Two phases are allowed in the expansion process, first, water molecules penetrate between the structural layers of the expansive clays, or between the flat surfaces of the adjacent particles tending to separate them, and second, the adsorption energy is small, leading to the repulsion of the double electric layer that tends to increase, driving away the particles [2], [15].

Additionally, the plasticity of soils is an important characteristic, especially for fine soils, which are often used in waterproofing barriers. Plasticity is the capacity of the soil to undergo irreversible deformation without rupture or crumbling, always dependent on the water content. The water is the main interconnection with compaction, exposed by Figure 15, these are geotechnical parameters dependent on the water within pores.

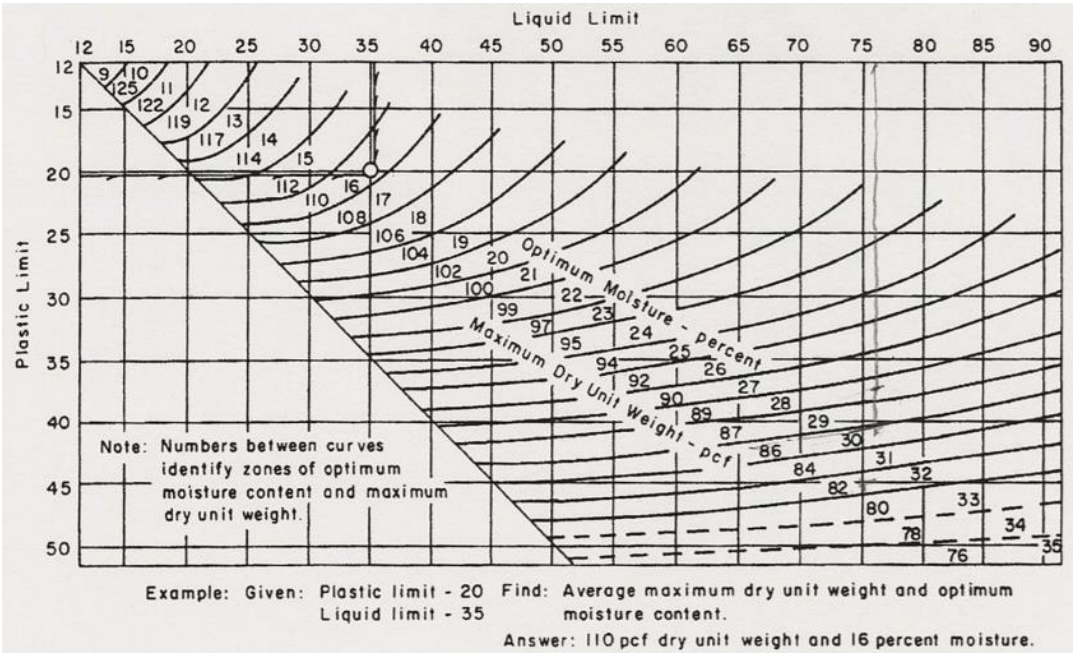

Figure 15. Relation of average maximum dry unit weight and optimum moisture content to plastic and liquid limit

Terzaghi and Casagrande developed methods to quantify plastic and liquid limits, which follow ISO 17892-12 [13]., The plastic limit of a soil is the water content at which a soil ceases to be plastic when dried further and it is measured along with liquid limit, samples were sieved and only the material under 0.4mm was used. For liquid limit, Casagrande apparatus, or Casagrande shell, is fullfilled with wetted soil sample in different portions trying to reach 15 to 35 hits in a created a path between slopes in the middle of the shell, and when this path is connected due impact of the shell, the hits are counted, and measured the water content in that specific touching sample. For the plastic limit, the procedure is to remold a paste with soil and distilled water into a 3mm diameter and 10cm length cylinder, then divide the cylinder in three parts and measure the water content of it.

2.4. Granulometric Distribution

Granulometry is the measurement of the size distribution of the grains of soils, particle size distribution curves are where the coordinate axis is plotted on a logarithmic scale with the diameter of the particles and the abscissa axis is the accumulated percentage, either in mass or volume of the corresponding diameter. Some nominal particle sizes are very importante such as D_{10}, D_{30}, D_{50}, D_{60}, D_{90}, corresponding to 10%, 30%, 50%, 60% and 90% passing by weight or volume, depending on the size distribution method applied. Granulometry analysis are through ISO 17892-4.

Unified Soil Classification System (USCS)

USCS classification of soils methods are not a differential parameter for soils with especial characteristics, or residue materials analysed as soil, but the range applied can qualify the material for the studied application. For instance, [17] studied lateritic fine-grained soils classified as CH and MH, or CL and ML, through USCS and concluded that they do not differ significantly in geotechnical behavior, but those classification can guarantee or not the soil's application for embankment, waste containment or other earthworks. There are several classification's systems for soils, they differ a little around the range for the grain size and the differentiation in silt and clay definitions, Table summarized it:

Classification System	Grain Size (mm)				
	Clay	Silt	Sand	Gravel	Cobbels/Boulders and Rocks
USCS	Plasticity characteristics		0.075-4.75	4.75-75	>75

AASHTO	<0.002	0.002-0.050	0.050-2.00	2.00-75	>75
ASTM	<0.005	0.005-0.060	0.060-2.00	2.00-100	>100

The USCS follows the Table 8 from ASTM D2487:

Table 8. USCS classification criterias

Criteria for Assigning Group Symbols and Group Names Using Laboratories Tests [A]				**Group Symbol**	**Group Name**
Coarse-grained Soils More than 50% retained on #200	Gravels More than 50% of coarse fraction retained on #4	Clean Gravels Less than 5% of fines [C]	$C_u \geq 4$ and $3 \geq C_c \geq 1$ [D]	GW	Well-graded gravel [E]
			$C_u > 4$ or $C_c < 1$ or $3 < C_c$ [D]	GP	Poorly graded gravel [E]
		Gravels with Fines More than 12% of fines	Fines as ML or MH	GM	Silty gravel [E,F,G]
			Fines as CL or CH	GC	Clayey gravel [E,F,G]
	Sands 50% or more of coarse fraction passes #4	Clean Sands Less than 5% of fines	$C_u \geq 6$ and $3 \geq C_c \geq 1$ [D]	SW	Well-graded sand [I]
			$C_u > 4$ or $C_c < 1$ or $3 < C_c$ [D]	SP	Poorly graded sand [I]
		Sand with Fines More than 12% of fines	Fines as ML or MH	SM	Silty sand [F,G,I]
			Fines as CL or CH	SC	Clayey sand [F,G,I]
Fine-Graned Soils 50% or more passes the #200	Silts and Clays Liquid limit less than 50%	Inorganic	PI > 7 and plots on or above "A" line [J]	CL	Lean clay [K, L, M]
			PI < 4 or plots below "A" line [J]	ML	Silt [K, L, M]
		Organic	Liquid limit oven dried < 0.75	OL	Organic clay [K, L, M, N]
			Liquid limit not dried < 0.75	OL	Organic silt [K, L, M, O]
	Silts and Clays Liquid limit more than 50%	Inorganic	PI plots on or above "A" line	CH	Fat clay [K, L, M]
			PI plots below "A" line	MH	Elastic silt [K, L, M]
		Organic	Liquid limit oven dried < 0.75	OH	Organic clay [K, L, M, P]
			Liquid limit not dried < 0.75	OH	Organic silt [K, L, M, Q]
Highly Organic Soils	Primarily organic matter, dark in color, and organic odor			PT	Peat

[A] Based on the material passing the 3-in. (75-mm) sieve.
[B] If field sample contained cobbles or boulders, or both, add "with cobbles or boulders, or both" to group name.
[C] Gravels with 5 to 12 % fines require dual symbols:
GW-GM well-graded gravel with silt
GW-GC well-graded gravel with clay
GP-GM poorly graded gravel with silt
GP-GC poorly graded gravel with clay
[D] For coarse soil classification, it is important to determine from abovementioned nominal particle sizes, the coefficient of curvature and the coefficient of uniformity, respectively by:

$$C_c = \frac{D_{30}^2}{D_{10} \cdot D_{60}}$$

$$C_u = \frac{D_{60}}{D_{10}}$$

[E] If soil contains >15 % sand, add "with sand" to group name.
[F] If fines classify as CL-ML, use dual symbol GC-GM, or SC-SM.
[G] If fines are organic, add "with organic fines" to group name.
[H] Sands with 5 to 12 % fines require dual symbols:
SW-SM well-graded sand with silt
SW-SC well-graded sand with clay
SP-SM poorly graded sand with silt

SP-SC poorly graded sand with clay

[I] If soil contains >15 % gravel, add "with gravel" to group name.
[J] If Atterberg limits plot in hatched area, soil is a CL-ML, silty clay.
[K] If soil contains 15 to <30% plus No. 200, add "with sand" or "with gravel," whichever is predominant.
[L] If soil contains >30 % plus No. 200, predominantly sand, add "sand" to group name.
[M] If soil contains >30 % plus No. 200, predominantly gravel, add "gravelly" to group name.
[N] PI < 4 and plots on or above "A" line.
[O] PI < 4 or plots below "A" line.
[P] PI plots on or above "A" line.
[Q] PI plots below "A" line.

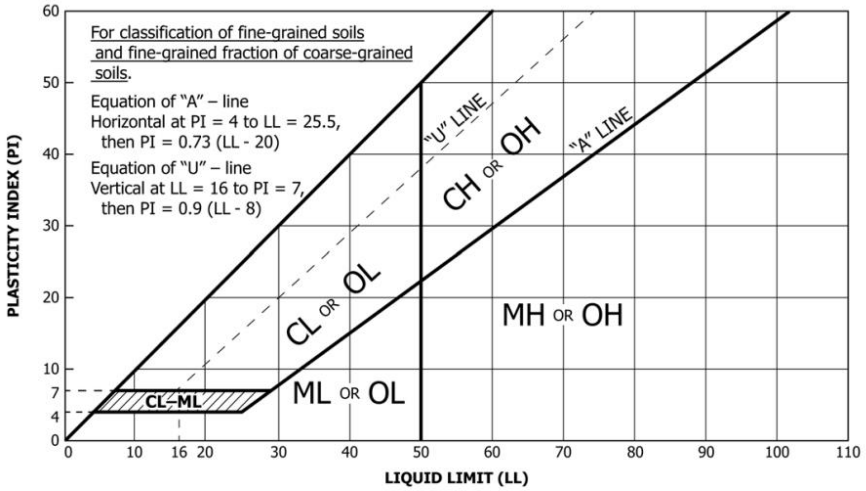

Figure 16. Plasticity chart [1].

The resume of the group symbol according to important properties relations is in Table below.

Table 9. Main properties according to granulometric classification

Group Symbol	**Permeability** When well compacted	**Shear strength** Compacted and saturated	**Compressibility** Compacted and saturated	**Workability** Construction material
GW	Regular	Excellent	None	Excellent
GP	High	Good	None	Good
GM	Low	Good	None	Good
GC	Low-Very low	Good-Regular	Very low	Good
SW	Regular	Excellent	None	Excellent
SP	Regular	Good	Very low	Regular
SM	Low-Very low	Good	Low	Regular
SC	Very low	Good-Regular	Low	Regular
ML	Low-Very low	Regular	Regular	Regular
CL	Very low	Regular	Regular	Good-Regular
OL	Low-Very low	Low	Regular	Regular
MH	Low-Very low	Regular-Low	High	Bad
CH	Very low	Loew	High	Bad
OH	Very low	Low	High	Bad
PT	-	-	-	-

The AASHTO follows the Table 10 and Figure 17.

Table 10. AASHTO soil classification system

General	Granular Materials 35% or less passing #200							Silt-clay Materials More than 35% passing #200			
Group	A-1			A-2							
	A-1-a	A-1-b	A-3	A-2-4	A-2-5	A-2-6	A-2-7	A-4	A-5	A-6	A-7-5 A-7-6
Sieve Analysis % passing											
#10	50max										
#40	30max	50max	51min								
#200	15max	25max	10max	35max	35max	35max	35max	36min	36min	36min	36min
Passing #40											
Liquid Limit	-		-	40max	41min	40max	41min	40max	41min	40max	41min
Plasticity Index	6max		NP	10max	10max	11min	11min	10max	10max	11min	11min
Usual Types	Stone Gravel and Sands	Parts,	Fine Sand	Silty or Clayey Gravel and Sand				Silty Soils		Clayey Soils	
Subgrade Rating	Excellent to Good							Fair to Poor			

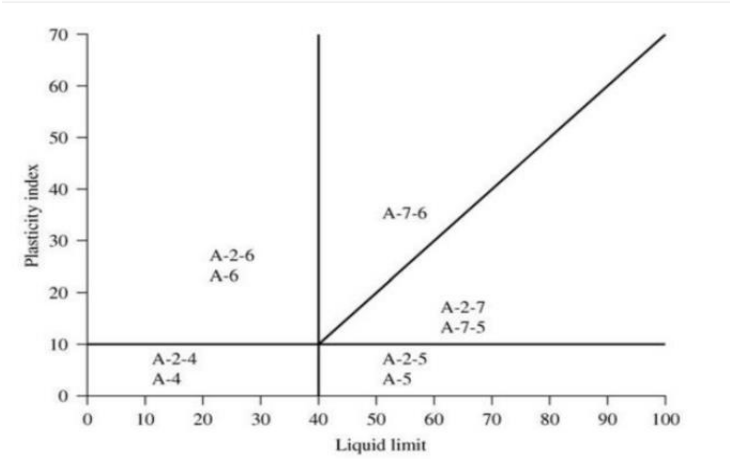

Figure 17. AASHTO plasticity chart [1].

3. Chemical and Mineralogical Composition

3.1. Diffratometry, Fluorescence and Microscopic

X-Ray Diffractometry (XRD), X-Ray Fluorescence (XRF) and Scanning Electron Microscopy (SEM) are the main chemical and mineralogical characterization techniques used.

In XRD, each mineral species is characterized by a systematic arrangement atomic (or ion) specific, with characteristic crystalline planes that can diffract X-rays. The diffraction of X-rays by atoms in a crystalline plane produces characteristic patterns when recorded (angles and intensities). These diffraction patterns are used as a fingerprint in the identification of mineral species, producing a series of dots or lines, called bands.

The XRF consists of the incidence of an X-ray beam on a sample, making with its electrons being ejected from the layers close to the nucleus, The vacancies created

are filled by electrons from the outermost layers, emitting X-rays (fluorescent or secondary), whose energies correspond to the difference between the energies of the levels and sublevels of the transitions. Each type of atom has a characteristic and unique X-ray spectrum that is used as a comparison for identification. The intensity of the XRF of a certain wavelength is related to the concentration of the element that emitted it. XRF analysis is semi-quantitative and provides the chemical composition expressed as the oxides of the elements.

The Scanning Electron Microscope (SEM) is one of the most versatile instruments to obtain information on the morphology of minerals. When they have detectors that capture characteristic X-rays by energy dispersion (Energy Dispersive Spectroscopy - EDS), they are called MEV-EDS, and provide information about the chemical elements that compose them. The SEM produces images with a three-dimensional appearance, a direct result of the great depth of field and allows the examination in successive increases, with great depth of focus, combining information from electronic and optical images. According to other authors, the main reason for its use is the high resolution obtained when observing the samples.

XRD was determined using the Rigaku equipment, model DMAXIII, USA, in which the clay mineralogy of the soil is obtained with a Phillips Analytical X-Ray B.V. diffractometer, composed of a PW 3710 mpd/00 controller and a high voltage generator PW 1830, P, operating at 40 kW and 30 mA with a copper bulb, Cu K-α radiation. An equivalence method by comparison in a database based on the characteristic peaks of the diffractions is also applied, expressing the estimated reflecting power for each type of mineral. SEM images were generated by the equipment S-2700 Hitachi, Rontec, USA. Oxides and elemental composition were determinated with EDS coupled in SEM equipment.

3.2. Cation Exchange Capacity

CEC is proporcionally inversed to mineral grain size particles [18]. Clay Activity values higher than 27 meq/100g correspond to high chemical activity [17]. Clay fraction's chemical activity of a soil can be determined through:

$$Clay\ Activity\ \left(\frac{meq}{100g}\right) = \frac{CEC(\frac{meq}{100g}) \cdot 100}{Clay\ Fraction\ (\%)}$$

Equation 33

CEC is is determined by the ammonium acetate method buffered to pH 7, described in Houba (1995), besides, organic matter content was also determined, by the Walkley-Black method, described in Nelson and Sommers (1996).

3.3. pH

The measument of pH was done following ASTM standard [19], mainly used in agricultural and environmental sciences, it determines the degree of acidity or alkalinity in soils suspended in distilled water and/or 0.01M calcium chloride solution, for calcium chloride is because the calcium displace exchangeable aluminum, this pH is slightly lower that within distilled water. For both suspensions, pH measurement can be made with either a potentiometer using a pH sensitive electrode system, or pH sensitive paper, the potentiometer must be calibrated with buffer solutions of known pH. The pH is useful for understand the solubility of soil minerals and ions' mobility viabilizing soil-environment compatibility.

As it is not a main parameter for this work analysis, pH measurement was done only with distilled water, although using a potentiometer. For the procedure, the soil was air-dried and sieved through 2mm mesh opening, mesh nº10 (#10) and the water was prepared by distillation, then approximately 10g of soil is placed into a glass container and 10mL of distilled water added, mixed and left stand for 1h, the mixture must be in the laboratory temperature, among 15-25ºC. The calibrated and well cleaned potentiometer was introduced into the suspensions of the mixtures, and the temperature and pH measured when values stabilized. For distilled water mixtures, the within laboratory standard deviations are 0.031 pH units, so the tests were conducted with a minimum of 3 times respecting this deviation.

4. Mechanical Performance

4.1. Normal Proctor

Proctor developed a relation among the dry unit weight, water content, compaction energy, soil type, and gradation to analyze compaction and its effect on physical and engineering properties. Compaction is a process where energy load is applied over soil increasing density or weight of the specimen causing a volume decrease of samples. It can be affected due several reasons - type and nature of the soil as its granulometry, density and plasticity, the water content at compaction, weather, layer thickness and type of machine used in field compaction. An equation to calculate the compaction energy follows Equation 12.

The sample is compacted according to [20] standard using different water contents, water addition permits the lubrication of soil particles, dry density, or unit dry weight, have an important hole for engineering constructions to adequate the soil for the required earthwork design, and the results should be plotted as the dry unit weight versus water content, with a minimum of five tests performed. Zero void air curve (ZVAC) is a curve corresponding to a 100% of saturation (S = 1), only usefull when the estimated point of intersecction is a solid, while several materials behave as a non-Newtonian fluid, mostly liquid, ZVAC use this equation:

$$\gamma_{ZAV} = \frac{\gamma_w}{w + \frac{1}{G_s}}$$

Compaction curves must achieve a peak, an optimum value for γ_d and w, although some soils have more complicated curves, Lee and Suedkomp defined four types of curves according to soil characteristics, for the single optimum are for soils which w_L is between 30-70%, and irregular shapes are for soils with liquid limit outside this range, being very usual when working with clays like montmorillonite found other shapes for compaction curves.

Compaction quality and methods influence in several aspects of a liner, when well compacted, it increases density and strength and decreases permeability, showing their importance for this type of earthwork. The moisture content and compaction method affect hydraulic conductivity and shear strength. Design field density and compaction moiture content are based on laboratory tests, which use standard or modified compaction, standard is the most common for basis design since it yields ans optimum moisture higher than modified one, compaction curves are essential for practical and trustworthy analysis for filed compaction quality [11].

4.2. Expansibility

The expansibility of soils is a relevant geotechnical characteristic directly dependent of clayey minerals of the fine fraction, expansible soils show volumetric variation due to water content variation, divided in swelling, volume increase when absorbing water, or shrinkage, decrease the volume losing water. It can damage earthworks structures immediately after construction or slowly while consolidation occurs, and the soil is subjected to movement. Potentially expansive soils can be found where vulcanic ashes were deposited or tropical regions, like Mediterraneum, South Africa, the southern of North America, and the northern of South America.

The expansibility (S) is defined by the volume increase of fine portion of compacted soil when absorving water by cappilarity and free to expand vertically, expressed in percentage of initial volume. The procedure is based on LNEC specification E 200, the representative sample is sieved in mesh opening 0,425mm, mesh nº40 (#40), and dried in 60-65ºC for 24h, the dried sil is placed in expansibility equipment and compacted in two equal layers, the surplus soil is carefully shoveled and leveled with the surface of the mold, a perspex plate is placed on top and a deflectometer is supported for readings. The entire assembly is placed in a container and water is placed in this container up to the level of the upper face, and the initial reading is taken on the deflectrometer. Periodic readings are taken on a logarithmic scale up to at least an interval of 2 h, to plot an expansion curve between S and time, S is the reason between the sample height and the initial height (15mm). Tests were performed at least 3 times, the final value being the average of them.

According to ASTM standard D4829, the expansibility index (I_S) can be calculated with the expansibility (S), and the percentage of the soil which passed the mesh #40 (F), following the equation:

$$I_S = S * F$$

Equation 34

And the expansibility potential, classified through the Table 3 below:

Table 11. Expansibility classification

I_S (%)	**Expansibility**
<20	Very low
20-50	Low
50-90	Regular
90-130	High
>130	Very high

4.3. Oedometric Consolidation

Terzaghi formulated an equation, for the one-dimensional consolidation case, that relates the change in pore pressure (Δu), time (t), and the depth (z) of a soil element subjected to a stress (Δσ) uniformly distributed over an infinite area of soil, and presents the solutions of the consolidation equation by two dimensionless quantities, the time factor (T_v) and the average degree of consolidation (U_v) within consolidation coefficient (c_v), for practical terms, it is adopted for the end of the consolidation when T_v equals to 1 and the consolidation reaches 90%. Terzaghi's teory is described:

$$\frac{\partial u}{\partial t} = c_v * \frac{\partial^2 u}{\partial z^2}$$

Equation 35

$$T_v = \frac{c_v * t}{d^2}$$

Equation 36

$$U_v = \frac{\Delta h(t)}{\Delta h_{last}}$$

Equation 37

$$T_v = 1 \leftrightarrow U_v = 90\% \rightarrow end\ of\ consolidation$$

Equation 38

Looking to determine the consolidation coefficient, two traditional methods are used, Taylor and Casagrande, to predict the speed at which the soil settles. Taylor method uses the square root of time on the x-axis to fit a tangent line, obtaining degrees of consolidation 0 and 90%. The Casagrande Method, on the other hand, plot time in logarithm scale, and uses an extension of the instantaneous consolidation part to obtain 0%, and two tangent lines, one in the primary consolidation and another in the secondary consolidation, where the intersection between them is the 100% point. Both methods seek to obtain the equivalent of 50% of the consolidation and its respective time.

Oedometric method through EN ISO 17892-5 used a specimen diameter:height (D:H) of 2.75 or greater mitigates ring friction, the used in this work respect ir with 63:20 (mm) of D:H relationship, with a fixed-ring, over a load increment following:

$$\frac{\Delta\sigma}{\sigma} \cong 1$$

Equation 39

During consolidation, the water flows upward at a certain rate, and following Darcy's law, it is possible to obtain permeability indirectly from oedometer, through coefficient of compressibility (a_v), coefficient of volume compressibility (m_v), and c_v, with:

$$a_v = m_v \cdot (1 + e)$$

Equation 40

$$k = c_v \cdot m_v \cdot \gamma_w$$

Equation 41

Compression index (Cc) can be estimated for inorganic soils with liquid limit less the 100% and for organic soils, respectively for:

$$C_C = 0.009 \cdot (W_L - 10)$$

Equation 42

$$C_C = 0.0115 \cdot w$$

Equation 43

Also, [21] established other relation for liquid limit and compression index:

$$C_C = 0.9 + 0.0105 \cdot W_L$$

Equation 44

Most clays have shown Cc values less than 1, and typically less than 0.5.

4.4. Consolidated Undrained Triaxial

Coulomb and Mohr strength theory express shear strength (τ_f) in terms of cohesion (c) and friction angle (φ) and utilizing Terzaghi concept of effective stress, parameters c' and φ' can be determined from triaxial tests. Triaxial tests consist in a cylindrical specimen enclosed in flexible membranes between a loading cap and a pedestal for drainage and axial load, this enclosed into a water pressure chamber. The load is applied in two stages, in the first, the water in the chamber confines the specimen and the second is applied axial load from a constant rate press. Theoretically, triaxial should apply three stresses, one for each axis, although in practice using cylindrical samples, there is an axial symetricallity resulting in $\sigma_1 \geq \sigma_2 = \sigma_3$, the major and axial stress being σ_1 and the fluid pressure from the cell being $\sigma_2 = \sigma_3$. Consolidated undrained assembly must not allow drainage during application of deviator stress.

For liner simulation, consolidated undrained (CU) triacial tests were performed through EN ISO 17892-9, the first stage is saturation and consolidation, where the specimen wets and consolidate at confining pressure (σ_c') and in the second stage, when drainage is not permitted but pore pressure may be measured. Different pressures are applied called deviator stress (σ_d), at least three, to generate a Mohr-

Coulomb line or determine the effective stress path due parameterizations with σ_3'= σ_c' and σ_1'= σ_c'+ σ_d, along with:

$$t = t' = \frac{\sigma_1{}' - \sigma_3{}'}{2}$$

Equation 45

$$s = \frac{\sigma_1 \ + \sigma_3}{2}$$

Equation 46

$$s' = \frac{\sigma_1' + \sigma_3{}'}{2}$$

Equation 47

The value of the effective angle of shearing resistance (φ') using the slope angle of the failure line to the horizontal s' axis (a'), and cohesion (c') based on the intersection with vertical t' axis (α') are following:

$$\sin\varphi' = \tan\alpha'$$

$$c' = \frac{a'}{\cos\varphi'}$$

According to [6], cohesion and friction angles can be estimated for normally consolidated plastic soils, respectively by:

$$c' = \frac{0.10 + 0.004 \cdot PI}{\sigma_V{}'}$$

Equation 48

$$\varphi' = \begin{cases} 36° - 0.25 \cdot PI \\ 31° - 0.20 \cdot (PI - 20), \\ 25° - 0.06 \cdot PI - 50) \end{cases} \begin{cases} PI < 20 \\ 20 < PI < 50 \\ 50 < PI < 100 \end{cases}$$

Equation 49

5. Hydraulic Conductivity

Laboratory tests through EN ISO 17892-11 fallling head permeability were performed, the procedure consists in a permeameter which can be measure from upward or downward through the soil, however, downward flow can transport fines and occurring clogging of the sample. The sample to be studied is inserted into a measured cylinder with a cross section (A) and specimen height (L), this cylinder is connected through tubes to another graduated cylinder with a cross section (a) that contains water to a certain level. At a certain initial moment (t_1), there is a certain hydraulic load

according to the height (h_1), at another moment (t2) there is another hydraulic load (h2). Hydraulic conductivity (k) is calculated through Equation 20 or Equation 21, and classified according to Graphic 4.

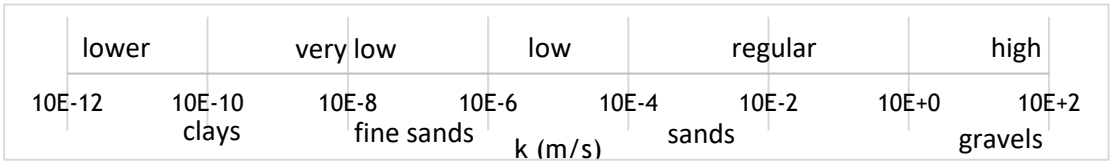

Graphic 4. Permeability range

6. In situ Tests

6.1. Compaction Degree

Gammadensimeter

The gamadensimeter is a Troxler 3440, an equipment which measure the density and water content, with these characteristics it can obtain the compaction degree of soils, rocks, and asphalt mixtures poured by layers. The equipment used operates in two modes, backscattering where the source rod is retracted in the meter, and in direct transmission mode, with the rod to the desired depth, resulting in gamma radiation. Both methods apply such radiation that they collide with the electrons in the ground, so, in summary, the greater the number of collisions, the lower the density of the material. Backscatter mode is deprecated for surfaces, direct transmission mode for deeper measurements.

Troxler 3440 methodology follows the recommendation by producer, first it is needed to make a calibration procedure, automatically, then it is introduced data from the laboratorial compaction tests, the Normal Proctor, the surface is properly leveled, with the help of a hammer and spike, drilled and inserted the rod to a depth of 30 cm, making sure that this depth is inserted in the device. After this preparation, it was measured by gamma radiation during 1min, and the data was saved, be sure to stay away from the device while readings are taken as radiation is harmful to health.

Soil Density Gauge

Soil Density Gauge (SDG) 200 is a Transtech Systems equipment, which uses electromagnetic method to measure soil density, based on electricity and magnetic principles, locating magnetic fields, and transforming in volumic weight and water content. It uses electrical impedance spectroscopy (EIS) measurements which make it possible to distinguish the influence of density and humidity against magnetic waves,

the degree of compaction is calculated by the response of the SDG detection field to EIS variations in the soil matrix. As the dielectric constant of air is much lower than that of the soil components, as the density/compaction increases, the combined dielectric also increases, as the percentage of air in the soil decreases. For reliable values, it is necessary to enter data on particle size, plasticity, and laboratory compaction using Proctor. The equipment's instruction manual advises to take as a reference, values of degree of compaction from other tests such as sand bottle or gamma densimeter, from this value, carry out 3-5 measurements with the SDG, the average values of these measurements will be the value of deviation to be used, if the deviation value is less than the reference value, it will have a positive deviation, otherwise, a negative deviation. In addition, if the values are very different from the reference, it may happen that the soil has some anomaly.

The procedure of the SDG200 is like the Troxler's, the device is automatically calibrated in the properly leveled measurement place, reaching calibration parameters A and B indicated by the reader, the index and laboratory properties of the soil are also inserted into the specifications. From the material, a new project is started, and measurements are taken at 5 points during the time necessary for each point to be read and following the location shown on the reader, with that, results are obtained and recorded in the project storage.

6.2. Drilling Tests

Many types of drilling tests are utilized for geotechnical and civil works around the world, the choice between them is related to several reasons, economic, resources, logistic, access, labor, type of the soil, and subsoil, among others. Dynamic penetration tests are divided in four, the dynamic penetration lightweight (DPL), medium weight (DPM), heavyweight (DPH), and super heavyweight (DPSH), they differ mainly with the weight of the pile, the height which the pile is released, and the characteristics of the penetration rod. Standard penetration test (SPT) and cone penetration test (CPT) are other usual boring tests used worldwide.

Such tests are coincident, except for one or the other case due to the heterogeneity of the massif. Several authors related the parameter for those abovementioned tests, and it varied according to the type of soil and the subsoil, some of them were summarized by [1] in:

- $\frac{N_{SPT}}{N_{DPSH}^{20}} \cong 2.00$, for residual granitic soils from the same region fo this work

- $1.50 > \frac{N_{SPT}}{N_{DPSH}^{30}} > 0.80$, for coarse-grained granite stones
- $\frac{N_{SPT}}{N_{DPSH}^{30}} \cong 1.40$, for residual soils from the studied region
- $\frac{N_{SPT}}{N_{DPSH}^{30}} \cong 1.15$, for sands, silty sands and silty clays
- $1.05 > \frac{N_{SPT}}{N_{DPSH}^{30}} > 1.00$, for sands, fine sands and gravels
- $\frac{N_{SPT}}{N_{DPSH}^{30}} \cong 0.57$, for fluvo-glacier terrain
- $\frac{N_{SPT}}{N_{DPSH}^{30}} \cong 0.50$, for a fluvio-lacustrine sand deposit with silt and gravel lenticules

SPT is conducted with a penetration procedure by dropping a 63.5kg mass from 75cm, and recording the blow counting for every 15cm, reported as penetration resistance (N_{SPT}), until the blow counting exceeds 100 or in the presence of rocks. CPT is conducted pushing a standard cone within a rate of 1-2 m/min into the soil, either mechanically or electrically, the cone has 60º and 3.6cm of diameter projecting an area of 10cm^2, and it is measured the point resistance (q_C), this test is related to undrained shear strength. Relations between SPT and CPT are very common, fluctuating around 2-6 for $\frac{q_c}{N_{SPT}}$.

Dinamic Penetration Lightweigh (DPL) and Superheavyweight (DPSH)

Dinamic penatrarion is a simple test that consists of penetrating a rod blowing a weight pile and counting the number of blows to penetrate 10 cm into compacted soil. It is possible to obtain a profile of the soil tip resistance with 10 to 10cm precision, in addition to correlating such values of DPL with DPSH, consequently with CPT and SPT. The advantage of DPL is that it is easy to perform and determine soil strengths without damaging the earthwork. The DPL versus DPSH specification is in Table 12.

Table 12. DPL x DPSH specifications

Specification	DPL	DPSH
Cone diameter	0.03 m	0.05 m
Rod diameter	0.02 m	0.03 m
Pile weight	10.0 kgf	63.5 kgf
Rod weight	2.0 kgf/m	3.0 kgf/m

6.3. Plate Load Test

Adapted from DIN 18134 (2012), the *in-situ* plate load test basically consists of loading a steel plate placed at the level where the actual load is to be applied and recording the deformation (settlement) corresponding to successive load increments. Plate load test were conducted after finishing the embankment construction to verify quality and consolidation ratios, devices were used for measuring the load applied and the settlement of the loading plate at right angles to the loaded surfaces.

Within deformation versus load curve, it is determined the strain modulus (E_V) and the modulus of subgrade reaction (k_S), parameters with the same importance as compressibility coeffient and pre-consolidation stress have for one-dimension consolidation tests. They follow:

$$E_V = 1.5 \cdot r \cdot \frac{1}{a_1 + a_2 \cdot \sigma_{0,max}}$$

Equation 50

$$k_S = \frac{\sigma_0}{s^*} = \frac{\sigma_0}{0.00125}$$

Equation 51

Where r the radius of the plate in mm, a_1 and a_2 coefficients from second-degree polynomial of deformation x tension curve, $\sigma_{0,max}$ from the first load cycle.

Chapter 3 development used [16], [20], [92], [156]–[190] references in addition to those abovementioned.

Chapter 4 – Results and Discussion

The results exposed were done by three authors, the author of this work Leonardo Marchiori (2022), a doctorate student of Civil Engineering at University of Beira Interior (UBI), Filipe Nunes (2017), and a master's in civil engineering at University of Beira Interior (UBI), Marta Lopes (2012); following the scheme below:

Table 13. Tests scheme by authors

Test	Marchiori (2022)	Nunes (2017)	Lopes (2012)
Specific gravity	✓		
Consistency limits	✓		
Normal Proctor	✓	✓	✓
Granulometry	✓	✓	✓
XRD	✓		
XRF	✓		
SEM	✓		
pH	✓		
CEC	✓		
Expansibility	✓		
Oedometer	✓		
Plate Load Test		✓	
Triaxial	✓		
Permeability	✓		
DPL	✓		
DPSH		✓	
CPT		✓	
SDG			✓
Troxler			✓

And the representation and location of the tested points of the embankment in Figure 18.

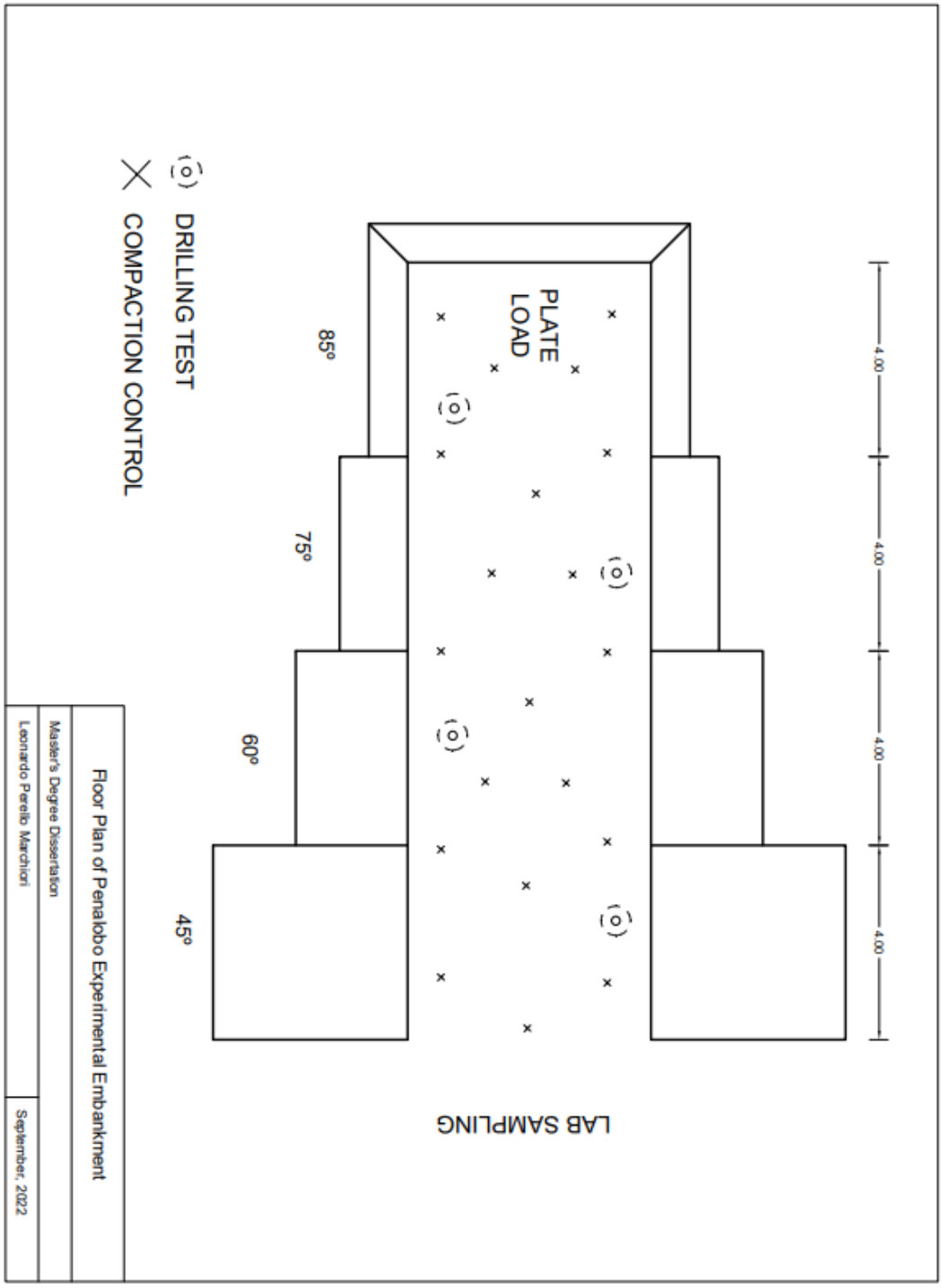

Figure 18. Embankment and tested points

1. Geotechnical Characterization

1.1. Specific Gravity

A JuneX heater, a Heidolph RZR1 mixed and a Memmert oven were used in several tests for heating, mixing, and drying purpose. Specific gravity tests were performed several times, showing results around 2.5-2.6, averaging 2.55. Those values are below

of Quartz (2.65), mostly explained due to high amounts of aluminum and silica. Figure 19 shows the used pycnometer for G_S test.

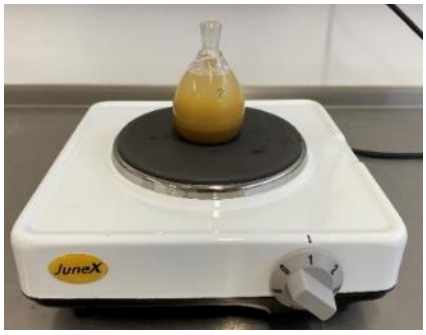

Figure 19. Specific gravity test

1.2. Consistency Limits

Following standard [16], the liquid limit is 28% based on graphic of Casagrande shell by ELE (Figure 20) results in Graphic 5.

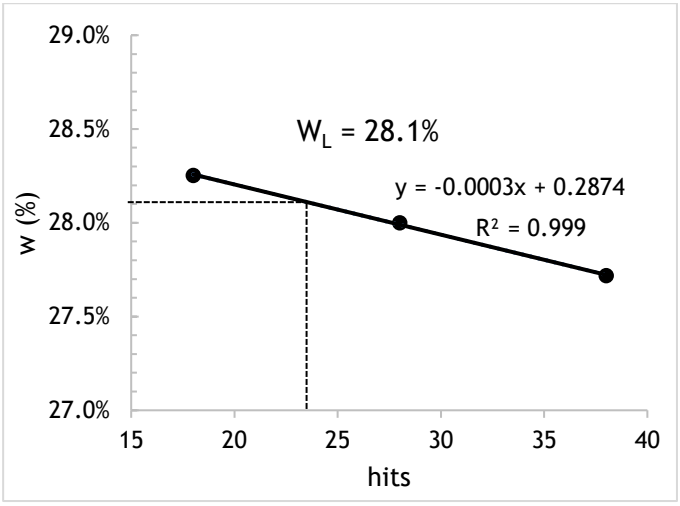

Graphic 5. Liquid limit results

Figure 20. Casagrande shell

Plastic limit was not able to perform because of non-plastic (NP) behavior of the soil.

1.1. Normal Proctor

Compaction curve is exposed in Graphic 6 when using a Normal Proctor compaction mold by UTEST model UTS-0600E, in addition, author's curve in comparison with other studies in the same site are in Graphic 7. It seems to have a tendency over time that compaction curve gets down along saturation curve, becoming a finer material, this can be explained by surface erodibility due to physical and chemical processes.

For example, Marta Lopes (2012) found optimum compaction was reached with 7.0% of water content (w) and almost 2.10 g/cm^3 of dry density, therefore in 2022, author's

values of w doubled to 14% and the dry density decreased to 1.86 g/cm^3, and in between Filipe Nunes (2017) found 8.0% and 2.0 g/cm^3 of w and density, respectively.

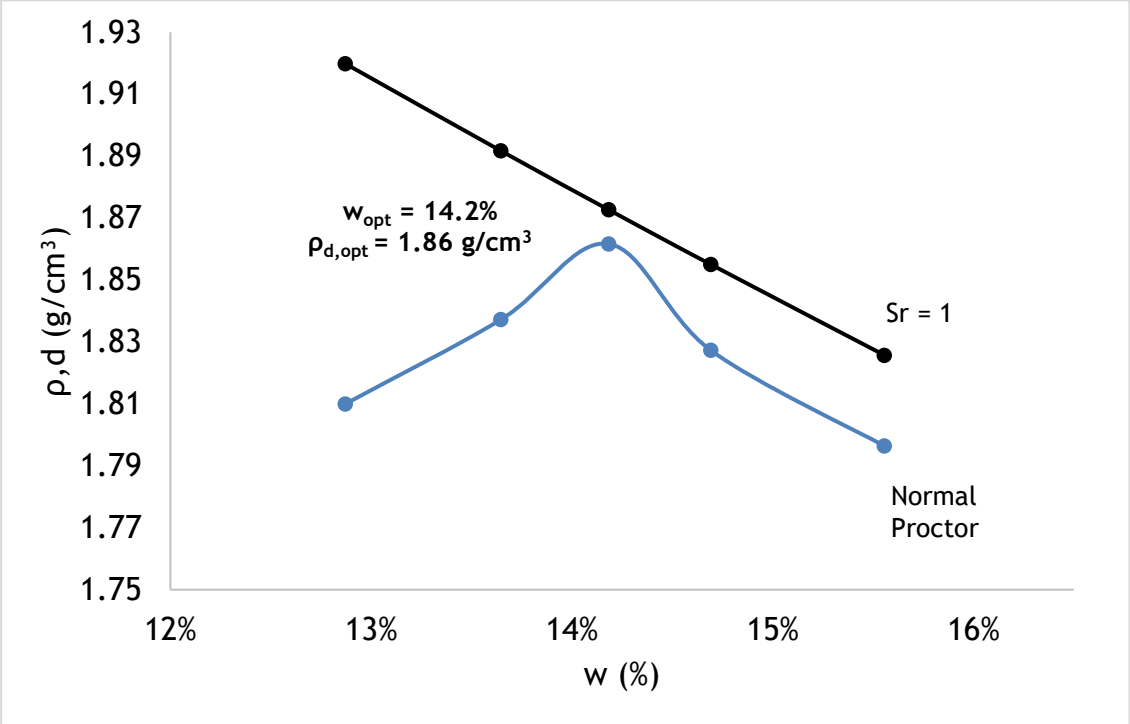

Graphic 6. Compaction curve

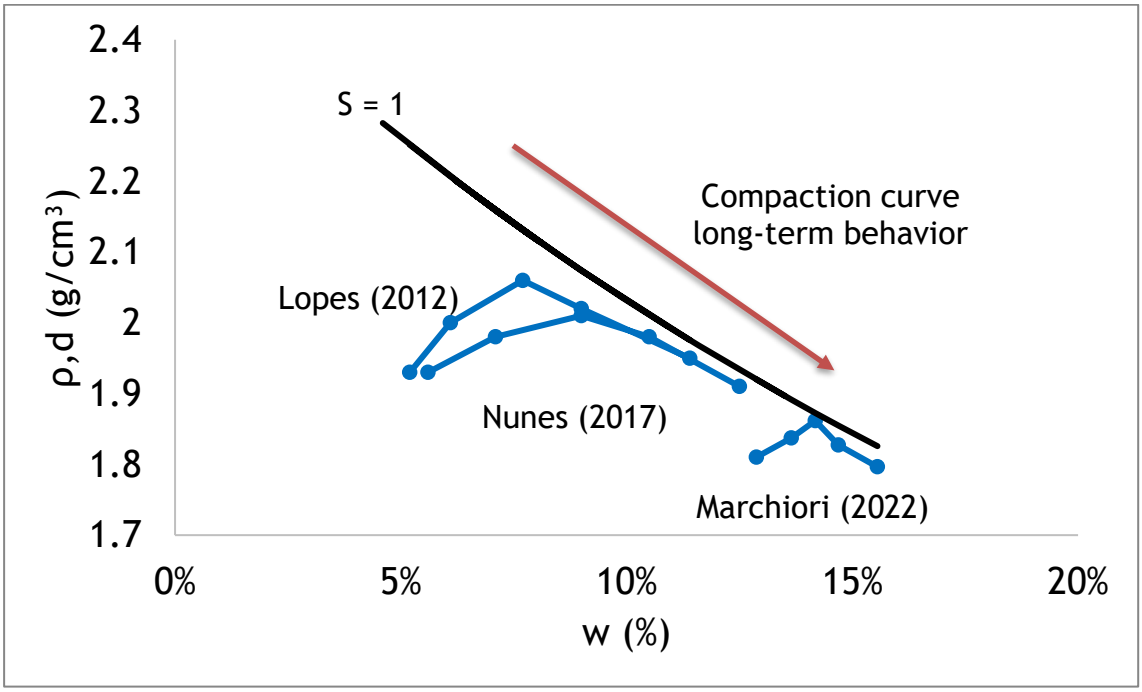

Graphic 7. Compaction curves comparison

1.2. Granulometric Distribution

Particle size distribution is showed in Graphic 8. Sieve analyzis were done until 0.075mm mesh by Retch, for the finer portion, Coulter LS200 laser was used.

Table 14 summarizes granulometric and geotechnical parameters. The granulometry parameter are the ratio among clay and silt, sand, and gravel percentages, nominal diameters of 10, 30, 50, 60, and 90% of size distribution, its uniformity coefficient (C_u) and distribution coefficient (C_d), the specific surface are (SS) calculated using D_{50}, and the classifications according to USCS and AASHTO. Geotechnical values are in accordance with specific gravity (G_S), plasticity limits and index, and Normal Proctor optimal compaction values.

Table 14. Geotechnical parameters

Parameter	Author (2022)	Nunes (2017)	Lopes (2012)
Granulometry			
Gravel	16%	13%	11%
Sand	64%	74%	80%
Clay and Silt	20%	13%	9%
D_{10}	0.01 mm	0.07 mm	0.08 mm
D_{30}	0.25 mm	0.30 mm	0.32 mm
D_{50}	1.10 mm	1.10 mm	1.00 mm
D_{60}	1.80 mm	1.70 mm	1.64 mm
D_{90}	7.00 mm	7.00 mm	7.00 mm
C_u	7.2	5.7	5.1
C_d	3.5	0.8	0.8
SS	5.0 mm^2/g	5.0 mm^2/g	5.6 mm^2/g
USCS	SW	SW	SW
AASHTO	A-1-b	A-1-b	A-1-b
Geotechnical			
G_s	2.5-2.6	-	-
W_L	28.1	-	-
W_P	NP	-	-
PI	NP	-	-
W_{opt}	14.0%	8.1%	7.6%
$\gamma_{d,max}$	18.3 kN/m^2	20.0 kN/m^2	20.2 kN/m^2

Following those results for the author, and according to Equation 1, Equation 18, Equation 31, Equation 34, Equation 42, Equation 43, and Equation 44:

$$h_c = \frac{1.50}{D_{10}} = \frac{1.50}{0.01} = 15000\ mm$$

$$k = D_{10}^2 \cdot 10^{-2} = 0.01^2 \cdot 10^{-2} = 10^{-6}\frac{m}{s} \rightarrow low\ to\ very\ low\ permeability$$

$$A_C = \frac{CEC}{Clay\%} = \frac{17.0}{1.0} = 17.0 \rightarrow inactive\ clay\ activity$$

$$C_C = 0.009 \cdot (w_L - 10) = 0.009 \cdot (28 - 10) = 0.162$$
$$C_C = 0.9 \cdot (0.0105 \cdot w_L) = 0.9 \cdot (0.0105 * 28) = 0.265 \rightarrow low\ compressibility$$
$$C_C = 0.0115 \cdot w = 0.0115 \cdot 14 = 0.161$$

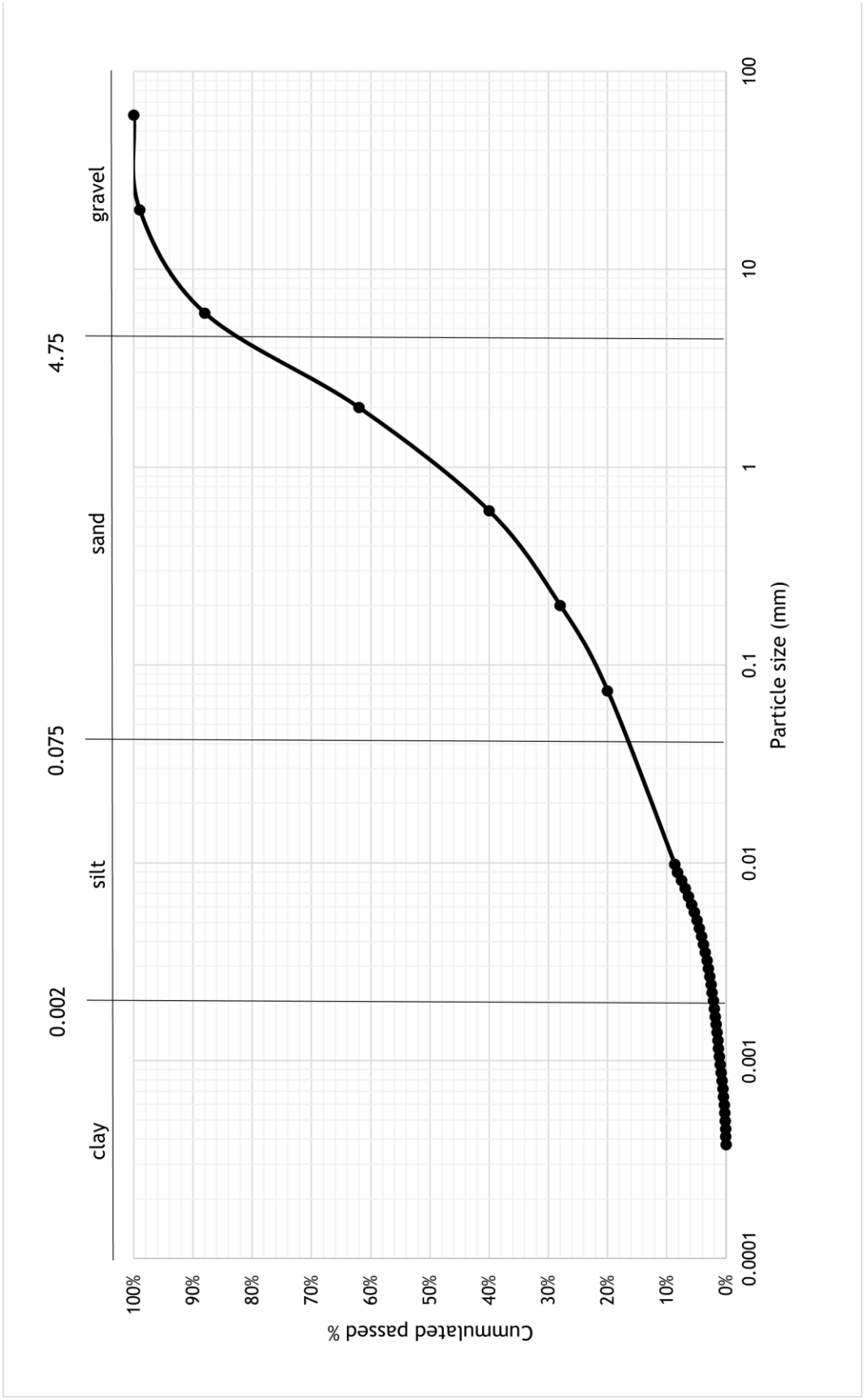

Graphic 8. Particle size distribution

2. Chemical Composition

Table 15 shows the percentages of each oxide and each element found in the soil composition. Typical results for region soils, high amounts of silica and aluminum, with lower percentages of iron and sodium oxides.

Results in distilled water showed pH = 6.0, typical to granitic soils. The soil had CEC = 17.0 meq/100g, characterized as medium CEC consequently having medium clay activity percentage.

Table 15. Oxides and Elemental composition

Oxides	Na_2O	MgO	Al_2O_3	SiO_2	K_2O	CaO	Cr_2O_3	Fe_2O_3
%	3.77	0.99	31.75	54.26	4.28	1.11	0.29	3.55

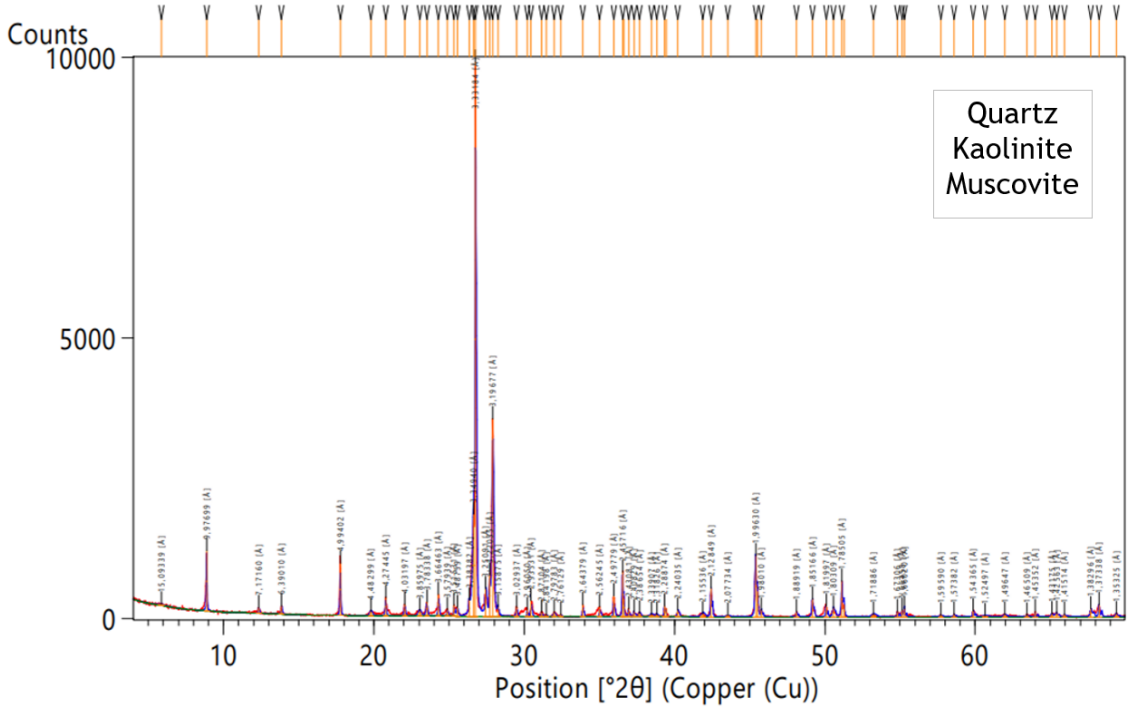

According to x-ray diffractures, the main minalogy is composed by quartz, kaolinite, and muscovite, corroborating with other studies in the region of Guarda [1].

Scanning Electron Microscopy (SEM) images for the soil are presented in two magnifications, 200x and 300x, for comparison and microscopic grain size analysis, exposed below. The grain size is very heterogeneous corroborating with the particle size distribution. Figure 21 to Figure 24 show in a microscopic scale grain of 1-100 μm representing the extensive granulometry of the samples.

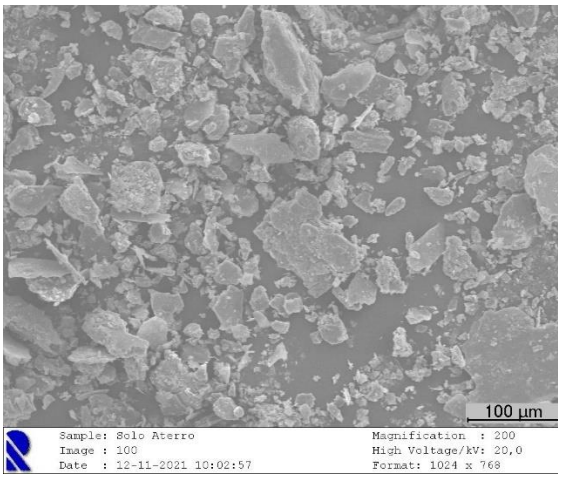

Figure 21. SEM 1 magnification 200x

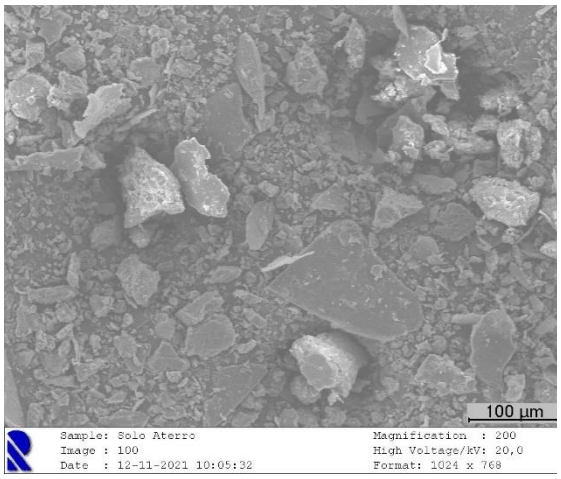

Figure 22. SEM 2 magnification 200x

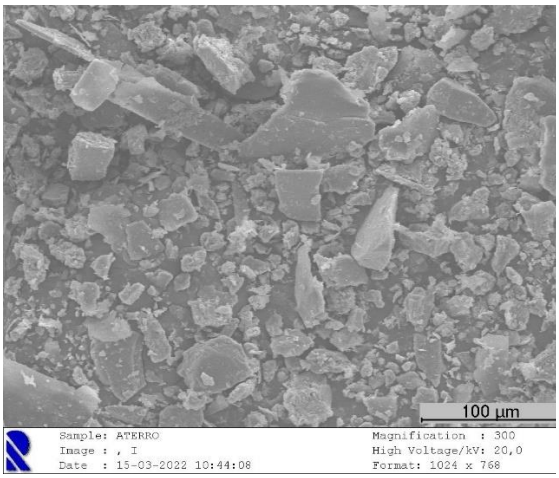

Figure 23. SEM 1 magnification 300x

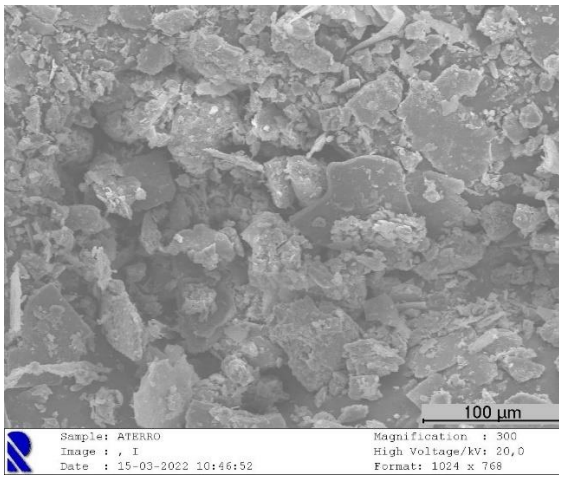

Figure 24. SEM 2 magnification 300x

3. Mechanical and Hydraulic Performance

3.1. Expansibility

Expansibility tests were performed 3 times using manual extensometers by Baty with 0.01mm precision, and the results are in Graphic 9, being the medium value found was:

$$S = 7.0\%$$

Resulting in:

$$I_S = 140$$

Having a very high free expansibility.

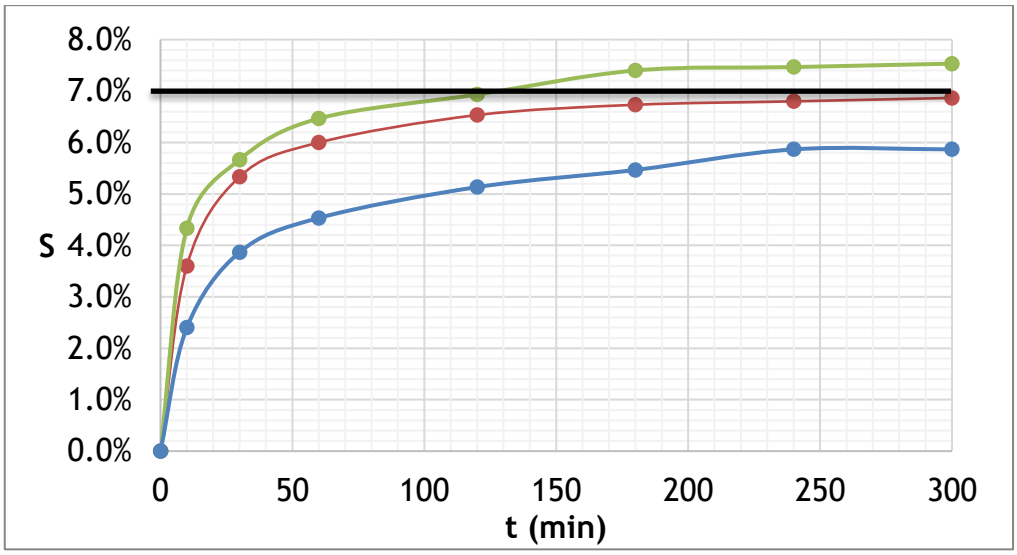

Graphic 9. Free expansibility curves

3.2. Oedometer

One-dimensional consolidation through oedometric cells were performed 3 times only using 1 stage of load and 1 of unload – called by oedometer, according to Graphic 10 and Table 16. Other round of tests was done to compare to plate load test, than was performed 3 load-unload stages – called oedometer stages, following Table 17. Table 18 and Table 19 summarize consolidation parameters due to loads and unloads for oedometer and oedometer stages tests, respectively. Figure 25 and Figure 26 show the used oedometric equipment by ELE with a data logger by VJ Tech with 0.001mm precision for automatic transducer by MPE model, and 1 sample after tested, respectively.

Initial void index (e) of the samples were always around 30-40%, in consequence of it, results are shown parametrizing e/e_0 and tensions in logarythim scale. Results were consistent with related soils from the same region. C_C lower than 0.100 characterize samples as a low compressible soil. Corroborating with Terzaghi consolidation theory, the average for the coefficients c_V and C_{SEC} increased with load increment, although the indirect k decreased.

Figure 25. 1D-Consolidation apparatus

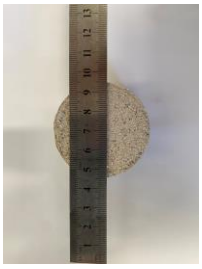

Figure 26. Oedometer sample

Table 16. Oedometric load-unload

Stage	kPa
Load 1	1
	30
	60
	120
	250
	500
	1000
Unload 1	1000
	250
	1

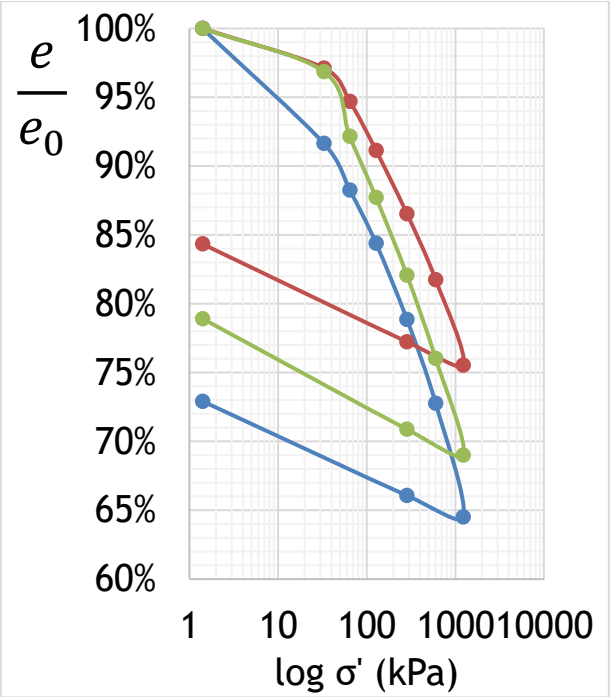

Graphic 10. Oedometric curves

Table 17. Oedometric stages load-unload

Stage	kPa
Load 1	1
	25
	50
	75
	125
	250
Unload 1	250
	75
	25
Load 2	75
	250
	500
	1000
Unload 2	250
	25
Load 3	250
	1000
	2000
Unload 3	1

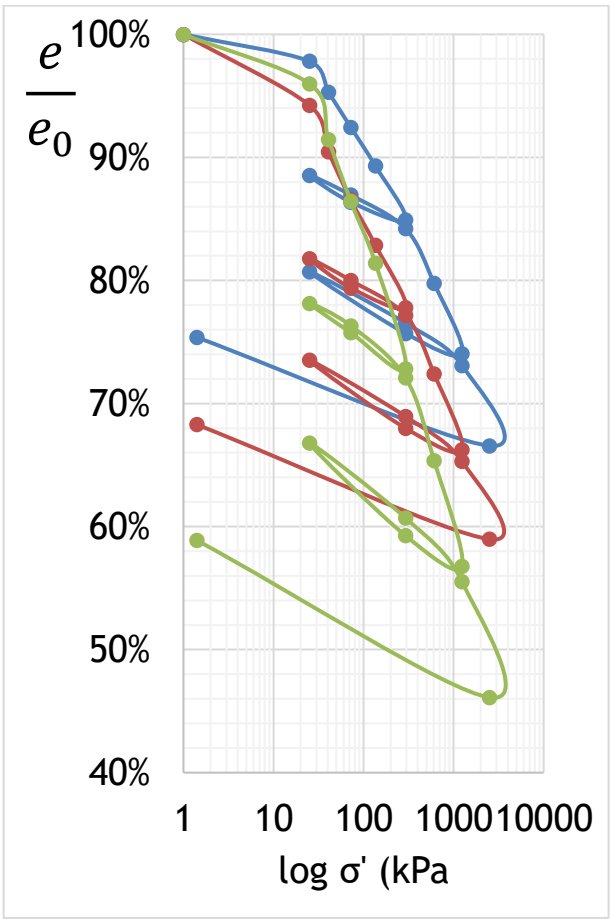

Graphic 10. Oedometric curves stages

Table 18. Oedometer consolidation parameters

Oedometer			σ (kPa)	c_V (m^2/ano)	C_{sec} (-)	k (m/s)
			30	99-496	0.0056-0.0110	1.17E-08 - 6.87E-09
			60	111-239	0.0058-0.0085	1.60E-08 - 6.69E-09
Compression	C_C	0.047-0.051	120	109-201	0.0053-0.0181	5.43E-09 - 8.96E-09
Recompression	C_R	0.006-0.130	250	107-400	0.0110-0.0130	1.45E-08 - 6.92E-09
Swelling	C_S	0.007-0.009	500	127-500	0.0070-0.0405	1.78E-09 - 9.44E-09
Pre-tension	σ'_{vm}	30 kPa	1000	20-134	0.0170-0.0180	2.65E-10 - 6.35E-10

Table 19. Oedometer Stages consolidation parameters

Oedometer Stages			σ (kPa)	c_V (m^2/ano)	C_{sec} (-)	k (m/s)
			25	83-207	0.0160-0.0240	3.48E-08 – 9.37E-09
			50	122-164	0.0066-0.0100	1.93E-08 - 2.71E-08
			75	132-202	0.0070-0.0105	1.15E-08 - 1.44E-08
			125	117-240	0.0050-0.0067	5.69E-09 - 8.93E-09
Compression	C_C	0.037-0.058	250	29-128	0.0101-0.0151	1.10E-09 - 2.95E-09
Recompression	C_R	0.005-0.013	500	111-193	0.0158-0.0160	1.37E-09 - 2.08E-09
Swelling	C_S	0.010-0.075	1000	15-129	0.0126-0.0148	1.48E-10 - 9.12E-10
Pre-tension	σ'_{vm}	30 kPa	2000	23-75	0.0081-0.0285	1.07E-10 - 9.55E-11

3.3. Plate Load Test

Used plates were squared (0.5 x 0.5m), although to compare with usual tests, it was considered a circular shape, therefore the diameter of each plate used is 0.5 m, resulting in an area of 0.20 m^2, they were placed in the end of the embankment. Each of them weighting 30 kN, resulting in 150 kN/m^2. While the plates were placed in the embankment, 3 deflectometers were reading the deformation and generated the results in Graphic 11. Deflectometers position, slope's topographic targets, and plate load view are exposed in Figure 27, Figure 28 and Figure 29, respectively.

All loose material was removed and the surface which received the loading plate was levelled, and the plate was in full contact with the surface, in place of a hydraulic jack, a pile of plates was used. Settlements were measured by displacement transducer protected from sunlight and wind.

Figure 27. Plate load deflectometers

Figure 28. Slope targets

Figure 29. Plate load test

The second-degree polynomial equation which describes settlement over tension is:

$$s = 1.2253 + 0.0063 \cdot \sigma_0 + 0.000003 \cdot \sigma_0^2$$

Equation 52

Thus, using Equation 50 and Equation 51:

$$E_V = 1.5 \cdot r \cdot \frac{1}{a_1 + a_2 \cdot \sigma_{0,max}} = 1.5 \cdot 500 \cdot \frac{1}{0.0063 + 0.000003 \cdot 500} = 96154\ mm/kPa$$

$$k_S = \frac{\sigma_0}{s^*} = \frac{150}{0.00125} = 120000\ kPa/mm = 120000\ MN/m^3$$

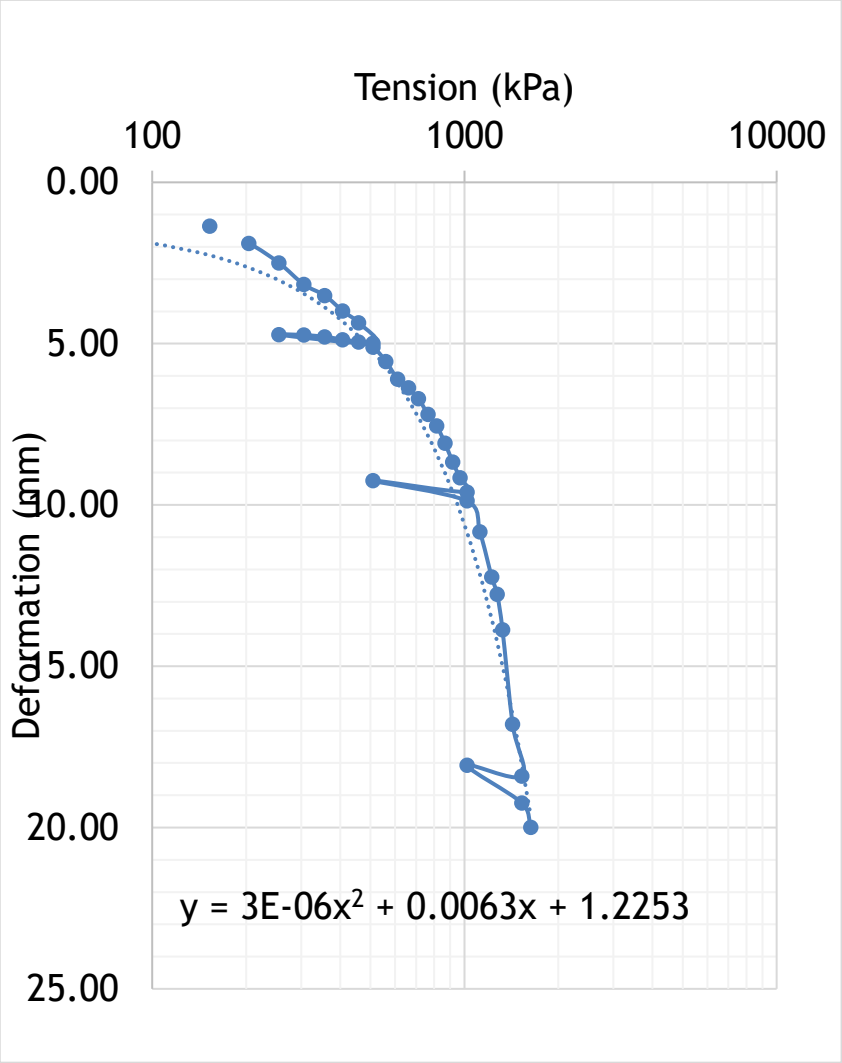

Graphic 11. Tension x deformation plate load test

3.4. Triaxial

Consolidated undrained (CU) triaxial shear test () were performed 5 times using differente confining tensions (σ_c), 50-100-200-300-500 kPa. The soil has no cohesion (c'=0), typical to sandy soil, and has a regular effective internal friction angle (φ') of 35°. Triaxial apparatus are GDSLab, and the water deaerator as well, the hydraulic press used for shearing is a Wykeham Farrance 50.

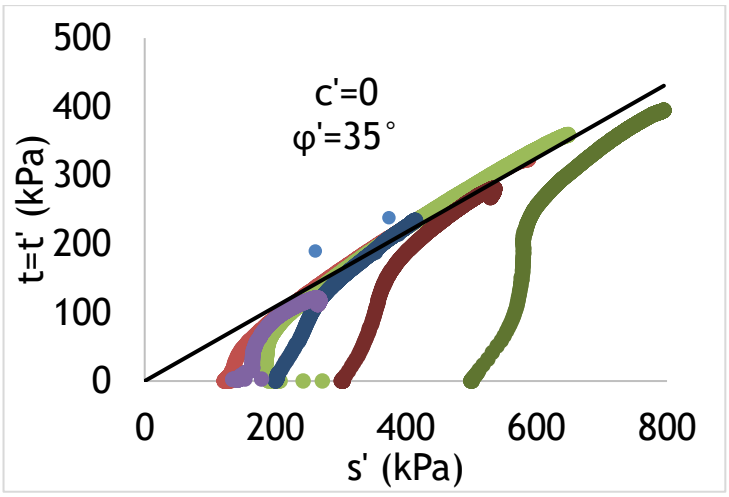

Graphic 12. CU triaxial stress paths

Figure 30. Triaxial test

3.5. Hydraulic Conductivity

Falling head permeability tests were performed during time, and after stabilization of hydraulic conductivity (k) values the average of results achieved 8 x 10^{-8} m/s, also a relationship with time was calculated, although being a regular relation within R^2 = 0.5, estimating k with time (t) in seconds according to:

$$k\,(t) = 8 \cdot 10^{-8} + (3 \cdot 10^{-13} \cdot t)$$

Characterizing as a low permeability soil.

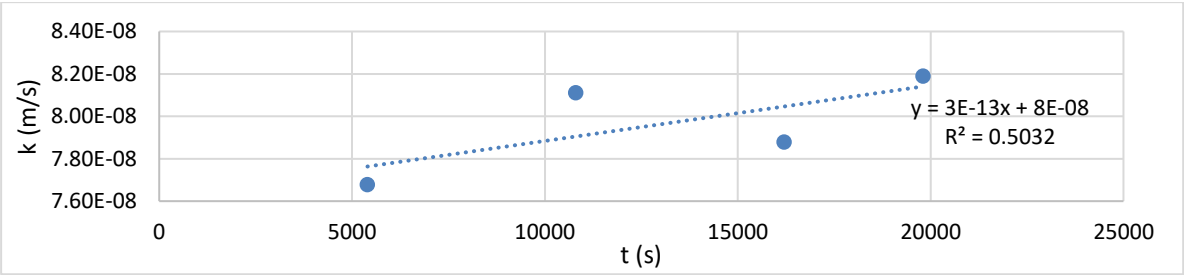

Graphic 13. Permeability during time

4. Drilling Tests

4.1. Dynamic Penetration Lightweight

Dynamic penetration lightweight (DPL) tests were performed for 4 points in the embankment, generating the following soil profile, literature's correlations around DPL and SPT were done, using N,DPL = 0.6 N,SPT. Figure 31 and Figure 32 show the author performing DPL tests and extruding samples for laboratorial analysis, respectively.

Figure 31. DPL test

Figure 32. Sampling extrudor

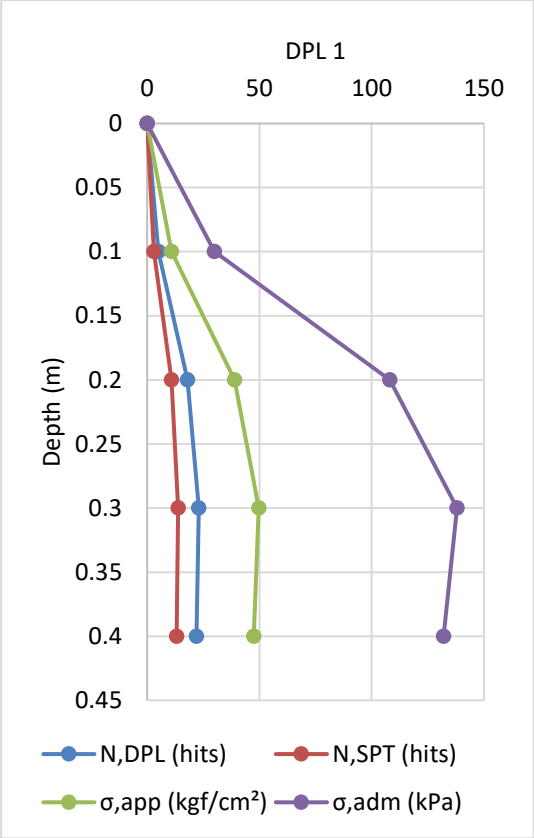

Graphic 14. DPL1

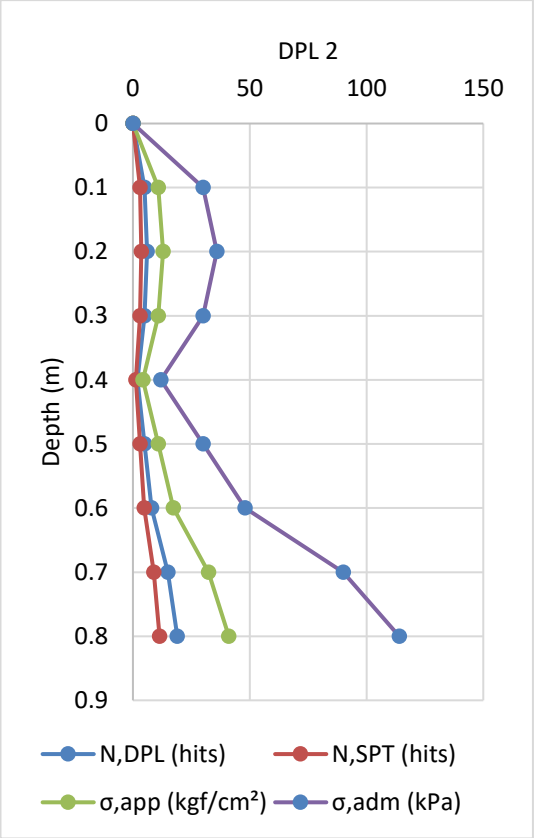

Graphic 15. DPL2

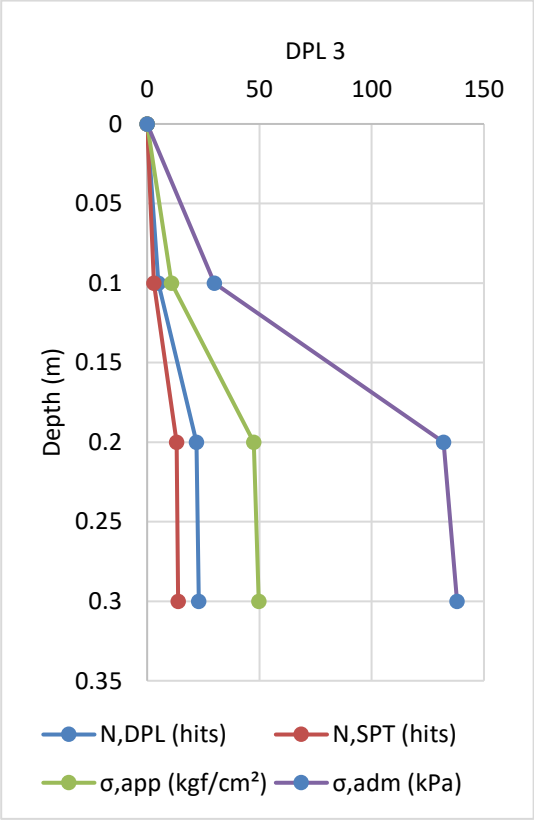

Graphic 16. DPL3

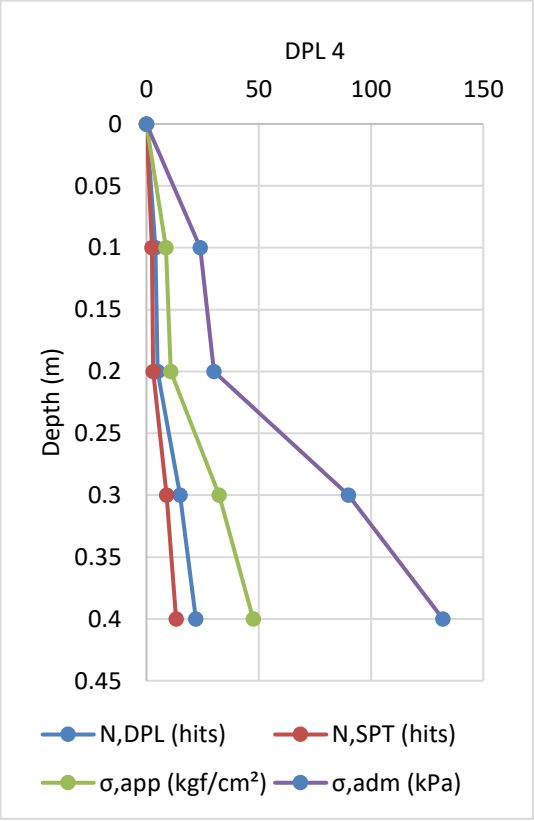

Graphic 17. DPL4

4.2. Dynamic Penetration Super-heavyweigth

Dynamic penetration super-heavyweight (DPSH) tests were performed for 8 points in the embankment, generating the following soil profile. Compaction degree results for 30cm layers during DPSH are shown, tests were performed until 5-7 m when it was too difficult to penetrate. DPSH tests were performed by doctoral student Filipe Nunes.

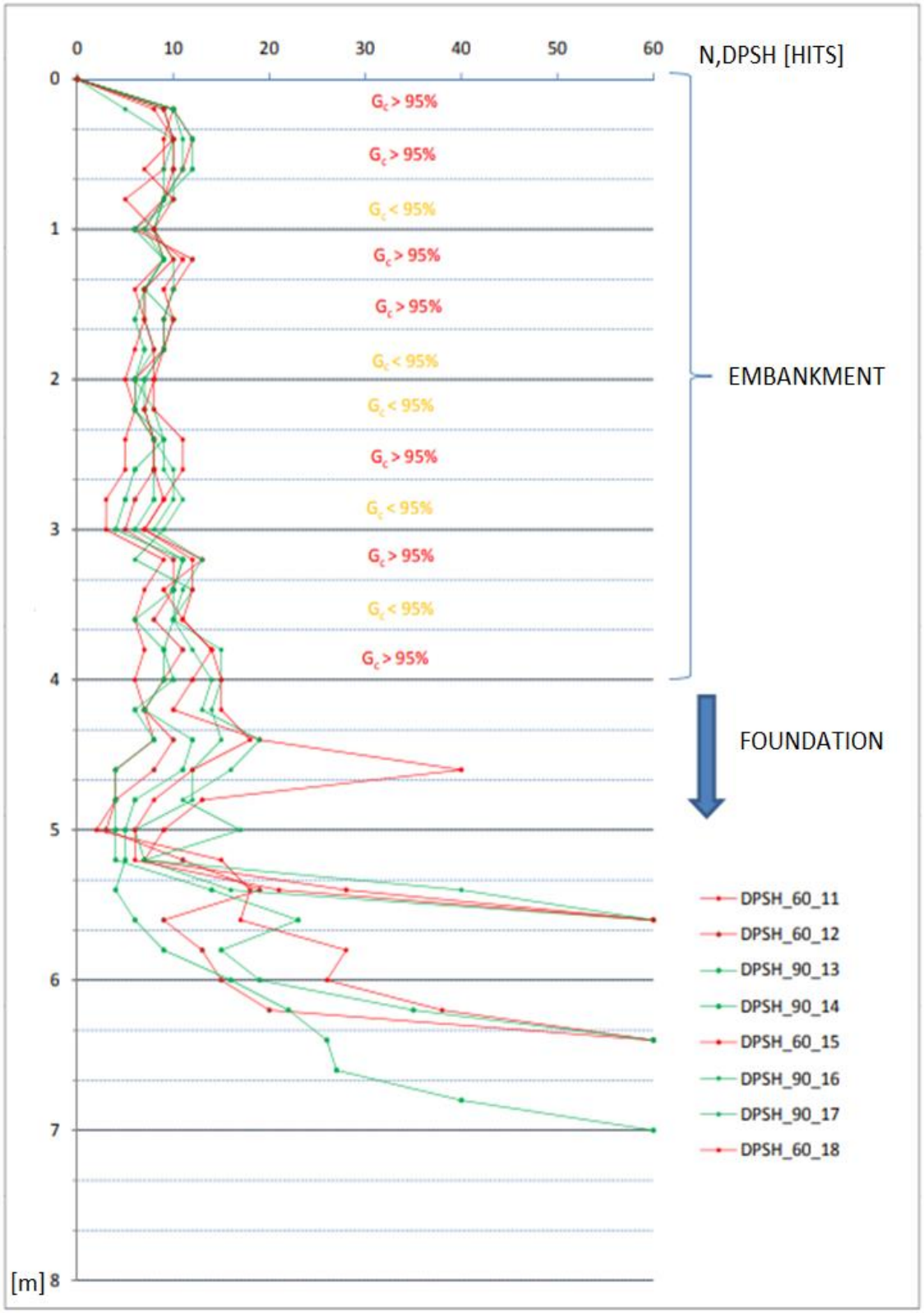

4.3. Cone Penetration Test

Cone penetration tests (CPT) were performed by Geocontrole for 8 points in the embankment, generating the following soil profile, those results are detailed in Appendices.

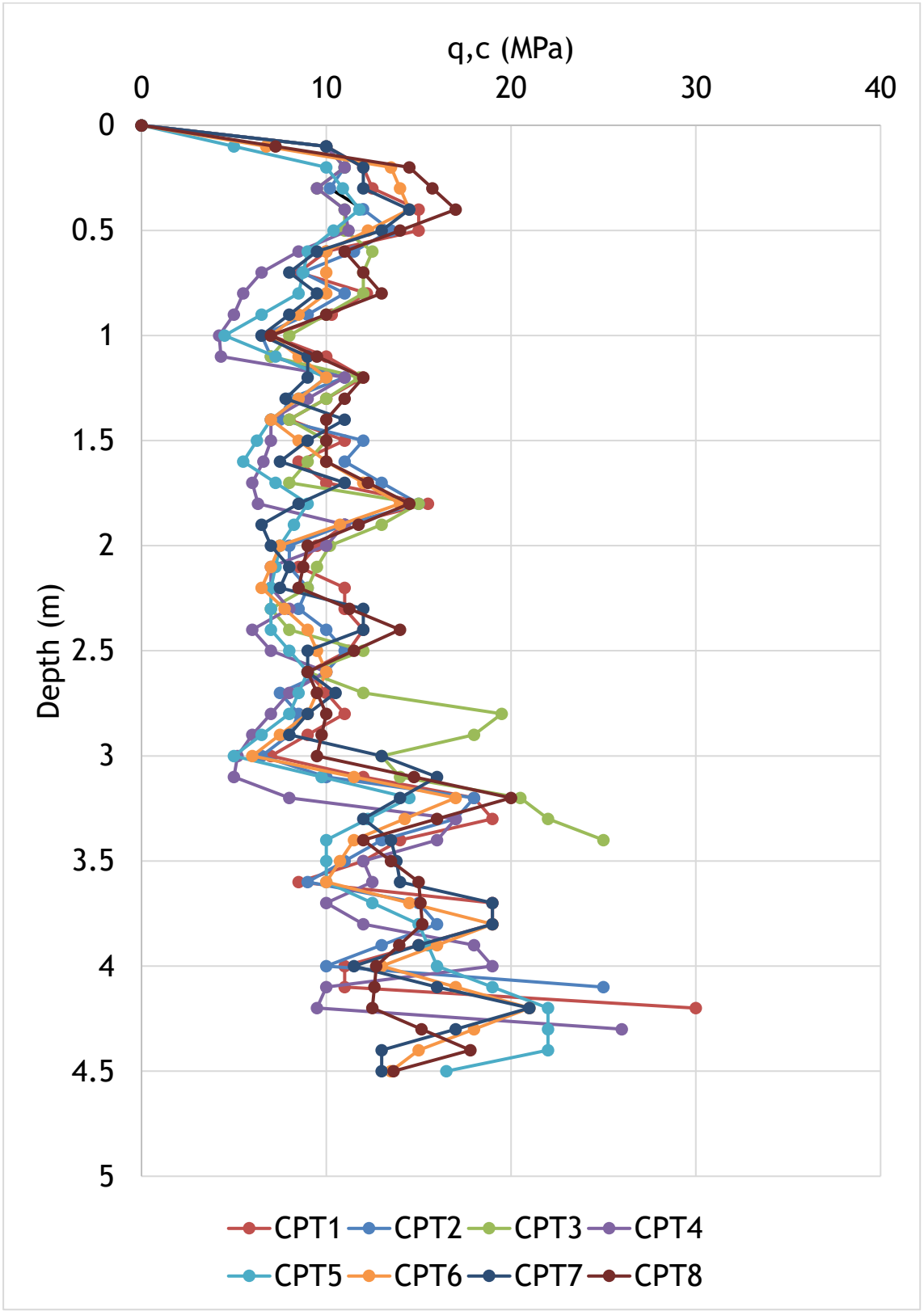

5. Long-term and Parameters Correlations

5.1. Proctor versus Soil Density Gauge versus Troxler

Gammadensimeter Troxler3440 and Soil Density Gauge SDG200 by TransTech data collected are summarized in Graphic 18, Lopes (2012) compared those two density measurement devices around their workability, practice, advantages, and disadvantages, explained in Table 20.

Table 20. Troxler and SDG comparative by Lopes (2012)

Parameter	Troxler	SDG
Handling	Easy	Easy
Perigosity	High	None
Worker Wear	High	Low
Technical Requirement	High	High
Practicle Obstacles	Steel structures	Rocks
Precision	High	High
Measurement Method	Drilling	Electromagnetic
Depth	Several specifications	30 cm
Costs	Low	Low
Device Calibration	Easy	Easy

Compaction must be controlled to reach enough compacity and optimal values not only mechanical, but also economically.

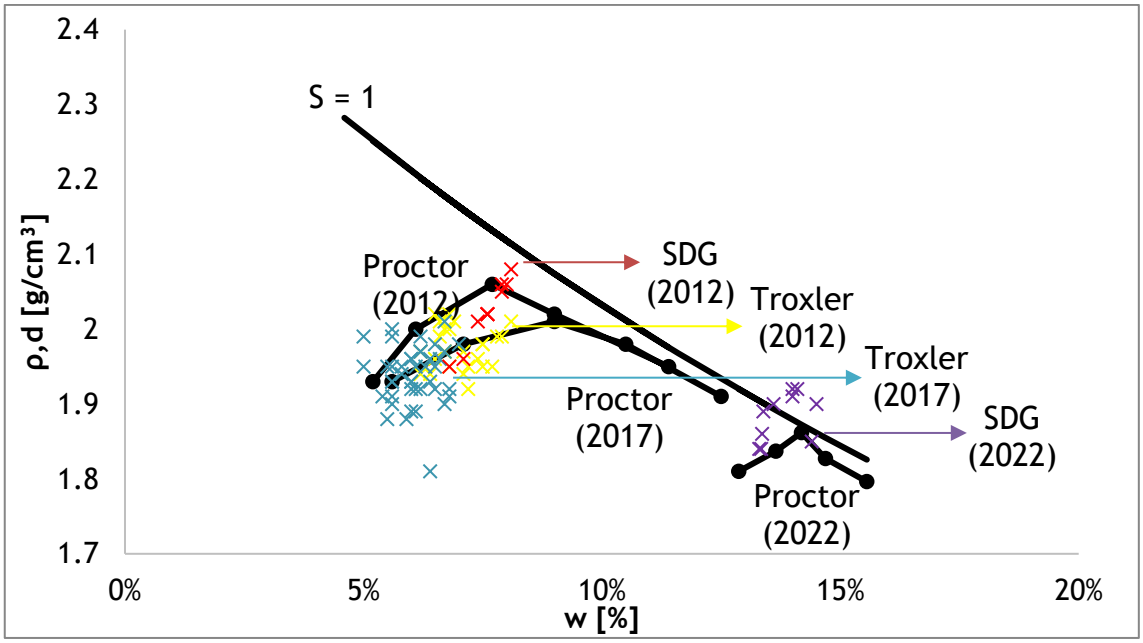

Graphic 18. Compaction degree during time

Compaction curves seems to have a tendency over time to get down along saturation curve, becoming a finer material, it can be explained by surface erodibility due to physical and chemical processes. Soil density gauge and gammadensimeter are very trustfull giving a good control of the embankment compaction.

5.2. Laboratorial Direct versus Indirect Permeability

Soils are permeable, some more like cobles and sands, others less like clays, they have pore pressure due to water pressure within the pores. Hydraulic conductivity is the capacity of water to flow through soil voids or pores. It is possible to obtain permeability parameter k through sample water flow or the capacity of compression and/or consolidation to expel the water inside pores.

A relationship was created along with oedometer one-dimensional consolidation, and the indirect values of k using Terzaghi theory and the actual falling head permeability measured in laboratory. Both had confined conditions, the same material, and geometry – cylindrical sample with 6.3 mm of diameter and 2.0 mm of height initially.

Values of k during consolidation are in Table 18 and Table 19, and falling head permeability in Graphic 13. Two behaviors can be observed when plotting those results together, the permeability decrease when the load upon the sample increase, and the permeability increase during time when the boundary conditions remain the same, like in a permeameter. Complementary behaviors which validate the average value of laboratorial k when for embankment construction time and load - flow and consolidation – are occurring during the process.

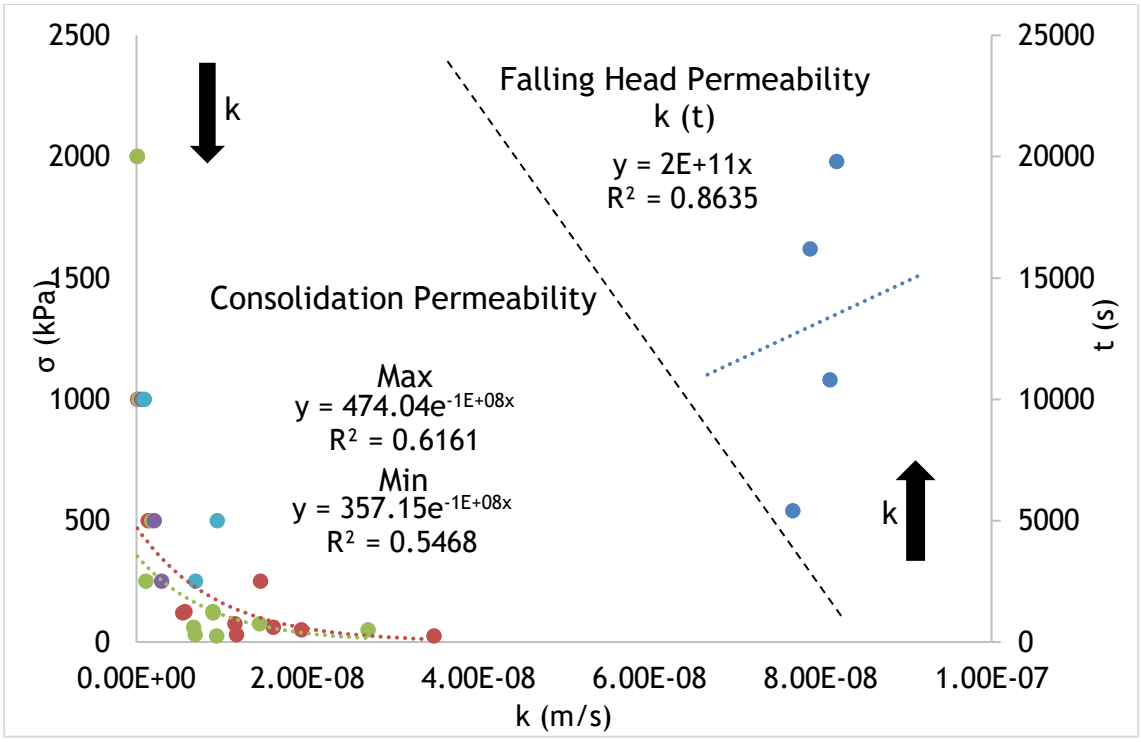

Graphic 19. Hydraulic conductivity due to consolidation and permeability

According to oedometer data, the permeability decreases when the load increase in a exponential trendline, this relationship is in between the maximum and minimum values obtained, with R^2 = 0.61 and R^2 = 0.55, respectively. Not a good relationship, but as those values are very low, in the order of 10^{-8}, it is valid. They follow, maximum and minimum values, respectively:

$$\sigma = 474 \cdot e^{10^{-8}} \cdot k \leftrightarrow k = \ln\left(\frac{\sigma}{474}\right) \cdot 10^{-8}$$

Equation 53

$$\sigma = 357 \cdot e^{10^{-8}} \cdot k \leftrightarrow k = \ln\left(\frac{\sigma}{357}\right) \cdot 10^{-8}$$

Equation 54

Where σ is in kPa and k in m/s.

Hydraulic conductivity (k) through falling head permeameter follows

$$t = 2 \cdot 10^{11} \cdot k \leftrightarrow k = \frac{t \cdot 10^{-11}}{2}$$

Equation 55

Where t is in s and k in m/s.

5.3. DPL versus DPSH versus SPT versus CPT

DPL values were limited due to difficulty to penetrate with lightweight pile. Anomalous values like DPL2 and SPT2 were discarded for this evaluation. Therefore, relationships DPL x DPSH were developed for 1m depth, making possible to compact three layers 30cm, and make possible to perform the most convenient drilling tests to measure the drilling resistance. SPT conversions were used literature's value of N,SPT = 0.6 x N,DPL.

[1] found for residual franitic soils from a similar region a relationship linking DPSH and SPT following: $\frac{N_{SPT}}{N_{DPSH}^{30}} \cong 2$, using the following data from Graphic 20 until 14m of depth.

It can be observed in Graphic 21 that the number of DPL and DPSH hits' coefficients were obtained for every 0.1m, with values fluctuating from 1.0-2.4, but limiting the confidence range, it can be defined the relationship in Equation 56. When the relation was not able to perform because of no data available, ND was indicated.

$$\frac{N_{DPL}}{N_{DPSH}} = 1.8 \; to \; 2.2 \approx 2.0$$

Equation 56

It can be observed in Graphic 22 that the number of SPT hits and q,c in MPa of CPT coefficients were obtained for every 0.1m, with values fluctuating from 1.9-5.0, but limiting the confidence range, it can be defined the relationship in Equation 57.

$$\frac{q_C}{N_{SPT}} = 2.5\ to\ 4.5 \approx 3.5$$

Equation 57

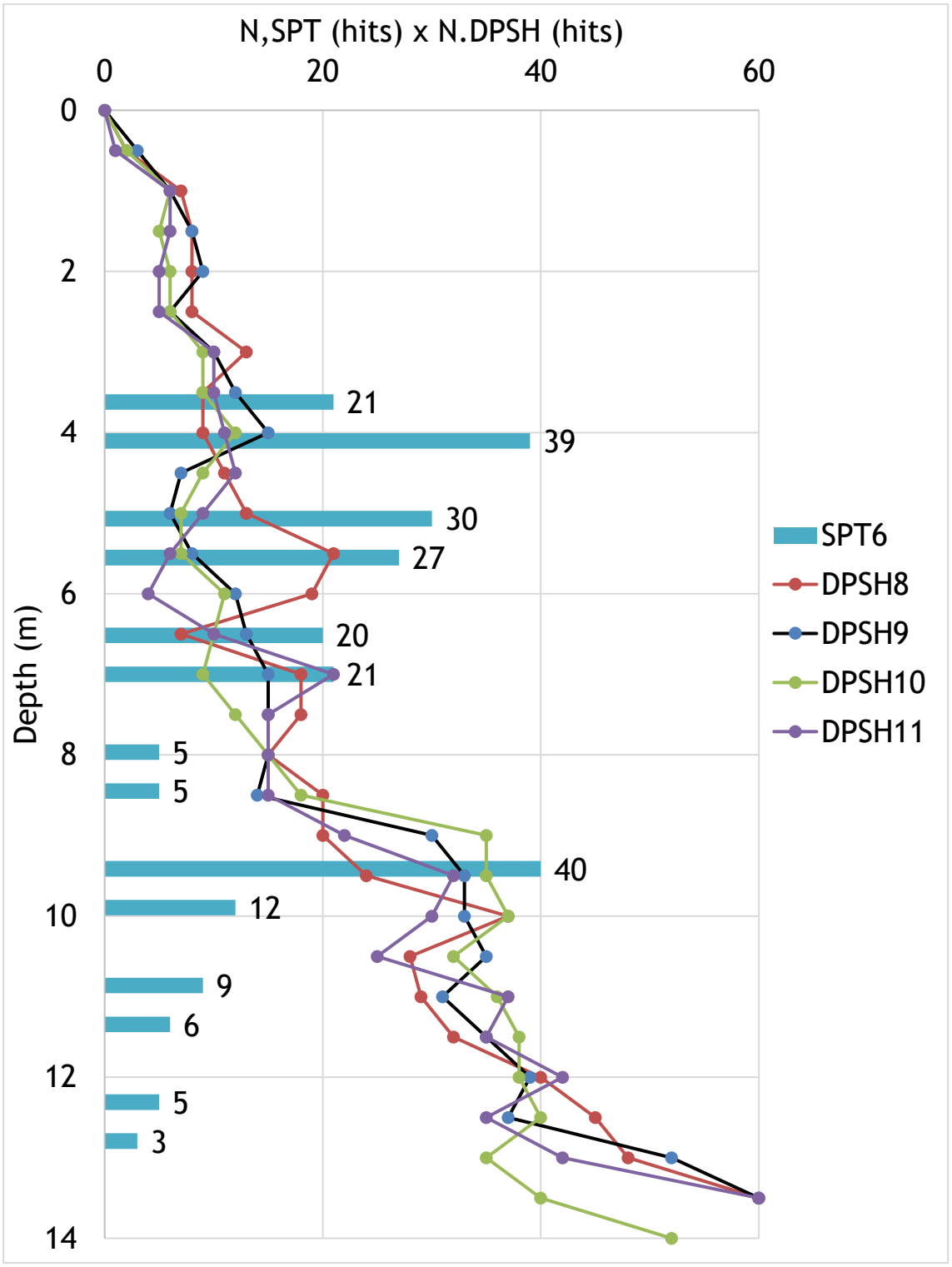

Graphic 20. DPSH x SPT relationship by [1]

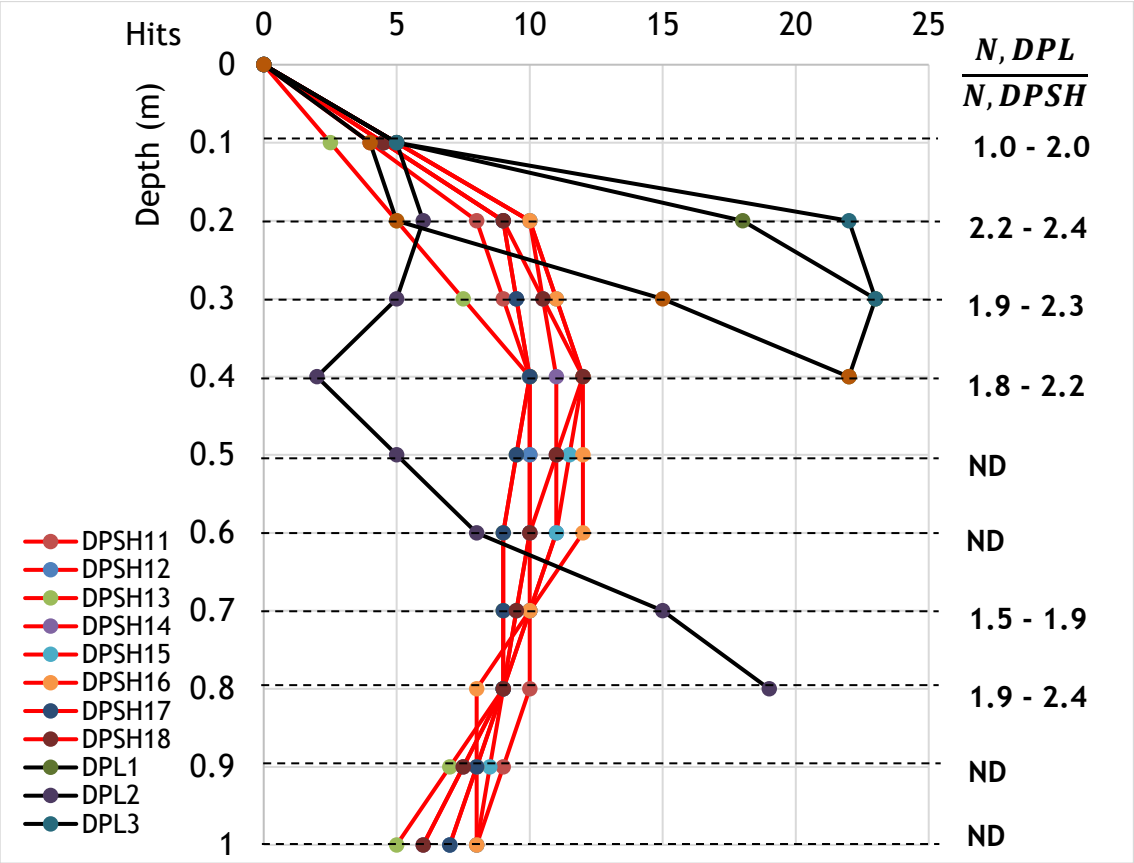

Graphic 21. DPL x DPSH relationship

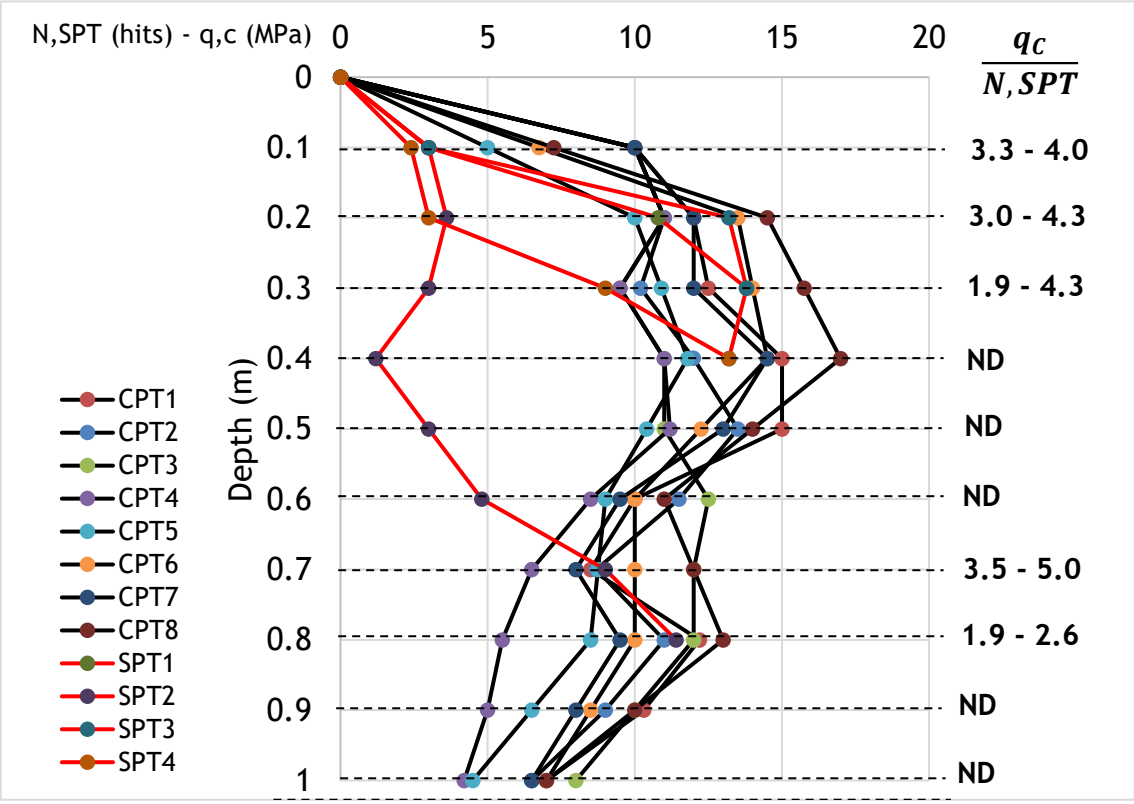

Graphic 22. SPT x CPT relationship

5.4. Oedometer versus Plate Load Test

Plate load test simulates in-situ oedometric consolidation, with some differences, mainly for the unconfined situation. Therefore, a relationship between those tests were made assuming premisses of the soil according to optimum compaction parameters and geotechnical parameters like:

- W_{opt} = 14%
- ρ_d = 1.85 g/cm^3
- G_S = 2.55

Although they have obvious geometrical differences, and using Terzaghi consolidation theory, compression coefficients were obtained, parameters exposed in Table 21.

Table 21. Geometry of oedometer and plate load test

	Oedometer	**Plate Load Test**
Diameter (mm)	63	500
Height (mm)	2	5 000
Area (mm^2)	3 200	20 000 000
Volume (mm^3)	6 5000	100 000 000 000
C_C	0.0500	0.0026
C_R	0.0130	0.0015
C_S	0.0070	0.0002

In-situ simulation of compression coefficients are much lower than laboratory tests, showing more stability of the structure due to compressibility, recompression, and swelling behavior, which seems to be good because laboratorial test gives a type of safety factor related to what is really happening in a construction site condition.

To analyse consolidation curves, oedometric and plate load results were plotted together in Graphic 23.

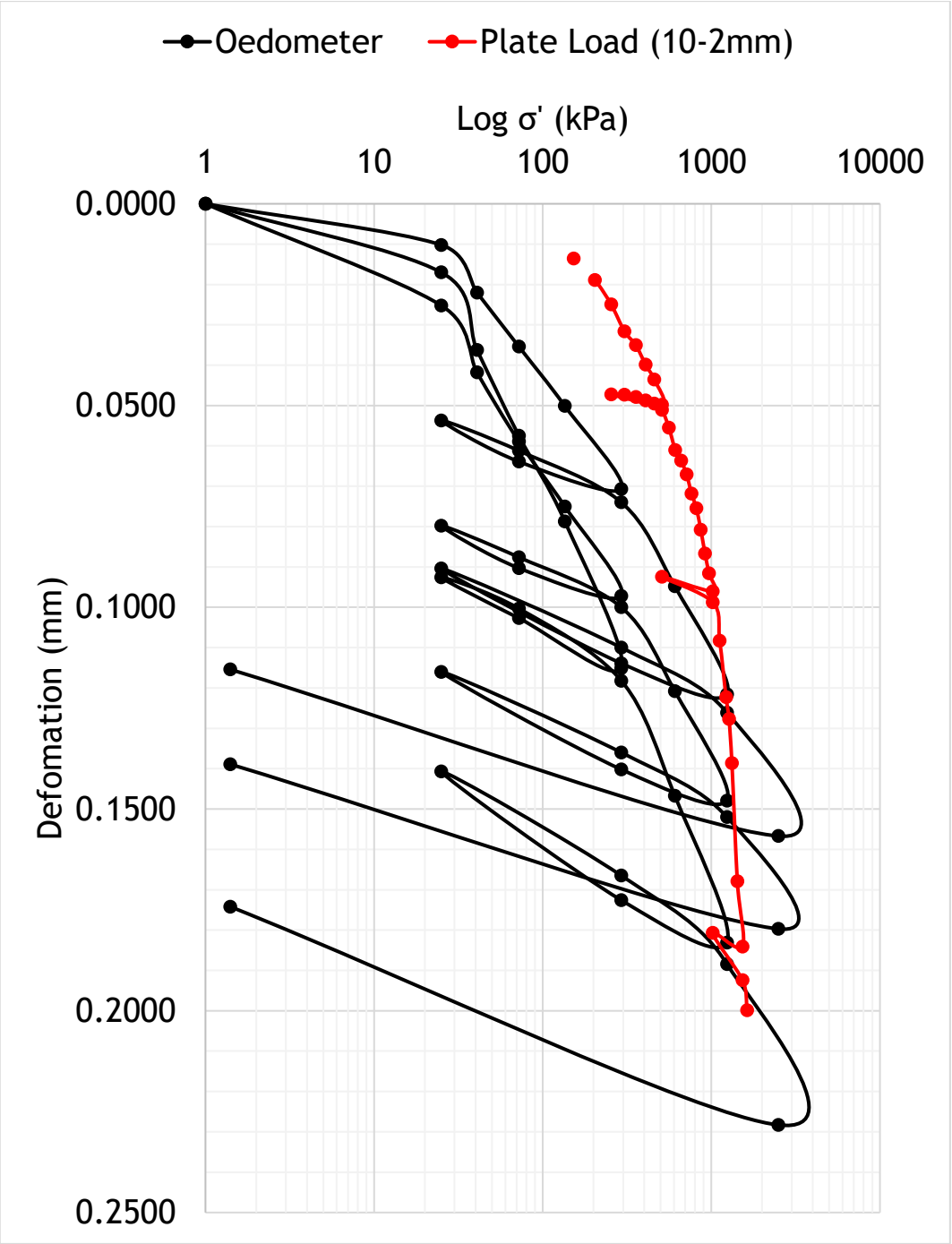

Graphic 23. Tension x deformation of oedometer and plate load

Chapter 5 – Conclusions and Proposals

It is intended to correlate laboratory and field geotechnical parameters, as well as their behavior over time.

Thus, the main conclusions around this study case and soil used are, according to laboratorial tests:

- Geotechnical characteristics encompass specific gravity of 2.55, non-plastic white color soil with liquid limit of 28%, optimal compaction on 14.0% humidity resulting in 1.86 g/cm3 dry density, it is a well graded sand classified as A-1-b for road embankments.

- Chemical compounds of high SiO_2 and Al_2O_3, and lower NaO_2 and Fe_2O_3 contributing for quartz, kaolinite, and muscovite mineralogy, besides its microscopic images show extense granulometris distribution.

- The soil has a high free expansibility, although a very low compressibility due to one-dimension consolidation, also have no cohesion and 35º of internal effective friction angle.

- The hydraulic conductivity fluctuates around 10^{-8} m/s.

And in situ performance:

- Compaction curves seems to have a tendency over time to get down along saturation curve, becoming a finer material, this can be explained by surface erodibility due to physical and chemical processes. Soil density gauge and gammadensimeter are very trustfull giving a good control of the embankment compaction.

- Two behaviors can be observed when analysing the permeability, it decreases when the load upon the sample increase, as in oedometric consolidation, and increases during time when the boundary conditions remain the same, like in a permeameter. Those complementary behaviors validate the average value of laboratorial k when for embankment construction time and load - flow and consolidation – are occurring during the process.

- Relationships among DPL x DPSH and SPT x CPT drilling tests were developed for 1m depth due to DPL's depth restrictions, following Equation 56 and Equation 57 below:

$$1.8 > \frac{N_{DPL}}{N_{DPSH}} > 2.2$$

$$2.5 > \frac{q_C}{N_{SPT}} > 4.5$$

- In-situ compression coefficients simulation with plate load tests are much lower than laboratory tests like oedometric compression, showing more stability of the structure due to compressibility, recompression, and swelling behavior, which seems to be good because laboratorial test gives a type of safety factor related to what is really happening in a construction site condition.

Besides, the author proposes for future research over the same studied site, which it should be perfomed the same, or an even more complete, testing program every 5 years at the same site, in order to give a consistent long-term behavior of the earthwork.

References

[1] V. Cavaleiro, "Condicionantes geotécnicas à expansão do núcleo urbano da Covilhã," Covilhã, 2001.

[2] C. Gomes, *Argilas: O que são e para que servem*. 1986.

[3] K. Terzaghi, R. B. Peck, and G. Mesri, *Soil Mechanics in Engineering Practice*, 3rd ed. New York, 1996.

[4] R. F. Craig, *Craig, mecânica dos solos*. LTC Editora, 2007. [Online]. Available: https://books.google.pt/books?id=zw8oOgAACAAJ

[5] A. W. Al-Khafaji and O. B. Andersland, *Geotechnical Engineering and Soil Testing*. 1992. [Online]. Available: https://www.researchgate.net/publication/322011747

[6] I. S. Oweis and R. P. Khera, "Geotechnology of waste management," p. 273, 1990.

[7] A. M. de A. C. de Brito, "Compactação de Aterros de Barragens: Novas Metodologias de Compactação," Lisboa, 2006.

[8] J. Kodikara, T. Islam, and A. Sounthararajah, "Review of soil compaction: History and recent developments," *Transportation Geotechnics*, vol. 17, pp. 24–34, Dec. 2018, doi: 10.1016/J.TRGEO.2018.09.006.

[9] R. N. Rosli, M. R. Selamat, and M. H. Ramli, "Shear strength and permeability properties of lateritic soils from North West Malaysia due to extended compaction," *Materials Today: Proceedings*, vol. 17, pp. 630–639, Jan. 2019, doi: 10.1016/J.MATPR.2019.06.344.

[10] L. J. Ebels, R. Lorio, and C. van der Merwe, "The importance of compaction from an historical perspective," in *The 23rd Annual Southern African Transport Conference*, Jul. 2004, pp. 34–43.

[11] S. Horpibulsuk, W. Katkan, and A. Apichatvullop, "An approach for assessment of compaction curves of fine grained soils at various energies using a one point test," *Soils and Foundations*, vol. 48, no. 1, pp. 115–125, Feb. 2008.

[12] S. Nam, M. Gutierrez, P. Diplas, and J. Petrie, "Laboratory and in situ determination of hydraulic conductivity and their validity in transient seepage analysis," *Water (Switzerland)*, vol. 13, no. 8, Apr. 2021, doi: 10.3390/w13081131.

[13] J. K. Tsugawa *et al.*, "Importance of Composing Representative Samples According to the Theory of Sampling (TOS) for the Reuse of Water Treatment Sludge ," *Geotechnical Engineering in the XXI Century: Lessons learned*, pp. 2450–2457, 2019, doi: 10.3233/STAL190314.

[14] F. C. M. Silva, "Avaliação da capacidade reativa de solos residuais destinados à infiltração de águas residuais tratadas," Universidade da Beira Interior, Covilhã, 2015.

[15] C. Gomes, *Argilas - Aplicações na Indústria*. 2002.

[16] L. Marchiori, A. Studart, A. Slva, A. Albuquerque, and V. Cavaleiro, "Geotechnical characterization of water treatment sludge for liner material production and soft soil reinforcement", *Material Science Forum*, no. 1046, pp. 83-88, 2021

[17] E. L. T. Montalvan, "Geotechnical properties of mixtures of water treatment sludge and residual lateritic soils from the State of São Paulo," Universidade de São Paulo, 2021.

[18] G. M. R. Coelho, "Avaliação da Capacidade Reativa de uma Lama de ETA para Remoção de Metais Pesados de Escorrências Rodoviárias," Universidade da Beira Interior, Covilhã, 2016.

[19] ASTM, "ASTM D4972-01 Standard Test Method for pH of Soils," 2007. [Online]. Available: www.astm.org

[20] BS 1377-4, "Methods of test for Soils for civil engineering purposes - Part 4: Compaction-related tests," British Standards Institution, UK, 1990.

[21] M. C. Wang, J. Q. Hull, and M. Jao, "Stabilization of water treatment plant sludge for possible use as embankment material.pdf," *Transportation Research Record*, no. 1345, pp. 36–43, 1992.

[22] R. Chen, S. Qi, W. Cheng, and H. Wang, "Effect of Compactness Degree on the Hydraulic Properties for Coarse Soils of High-Speed Railway Embankment," *Procedia Engineering*, vol. 143, pp. 237–243, Jan. 2016, doi: 10.1016/J.PROENG.2016.06.030.

[23] Y. Al-Badran and T. Schanz, "Modelling the compaction curve of fine-grained soils," *Soils and Foundations*, vol. 54, no. 3, pp. 426–438, Jun. 2014, doi: 10.1016/J.SANDF.2014.04.011.

[24] S. Anjan Kumar, R. Aldouri, S. Nazarian, and J. Si, "Accelerated assessment of quality of compacted geomaterials with intelligent compaction technology," *Construction and Building Materials*, vol. 113, pp. 824–834, Jun. 2016, doi: 10.1016/J.CONBUILDMAT.2016.03.117.

[25] Y. Zhao, Y. Cui, H. Zhou, X. Feng, and Z. Huang, "Effects of void ratio and grain size distribution on water retention properties of compacted infilled joint soils," *Soils and Foundations*, vol. 57, no. 1, pp. 50–59, Feb. 2017, doi: 10.1016/J.SANDF.2017.01.004.

[26] H. B. Nagaraj, B. Reesha, M. V. Sravan, and M. R. Suresh, "Correlation of compaction characteristics of natural soils with modified plastic limit," *Transportation Geotechnics*, vol. 2, pp. 65–77, Mar. 2015, doi: 10.1016/J.TRGEO.2014.09.002.

[27] K. Kawai, V. Phommachanh, T. Kawakatsu, and A. Iizuka, "Explanation of Dry Density Distribution Induced by Compaction through Soil/Water/Air Coupled Simulation," *Procedia Engineering*, vol. 143, pp. 276–283, Jan. 2016, doi: 10.1016/J.PROENG.2016.06.035.

[28] S. Horpibulsuk, A. Suddeepong, P. Chamket, and A. Chinkulkijniwat, "Compaction behavior of fine-grained soils, lateritic soils and crushed rocks," *Soils and Foundations*, vol. 53, no. 1, pp. 166–172, Feb. 2013, doi: 10.1016/J.SANDF.2012.12.012.

[29] Y. Minabe, S. Kawajiri, T. Kawaguchi, D. Nakamura, and S. Yamashita, "Correlation between Mechanical Properties and Suction Calculated by X-ray CT of Unsaturated Sandy Soil," *Procedia Engineering*, vol. 143, pp. 292–299, Jan. 2016, doi: 10.1016/J.PROENG.2016.06.037.

[30] H. F. Aghajani, M. G. Yengejeh, A. Karimzadeh, and H. Soltani-Jigheh, "A new procedure for determining dry density of mixed soil containing oversize gravel," *J Cent South Univ*, vol. 25, no. 12, pp. 2841–2856, Dec. 2018, doi: 10.1007/S11771-018-3957-7.

[31] K. Xia, "Numerical prediction of soil compaction in geotechnical engineering," *Comptes Rendus Mécanique*, vol. 342, no. 3, pp. 208–219, Mar. 2014, doi: 10.1016/J.CRME.2014.01.007.

[32] H. M. A. Rashid *et al.*, "Characterization of locally available soil as a liner material for solid waste landfills in Sri Lanka," *Environmental Earth Sciences*, vol. 76, no. 11, Jun. 2017, doi: 10.1007/s12665-017-6717-3.

[33] D. E. Daniel, *Geotechnical practice for waste disposal*. 2012. doi: 10.1016/0956-053x(94)90012-4.

[34] S. A. Naeini, N. Gholampoor, and M. A. Jahanfar, "Effect of leachate's components on undrained shear strength of clay-bentonite liners," *European Journal of Environmental and Civil Engineering*, vol. 23, no. 3, pp. 395–408, Mar. 2019, doi: 10.1080/19648189.2017.1278725.

[35] R. K. Rowe, R. M. Quigley, and J. R. Booker, *Clayey Barrier Systems for Waste Disposal Facilities*. Taylor & Francis, 1997.

[36] H. Soltani-Jigheh, V. Marefat, and A. Ersizad, "Behavior of Clay-Tire Mixtures Subjected to Undrained Monotonic Loading," *Soils and Rocks*, vol. 36, no. 3, pp. 283–292, Sep. 2013.

[37] V. Srikanth and A. K. Mishra, "Atterberg Limits of Sand-Bentonite Mixes and the Influence of Sand Composition," *Geotechnical Characterisation and Geoenvironmental Engineering*, vol. 16, pp. 139–145, 2016.

[38] M.-L. Lopes, F. Ferreira, R. Carneiro, & Castorina, S. Vieira, and C. S. Vieira, "Soil-geosynthetic inclined plane shear behavior: influence of soil moisture content and geosynthetic type," *International Journal of Geotechnical Engineering*, vol. 8, no. 3, pp. 335–342, 2014, doi: 10.1179/1939787914Y.0000000047.

[39] F. M. L. Ferreira, "CARACTERIZAÇÃO GEOTÉCNICA DE SOLOS DE ALTA MONTANHA," Universidade da Beira Interior, Covilhã, 2015.

[40] J. Colin JFP, *Earth Reinforcement and Soil Structures*. Butterworth-Heinemann, 1985.

[41] M. Julina and T. Thyagaraj, "Effect of Induced Osmotic Suction on Swell and Hydraulic Conuctivity of an Expansice Soil," *Geotechnical Characterisation and Geoenvironmental Engineering*, vol. 16, pp. 193–200, 2016.

[42] M. Kowalska and M. Ptaszek, "Influence of Rubber and Mineral Admixtures on Selected Swelling Properties of Red Clay," in *IOP Conference Series: Materials Science and Engineering*, Feb. 2019, vol. 471, no. 4. doi: 10.1088/1757-899X/471/4/042012.

[43] Y. P. Matos, B. R. Soares, F. F. Monteiro, I. C. Marques, R. O. Ribeiro, and M. F. P. Aguiar, "Avaliação dos Resultados de Ensaios de Compressão Triaxial em Solos Granulares e Finos," 2014.

[44] S. A. Bernal, E. D. Rodríguez, A. P. Kirchheim, and J. L. Provis, "Management and valorisation of wastes through use in producing alkali-activated cement materials," *Journal of Chemical Technology and Biotechnology*, vol. 91, no. 9, pp. 2365–2388, Sep. 2016, doi: 10.1002/jctb.4927.

[45] A. A. Firoozi, A. A. Firoozi, and M. Shojaei, "A Review of Clayey Soils," *Asian Journal of Applied Sciences*, vol. 04, no. 06, p. 13, 2017.

[46] G. P. Karunaratne, S. H. Chew, S. L. Lee, and A. N. Sinha, "Ben-tonite:Kaolinite Clay Liner," *Geosynthetics International*, vol. 8, no. 2, pp. 113–133, 2001.

[47] C. B. Gupt, S. Bordoloi, R. K. Sahoo, and S. Sekharan, "Mechanical performance and micro-structure of bentonite-fly ash and bentonite-sand mixes for landfill liner application," *Journal of Cleaner Production*, vol. 292, p. 126033, Apr. 2021, doi: 10.1016/j.jclepro.2021.126033.

[48] G. Wei and J. Dong, "Swelling Research of Expansive Soil Under Drying-Wetting Cycles: A NMR Method," *Soils and Rocks*, vol. 43, no. 1, pp. 21–30, Mar. 2020, doi: 10.28927/sr.431021.

[49] A. Benvindo Da Luz and C. Honório De Oliveira, "Argila - Bentonita," in *Rochas e Minerais Industriais - CETEM*, 2nd ed., 2008, pp. 239–253.

[50] R. K. Rowe, J. D. D. Garcia, R. W. I. Brachman, and M. S. Hosney, "Chemical interaction and hydraulic performance of geosynthetic clay liners isothermally hydrated from silty sand subgrade," *Geotextiles and Geomembranes*, vol. 47, no. 6, pp. 740–754, Dec. 2019, doi: 10.1016/j.geotexmem.2019.103486.

[51] M. Kowalska and M. Jastrzebska, "Triaxial Tests on Weak Cohesive Soils - Some Practical Remarks (Part 1)," *Architecture, Civil Engineering, Environment*, vol. 9, no. 3, pp. 71–80, 2016, doi: 10.21307/acee-2016-036.

[52] K. André and P. Amann, "Metodologia Semiempírica Unificada Capacidade de Carga de Estacas para Previsão de," in *COBRAMSEG 2010*, 2010, no. 2010, pp. 1–8.

[53] Y.-C. Li, P. J. Cleall, Y.-D. Wen, Y.-M. Chen, and Q. Pan, "Stresses in soil–bentonite slurry trench cut-off walls," *Géotechnique*, vol. 65, no. 10, pp. 843–850, Oct. 2015, doi: 10.1680/jgeot.14.p.219.

[54] T. Kozlowski and A. Ludynia, "Permeability coefficient of low permeable soils as a single-variable function of soil parameter," *Water (Switzerland)*, vol. 11, no. 12, Dec. 2019, doi: 10.3390/w11122500.

[55] S. P. Singh and S. Rout, "An Experimental Investigation on the Geoengineering Properties of Pond Ash-Bentonite Mixes," *Geotechnical Characterisation and Geoenvironmental Engineering*, vol. 16, pp. 211–218, 2016.

[56] C. P. Sarma, A. M. Krishna, and A. Dey, "Geotechnical Characterization of Hillslope Soils of Guwahati Region," *Geotechnical Characterisation and Geoenvironmental Engineering*, vol. 16, pp. 103–110, 2016.

[57] N. Touze-Foltz, H. Xie, and G. Stoltz, "Performance issues of barrier systems for landfills: A review," *Geotextiles and Geomembranes*, vol. 49, no. 2, pp. 475–488, Apr. 2021, doi: 10.1016/j.geotexmem.2020.10.016.

[58] F. Tatsuoka and A. G. Correia, "Importance of Controlling the Degree of Saturation in Soil Compaction," *Procedia Engineering*, vol. 143, pp. 556–565, Jan. 2016, doi: 10.1016/J.PROENG.2016.06.070.

[59] G. P. Karunaratne, S. H. Chew, S. L. Lee, and A. N. Sinha, "Bentonite: Kaolinite clay liner," *Geosynthetics International*, vol. 8, no. 2, pp. 113–133, 2001, doi: 10.1680/gein.8.0189.

[60] S. C. Prado, G. C. de M. Mendes, and M. F. P. de Aguiar, "Correlação Entre Dpl E Spt Para Camada De Areia Em Depósito Eólico De Fortaleza, Ceará," *Ciências Exatas e da Terra: Exploração e Qualificação de Diferentes Tecnologias 3*, no. October, pp. 107–114, 2021, doi: 10.22533/at.ed.1232113018.

[61] D. M. Moore and R. C. Reynolds Jr, *X-Ray Diffraction and the Identification and Analysis of Clay Minerals*. 1989.

[62] M. K. Uddin, "A review on the adsorption of heavy metals by clay minerals, with special focus on the past decade," *Chemical Engineering Journal*, vol. 308, pp. 438–462, Jan. 2017, doi: 10.1016/j.cej.2016.09.029.

[63] M. Banar, Y. Güney, A. Özkan, Z. Günkaya, E. Bayrakcı, and D. Ulutaş, "Utilisation of waste clay from boron production as a landfill liner material," *International Journal of Mining, Reclamation and Environment*, vol. 33, no. 3, pp. 206–222, Apr. 2019, doi: 10.1080/17480930.2017.1402854.

[64] D. Carrol, "Clay Minerals: A Guide to Their X-ray Identification," *The Geological Society of America*, vol. 126, 1970.

[65] A. F. Elhakim, "Estimation of soil permeability," *Alexandria Engineering Journal*, vol. 55, no. 3, pp. 2631–2638, Sep. 2016, doi: 10.1016/J.AEJ.2016.07.034.

[66] M. Jastrzebska and M. Kowalska, "Triaxial Tests on Weak Cohesive Soils - Some Practical Remarks (Part 2)," *Architecture, Civil Engineering, Environment*, vol. 9, no. 3, pp. 81–94, 2016, doi: 10.21307/acee-2016-037.

[67] IPB, "Avaliação e Capacidade de Carga da Plataforma de um Aterro," 2017.

[68] T. L. C. Morandini and A. L. Leite, "Shear Strength of Tropical Soils and Bentonite Mixtures for Barrier Design," *Soils and Rocks*, vol. 39, no. 3, pp. 239–248, Sep. 2016.

[69] K. Nivedya, "Study on the Effect of pH on the Atterberg Limits of Kaolinitic and Montmorillonitic Clay," *Geotechnical Characterisation and Geoenvironmental Engineering*, vol. 16, pp. 251–256, 2016.

[70] O. Bahmani and M. Bayram, "Investigating the hydraulic conductivity and soil characteristics under compaction and soil texture and performances as landfill liner," *Arabian Journal of Geosciences*, vol. 11, no. 16, Aug. 2018, doi: 10.1007/s12517-018-3817-7.

[71] M. Kowalska and M. Chmielewski, "Mechanical Parameters of Rubber-Sand Mixtures for Numerical Analysis of a Road Embankment," in *IOP Conference Series: Materials Science and Engineering*, Nov. 2017, vol. 245, no. 5. doi: 10.1088/1757-899X/245/5/052003.

[72] N. Saranya and D. N. Arnepalli, "Effect of Pore Size Distribution on Unconfined Compressive Shear Strength," *Geotechnical Characterisation and Geoenvironmental Engineering*, vol. 16, pp. 75–82, 2016.

[73] E. Emmanuel, V. Anggraini, and S. S. R. Gidigasu, "A critical reappraisal of residual soils as compacted soil liners," *SN Applied Sciences*, vol. 1, no. 5. Springer Nature, May 01, 2019. doi: 10.1007/s42452-019-0475-7.

[74] M. Heidemann, L. A. Bressani, and J. A. Flores, "Residual Shear Strength of a Residual Soil of Granulite," *Soils and Rocks*, vol. 43, no. 1, pp. 31–41, Mar. 2020, doi: 10.28927/sr.431031.

[75] G. Spagnoli and S. Shimobe, "An overview on the compaction characteristics of soils by laboratory tests," *Engineering Geology*, vol. 278. Elsevier B.V., p. 105830, Dec. 05, 2020. doi: 10.1016/j.enggeo.2020.105830.

[76] B. Sharma and P. Deka, "A Study on Compressibility, Swelling and Permeability Behaviour of Bentonite-Sand Mixture," *Geotechnical Characterisation and Geoenvironmental Engineering*, vol. 16, pp. 43–50, 2019.

[77] D. Abdellah, M. K. Gueddouda, I. Goual, H. Souli, and M. S. Ghembaza, "Effect of landfill leachate on the hydromechanical behavior of bentonite-geomaterials mixture," *Construction and Building Materials*, vol. 234, p. 117356, Feb. 2020, doi: 10.1016/j.conbuildmat.2019.117356.

[78] B. R. Phanikumar and E. Ramanjaneya Raju, "Compaction and strength characteristics of an expansive clay stabilised with lime sludge and cement," *Soils and Foundations*, vol. 60, no. 1, pp. 129–138, Feb. 2020, doi: 10.1016/j.sandf.2020.01.007.

[79] B. Wang, J. Xu, B. Chen, X. Dong, and T. Dou, "Hydraulic conductivity of geosynthetic clay liners to inorganic waste leachate," *Applied Clay Science*, vol. 168, pp. 244–248, Feb. 2019, doi: 10.1016/j.clay.2018.11.021.

[80] A. I. de Oliveira Júnior, J. F. T. Jucá, J. A. Ferreira, and L. C. Guilherme, "Geotechnical Behavior and Soil-Fiber Interaction of Clayey Soil Mixed with

Randomly Dispersed Coconut Fibers," *Soils and Rocks*, vol. 42, no. 2, pp. 127–138, Aug. 2019, doi: 10.28927/sr.422127.

[81] F. Rocha, "Argilas aplicadas a estudos litoestratigráficos e paleoambientais na bacia sedimentar de Aveiro," Universidade de Aveiro, Aveiro, 1993.

[82] L. Marchiori, A. Albuquerque, and V. Cavaleiro, "Critical Review of Industrial Solid Wastes as Barrier Material for Impermeabilization of Storage Waste Facilities", *Proceeding of SUM2020 – Symposium on Urban Mining and Circular Economy,* Nov. 2020.

[83] L. Marchiori, A. Studart, M.V. Morais, A. Albuquerque, and V. Cavaleiro, "Evaluation of the potential use of water treatment sludge (WTS) as a waterproofing material for waste containment earthworks", *Coleção desafios das engenharias – Engenharia sanitaria 2,* 2021.

[84] L. Marchiori, A. Studart, M.V. Morais, A. Albuquerque, V. Cavaleiro, "Avaliação do potencial de utilização de resíduo de ETA como impermeabilizante de obras de terra para contenção de resíduos", *Proceedings of LETA21 – 1º Encontro Nacional de Lodo de Estação de Tratamento de Água,* 2021.

[85] L. Marchiori, A. Studart, M.V. Morais, A. Albuquerque, L. Andrade Pais, M.E.G. Boscov, "Geotechnical characterization of biomass ashes for soil reinforcement and liner material", *KnE Materials Science,* pp. 219-224, 2021.

[86] L. Marchiori, A. Studart, M.V. Morais, A. Albuquerque, P.G. Almeida, L. Andrade Pais, M.E.G. Boscov, V. Cavaleiro, "A substituição de geossintéticos e solos através da valorização de resíduos de estação de tratamento de água em obras de terra", *Proceedings of 17CNG - XVII Congresso Nacional de Geotecnia,* 2021.

[87] A. Studart, L. Marchiori, M.V. Morais, A. Albuquerque, P.G. Almeida, V. Cavaleiro, "Chemical and Mineralogical Characterization of Biomass Ashes for Soil Reinforcement and Liner Material", *KnE Materials Science,* pp. 212-218, 2021.

[88] F. Parastar, S. M. Hejazi, M. Sheikhzadeh, and A. Alirezazadeh, "A parametric study on hydraulic conductivity and self-healing properties of geotextile clay liners used in landfills," *Journal of Environmental Management*, vol. 202, pp. 29–37, Nov. 2017, doi: 10.1016/j.jenvman.2017.07.013.

[89] J. T. F. Wong, Z. Chen, C. W. W. Ng, and M. H. Wong, "Gas permeability of biochar-amended clay: potential alternative landfill final cover material," *Environmental Science and Pollution Research*, vol. 23, no. 8, pp. 7126–7131, Apr. 2016, doi: 10.1007/s11356-015-4871-2.

[90] H. Yoshida and R. K. Rowe, "Consideration of Landfill Liner Temperature," in *Proceedings Sardinia 2003, Ninth International Waste Management and Landfill Symposium*, Oct. 2003, pp. 6–10.

[91] L. Marchiori, A. Albuquerque, V. Cavaleiro, "Industrial solid wastes acting as barrier material for storing solid wastes (SW) and wastewaters: A critical review", *Proceedings of ICSMGE2022 – 20th International Conference on Soil Mechanics and Geotechnical Engineering,* Sydney, May 2022.

[92] ABNT, "NBR 13896 - Aterro de Resíduos Não Perigosos - Critérios para Projeto, Implantação e Operação," Rio de Janeiro, Jun. 1997.

[93] L. Marchiori, A. Studart, M.V. Morais, A. Albuquerque, and V. Cavaleiro, "Laboratory testing of vegetable biomass ashes with soils for liner production and soil strengthening", *Proceedings of TESTE2022 . 3rd Congress on Testing and Experimentation on Civil Engineering*, Jul. 2022.

[94] L. Marchiori, A. Albuquerque, V. Cavaleiro, "Granitic mining waste feasibility for liner material production", *Proceedings of ICEPTP'22 – 7th World Congress on Civil, Structural, and Environmental Engineering*, Apr. 2022.

[95] V. Cavaleiro, L. Marchiori, G. Marchi, M. Cocchiaralle, "New methodology for rock's geomechanical characterization with Schmidt sclerometer", *Proceedings of TESTE2022 . 3rd Congress on Testing and Experimentation on Civil Engineering*, Jul. 2022..

[96] M.V. Morais, L. Marchiori, A. Albuquerque, and V. Cavaleiro, "Simultaneous application of physical methods and scanning electron microscopy for evaluation of bioclogging in geotextiles", *Proceedings of TESTE2022 . 3rd Congress on Testing and Experimentation on Civil Engineering*, Jul. 2022..

[97] G. Varank *et al.*, "Migration behavior of landfill leachate contaminants through alternative composite liners," *Science of the Total Environment*, vol. 409, no. 17, pp. 3183–3196, Aug. 2011, doi: 10.1016/j.scitotenv.2011.04.044.

[98] M. Regadío, J. A. Black, and S. F. Thornton, "The Role of Natural Clays in the Sustainability of Landfill Liners," *Detritus*, 2019.

[99] A. B. C. Junior, V. M. Zanta, L. C. Lange, L. P. Gomes, and N. Pessin, "Alternativas de Disposição de Resíduos Sólidos Urbanos para Pequenas Comunidades," Florianópolis, 2003.

[100] G. Tchobanoglous, H. Theisen, and V. Samuel, *Integrated solid waste management : engineering principles and management issues*. 1993.

[101] P. Agamuthu, "Landfilling in developing countries," *Waste Management and Research*, vol. 31, no. 1, pp. 1–2, Jan. 2013, doi: 10.1177/0734242X12469169.

[102] P. Kjeldsen, M. A. Barlaz, A. P. Rooker, A. Baun, A. Ledin, and T. H. Christensen, "Present and longterm composition of MSW landfill leachate - a review," *Critical Reviews in Environmental Science and Technology*, vol. 32, no. 4, pp. 297–336, 2002.

[103] S. R. Qasim and W. Chiang, "Sanitary Landfill Leachate: Generation, Treatment and Control," *Control and Treatment*, vol. 1. Lancaster, p. 339, 1994.

[104] M. O. Portella and J. C. J. Ribeiro, "Aterros Sanitários - Aspectos Gerais e Destino Final dos Resíduos," *Revista Direiro Ambiental e Sociedade*, vol. 4, no. 1, pp. 115–134, 2014.

[105] US Environmental Protection Agency, "Principles of Design and Operations of Wastewater Treatment Pond Systems for Plant Operators, Engineers, and ManagersDevelopment National Risk Management Research Laboratory-Land Remediation and Pollution Control Division," Cincinnati, Ohio, Aug. 2011.

[106] R. K. Mohan, J. B. Herbich, L. R. Hossner, and F. S. Williams, "Reclamation of solid waste landfills by capping with dredged material," *Journal of Hazardous Materials*, vol. 53, no. 1–3, pp. 141–164, May 1997, doi: 10.1016/S0304-3894(96)01831-6.

[107] R. Iranpour, H. H. J. Cox, R. J. Kearney, J. H. Clark, A. B. Pincince, and G. T. Daigger, "Regulations for Biosolids Land Application in U.S. and European Union," *Journal of Residuals Science & Technology*, vol. 1, no. 4, pp. 209–222, Oct. 2004.

[108] D. P. Duffy, "Landfill Economics - Part 1 - Getting Down to Business," *MSW Management*, Apr. 06, 2015.

[109] M. K. Widomski, W. Stępniewski, and A. Musz-Pomorska, "Clays of different plasticity as materials for landfill liners in rural systems of sustainable waste management," *Sustainability (Switzerland)*, vol. 10, no. 7, Jul. 2018, doi: 10.3390/su10072489.

[110] V. Soares, "Utilização de Mistura de Solo Saprolítico com Bentonita na Construção de Revestimento de Fundo de Aterros Sanitários," Escola Politécnica da Universidade de São Paulo, São Paulo, 2012.

[111] K. Binnemans, P. T. Jones, B. Blanpain, T. Van Gerven, and Y. Pontikes, "Towards zero-waste valorisation of rare-earth-containing industrial process residues: A critical review," *Journal of Cleaner Production*, vol. 99, pp. 17–38, Jul. 2015, doi: 10.1016/j.jclepro.2015.02.089.

[112] E. J. Murray, N. Dixon, and D. R. V Jones, "Geotechnical Engineering of Landfills," Sep. 1998.

[113] J. F. Wagner and C. Schnatmeyer, "Test field study of different cover sealing systems for industrial dumps and polluted sites," *Applied Clay Science*, vol. 21, no. 1–2, pp. 99–116, Apr. 2002, doi: 10.1016/S0169-1317(01)00096-5.

[114] S. Shu, W. Zhu, and J. Shi, "A new simplified method to calculate breakthrough time of municipal solid waste landfill liners," *Journal of Cleaner Production*, vol. 219, pp. 649–654, May 2019, doi: 10.1016/j.jclepro.2019.02.050.

[115] USEPA, "Safer Disposal For Solid Waste The Federal Regulations for Landfills," 1993.

[116] I. Travar, L. Andreas, J. Kumpiene, and A. Lagerkvist, "Development of drainage water quality from a landfill cover built with secondary construction materials," *Waste Management*, vol. 35, pp. 148–158, 2015.

[117] Ontario Regulations, "Landfill standards: A guideline on the regulatory and approval requirements for new or expanding landfilling sites," Jul. 15, 2020. https://www.ontario.ca/page/landfill-standards-guideline-regulatory-and-approval-requirements-newexpanding-land#section-4

[118] X. Zhao, T. Voice, and S. A. Hashsham, "Bioreactor Landfill Research and Demonstration Project Northern Oaks Landfill, Harrison, MI," Harrison, MI, Aug. 2006.

[119] D. P. Duffy, "Landfill Economics - Getting Down to Business - Part 2," *MSW Management*, Jun. 02, 2016.

[120] J. K. Locastro and B. L. De Angelis, "Barreiras de Impermeabilização: Configurações Aplicadas em Aterros Sanitários," *Revista Eletrônica em Gestão, Educação e Tecnologia Ambiental*, vol. 20, no. 1, pp. 200–210, 2016.

[121] C. D. Shackelford, C. H. Benson, T. Katsumi, T. B. Edil, and L. Lin, "Evaluating the hydraulic conductivity of GCLs permeated with non-standard liquids," *Geotextiles and Geomembranes*, vol. 18, no. 2–4, pp. 133–161, Apr. 2000, doi: 10.1016/S0266-1144(99)00024-2.

[122] T. L. C. Morandini and A. D. L. Leite, "On the compatibility and theoretical equations for mixtures of tropical soils and bentonite for barrier purposes," *Soils and Rocks*, vol. 41, no. 3, pp. 345–357, Sep. 2018, doi: 10.28927/SR.413345.

[123] B. Zainab, C. Wireko, D. Li, K. Tian, and T. Abichou, "Hydraulic conductivity of bentonite-polymer geosynthetic clay liners to coal combustion product leachates," *Geotextiles and Geomembranes*, Apr. 2021, doi: 10.1016/j.geotexmem.2021.03.007.

[124] R. K. Rowe, "Long-term performance of contaminant barrier systems," *Géotechnique*, vol. 55, no. 9, pp. 631–678, 2005.

[125] J. C. Vertematti, *Manual Brasileiro de Geossintéticos*. 2015.

[126] Y. Guney, B. Cetin, A. H. Aydilek, B. F. Tanyu, and S. Koparal, "Utilization of sepiolite materials as a bottom liner material in solid waste landfills," *Waste Management*, vol. 34, no. 1, pp. 112–124, Jan. 2014, doi: 10.1016/j.wasman.2013.10.008.

[127] N. Khalid, M. Mukri, M. Fadzil Arshad, N. Sidek, and F. Kamarudin, "Effect on Salak Tinggi residual soil mixed Bentonite as compacted clay liner," in *IOP Conference Series: Materials Science and Engineering*, Apr. 2019, vol. 513, no. 1. doi: 10.1088/1757-899X/513/1/012024.

[128] C. A. Hidalgo and J. J. Bustamante-Hernández, "A new sustainable geotechnical reinforcement system from old tires: Experimental evaluation by pullout tests," *Sustainability (Switzerland)*, vol. 12, no. 11, Jun. 2020, doi: 10.3390/su12114582.

[129] Y. B. Yamusa, K. Ahmad, and N. A. Rahman, "Sustainable design of compacted laterite soil liner," *Lecture Notes in Civil Engineering*, vol. 9, pp. 1211–1222, 2019, doi: 10.1007/978-981-10-8016-6_84.

[130] Y. Wan, Q. Xue, and L. Liu, "Study on the permeability evolution law and the micro-mechanism of CCL in a landfill final cover under the dry-wet cycle," *Bulletin of Engineering Geology and the Environment*, vol. 73, no. 4, pp. 1089–1103, Oct. 2014, doi: 10.1007/s10064-014-0604-x.

[131] C. A. Bareither, C. H. Benson, E. M. Rohlf, and J. Scalia, "Hydraulic and mechanical behavior of municipal solid waste and high-moisture waste mixtures," *Waste Management*, vol. 105, pp. 540–549, Mar. 2020, doi: 10.1016/j.wasman.2020.02.030.

[132] I. Herrmann, L. Andreas, S. Diener, and L. Lind, "Steel slag used in landfill cover liners: Laboratory and field tests," *Waste Management and Research*, vol. 28, no. 12, pp. 1114–1121, Dec. 2010, doi: 10.1177/0734242X10365095.

[133] K. Mukherjee and A. Kumar Mishra, "Undrained performance of sustainable compacted sand-bentonite–glass fiber composite for landfill application," *Journal of Cleaner Production*, vol. 244, p. 118662, Jan. 2020, doi: 10.1016/j.jclepro.2019.118662.

[134] A. Raheem *et al.*, "Opportunities and challenges in sustainable treatment and resource reuse of sewage sludge: A review," *Chemical Engineering Journal*, vol. 337, pp. 616–641, Apr. 2018, doi: 10.1016/j.cej.2017.12.149.

[135] M. Eugenia Gimenez Boscov and P. Scarano Hemsi, "Some topics of current practical relevance in environmental geotechnics," *Soils and Rocks*, vol. 43, no. 3, pp. 461–495, Sep. 2020, doi: 10.28927/SR.433461.

[136] A. M. Al-Mahbashi and M. Dafalla, "Impact of placement and field conditions on hydraulic conductivity and lifetime of liners," *Journal of King Saud University - Science*, vol. 33, no. 4, p. 101410, Jun. 2021, doi: 10.1016/j.jksus.2021.101410.

[137] M. Mukri, A. N. Zainuddni, N. A. Abdullah, N. Ibrahim, and T. Mara Johor Bahru, "Performance of different percentage on nano-kaolin as additives in soil liner application," *Materials Today: Proceedings*, vol. 5, pp. 21604–21611, 2018.

[138] M. Almeida, M. Ehrlich, and D. Curcio, "Hydro-mechanical behavior of a lateritic fiber-soil composite as a waste containment liner," *Geotextiles and Geomembranes*, vol. 47, pp. 42–47, Oct. 2019.

[139] M. Regadío, A. Cargill, J. Black, and S. F. Thornton, "High Attenuation Recycled Materials as landfill liners (the HARM project) – A new concept for improved landfill liner design," Sheffield, 2020. doi: 10.31223/osf.io/b49hd.

[140] G. Spagnoli, F. Clement, B. Dilnesa, F. Cao, and P. Feng, "A new waterproofing membrane for tailings ponds," *Paste 2019*, pp. 153–164, 2019.

[141] B. A. Marcotte and I. R. Fleming, "Damage to geomembrane liners from tire derived aggregate," *Geotextiles and Geomembranes*, vol. 48, no. 2, pp. 198–209, Apr. 2020, doi: 10.1016/j.geotexmem.2019.11.005.

[142] T. Özdamar Kul and A. H. Ören, "Liquid limit based assessment of geosynthetic clay liners subject to hydration and hydraulic conductivity testings," *Geotextiles and Geomembranes*, vol. 46, no. 4, pp. 436–447, Aug. 2018, doi: 10.1016/j.geotexmem.2018.03.009.

[143] R. K. Rowe and Y. Yu, "Magnitude and significance of tensile strains in geomembrane landfill liners," *Geotextiles and Geomembranes*, vol. 47, no. 3, pp. 439–458, Jun. 2019, doi: 10.1016/j.geotexmem.2019.01.001.

[144] X. Xu, X. Liu, M. Oh, and J. Park, "Development of a novel base liner material for offshore final disposal sites and the assessment of its hydraulic conductivity," *Waste Management*, vol. 102, pp. 190–197, Feb. 2020, doi: 10.1016/j.wasman.2019.10.047.

[145] J.-F. Wagner and C. Schnatmeyer, "Test field study of different cover sealing systems for industrial dumps and polluted sites," *Applied Clay Science*, pp. 99–116, 2002.

[146] P. V. Divya, B. V. S. Viswanadham, and J. P. Gourc, "Influence of geomembrane on the deformation behaviour of clay-based landfill covers," *Geotextiles and Geomembranes*, vol. 34, pp. 158–171, Oct. 2012, doi: 10.1016/j.geotexmem.2012.06.002.

[147] O. Ojuri and O. Oluwatuyi, "Strength and hydraulic conductivity characteristics of sand-bentonite mixtures designed as a landfill liner," *Jordan Journal of Civil Engineering*, vol. 11, no. 4, pp. 614–622, 2017.

[148] M. Mukri, A. N. Zainuddni, Nur. A. Abdullah, and N. Ibrahim, "Performance of different percentage on nano-kaolin as additives in soil liner application," *The 3rd International Conference on Green Chemical Engineering Technology (3rd GCET_2017): Materials Science*, vol. 5, pp. 21604–21611, Nov. 2018.

[149] M. Guo *et al.*, "Study on water permeability, shear and pull-off performance of waterproof bonding layer for highway bridge," *International Journal of Pavement Research and Technology*, vol. 11, no. 4, pp. 396–400, Jul. 2018, doi: 10.1016/j.ijprt.2017.09.013.

[150] J. He, F. Li, Y. Li, and X. L. Cui, "Modified sewage sludge as temporary landfill cover material," *Water Science and Engineering*, vol. 8, no. 3, pp. 257–262, Jul. 2015, doi: 10.1016/j.wse.2015.03.003.

[151] M. Barroso *et al.*, "Semi-automatic mobile system for detecting defects in landfill liners: Tests in a pilot plant LNEC," 2013.

[152] R. P. Chapuis, "The 2000 R.M. Hardy lecture: Full-scale hydraulic performance of soil-bentonite and compacted clay liners," *Canadian Geotechnical Journal*, vol. 39, no. 2, pp. 417–439, 2002, doi: 10.1139/t01-092.

[153] X. Xu, X. Liu, M. Oh, and J. Park, "Development of a novel base liner material for offshore final disposal sites and the assessment of its hydraulic conductivity," *Waste Management*, vol. 102, pp. 190–197, Feb. 2020, doi: 10.1016/j.wasman.2019.10.047.

[154] J. H. Li, L. Li, R. Chen, and D. Q. Li, "Cracking and vertical preferential flow through landfill clay liners," *Engineering Geology*, vol. 206, pp. 33–41, May 2016, doi: 10.1016/j.enggeo.2016.03.006.

[155] D. A. Rubinos and G. Spagnoli, "Utilization of waste products as alternative landfill liner and cover materials – A critical review," *Critical Reviews in Environmental Science and Technology*, vol. 48, no. 4, pp. 376–438, Feb. 2018, doi: 10.1080/10643389.2018.1461495.

[156] ASTM, "ASTM D2434-00 Standard Test Method for Permeability of Granular Soils (Constant Head)," 2000.

[157] ABNT, "NBR 6457 Amostras de solo - preparação para ensaios de compactação e ensaios de caracterização," 2016.

[158] ASTM, "ASTM D2488-09a Standard Practice for Description and Identification of Soils (Visual-Manual Procedure)," 2015. doi: 10.1520/D2488-09A.

[159] ASTM, "ASTM D2974-20 Determining the Water (Moisture) Content, Ash Content, and Organic Material of Peat and Other Organic Soils," 2020. doi: 10.1520/D2974-20E01.

[160] BS 1377-9, "Methods of test for Soils for civil engineering purposes - Part 9: In-situ tests," British Standards Institution, 1990.

[161] ASTM, "ASTM D698- 12e2 Standard Test Methods for Laboratory Compaction Characteristics of Soil Using Standard Effort (12 400 ft-lbf/ft3 (600 kN-m/m3))," 2012.

[162] ASTM, "ASTM D854-14 Standard Test Methods for Specific Gravity of Soil Solids by Water Pycnometer," 2014.

[163] ASTM, "ASTM D6913-17 Standard Test Methods for Particle-Size Distribution (Gradation) of Soils Using Sieve Analysis," West Conshohocken, PA, 2017, 2017.

[164] ASTM, "ASTM D2216-19 Standard Test Methods for Laboratory Determination of Water (Moisture) Content of Soil and Rock by Mass," 2019.

[165] ASTM, "ASTM D1140-17 Standard Test Methods for Amount of Material in Soils Finer Than the 75-µm (No. 200) Sieve in Soils by Washing," 2017. doi: 10.1520/D1140-17.

[166] ASTM, "ASTM D1556-00 Standard Test Method for Density and Unit Weight of Soil in Place by the Sand-Cone Method," 2000.

[167] ASTM, "ASTM D2434-19 Standard Test Method for Permeability of Granular Soils (Constant Head)," 2019.

[168] ASTM, "ASTM D3080-11 Standard Test Method for Direct Shear Test of Soils Under Consolidated Drained Conditions," 2014. doi: 10.1520/D3080_D3080M-11.

[169] ASTM, "ASTM D4318-17e1 Standard Test Methods for Liquid Limit, Plastic Limit, and Plasticity Index of Soils," 2017.

[170] ASTM, "ASTM D3385-09 Standard Test Method for Infiltration Rate of Soils in Field Using Double-Ring Infiltrometer," 2015. doi: 10.1520/D3385-09.

[171] ASTM, "ASTM D3385-18 Infiltration Rate of Soils in Field Using Double-Ring Infiltrometer," 2018. doi: 10.1520/D3385-18.2.1.

[172] ASTM, "ASTM D7181-20 Standard Test Method for Consolidated Drained Triaxial Compression Test for Soils," 2020. doi: 10.1520/D7181-20.

[173] ASTM, "ASTM D5084-10 Standard Test Methods for Measurement of Hydraulic Conductivity of Saturated Porous Materials Using a Flexible Wall Permeameter," 2015. doi: 10.1520/D5084-10.

[174] ASTM, "ASTM D4767-11 Standard Test Method for Consolidated Undrained Triaxial Compression Test for Cohesive Soils," 2020. doi: 10.1520/D4767-11R20.

[175] ASTM, "ASTM D4254-00 Standard Test Methods for Minimum Index Density and Unit Weight of Soils and Calculation of Relative Density," 2006.

[176] ABNT, "NBR 6122 - Projeto e Execucao de Fundacoes," 1996.

[177] ASTM, "ASTM D2937-04 Standard Test Method for Density of Soil in Place by the Drive-Cylinder Method," 2004.

[178] ASTM, "ASTM D1883-07 Standard Test Methods for CBR (California Bearing Ratio) of Laboratory-Compacted Soils," 2007.

[179] BS 1377-2, "Methods of test for Soils for civil engineering purposes - Part 2: Classification tests," British Standards Institution, 1990.

[180] ASTM, "ASTM D4829-08a Standard Test Method for Expansion Index of Soil," 2008.

[181] ISO17892-11, "Geotechnical investigation and testing - Laboratory testing of soil - Part 11: Permeability tests," 2019.

[182] ISO17892-7, "Geotechnical investigation and testing - Laboratory testing of soil - Part 7: Unconfined compression test," 2017.

[183] ISO17892-9, "Geotechnical investigation and testing - Laboratory testing of soil - Part 9: Consolidated triaxial compression tests on water saturated soils," 2018.

[184] ISO17892-8, "Geotechnical investigation and testing - Laboratory testing of soil - Part 8: Unconsolidated undrained triaxial test," 2004.

[185] ISO17892-5, "Geotechnical investigation and testing - Laboratory testing of soil - Part 5: Incremental loading oedometer test," 2017.

[186] ISO17892-6, "Geotechnical investigation and testing - Laboratory testing of soil - Part 6: Fall cone test," 2014.

[187] ISO17892-3, "Geotechnical investigation and testing - Laboratory testing of soil - Part 3: Determination of particle density," 2015.

[188] ISO17892-2, "Geotechnical investigation and testing - Laboratory testing of soil - Part 2 : Determination of bulk density," 2014.

[189] ISO17892-1, "Geotechnical investigation and testing - Laboratory testing of soil - Part 1: Determination of water content," 2014.

[190] ISO17892-4, "Geotechnical investigation and testing - Laboratory testing of soil - Part 4: Determination of particle size distribution," 2016.

Appendices List

Appendices

Appendices 1 – Cone Penetration Tests

CPT1

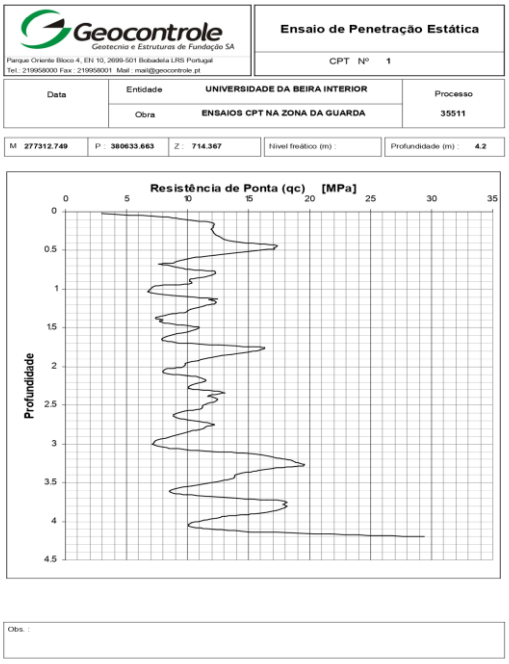

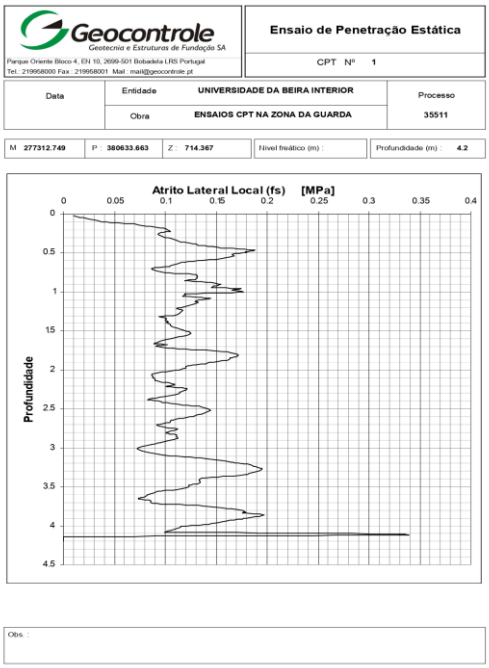

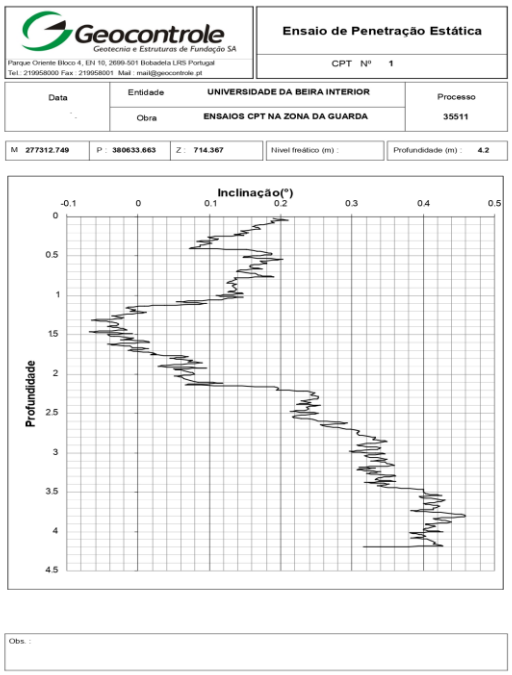

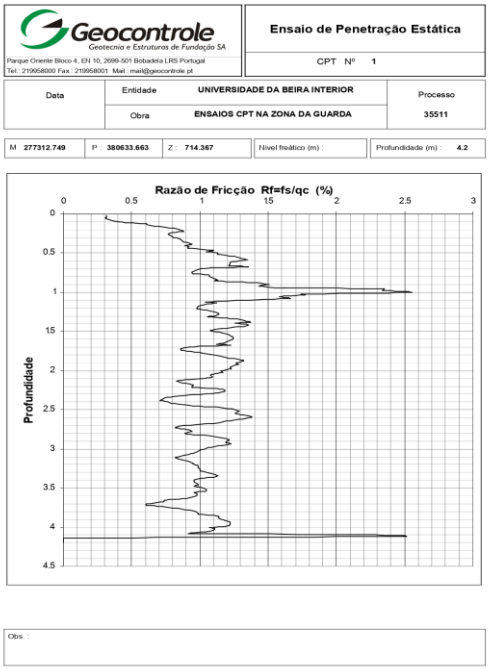

CPT2

Geocontrole
Geotecnia e Estruturas de Fundação SA
Parque Oriente Bloco 4, EN 10, 2699-501 Bobadela LRS Portugal
Tel.: 219958000 Fax : 219958001 Mail : mail@geocontrole.pt

Ensaio de Penetração Estática

CPT Nº 2

Data	Entidade	UNIVERSIDADE DA BEIRA INTERIOR	Processo
	Obra	ENSAIOS CPT NA ZONA DA GUARDA	35511

M	P	Z	Nivel freático (m) :	Profundidade (m) :
277313.532	380633.692	714.367		4.2

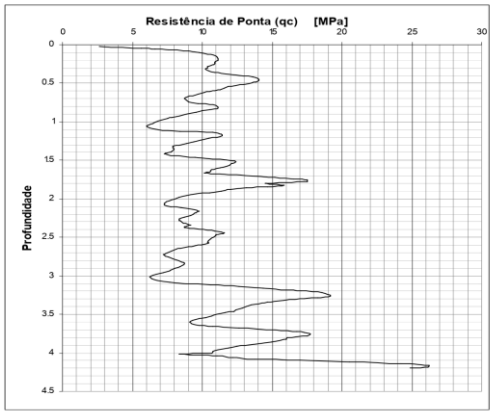

Obs. :

Geocontrole
Geotecnia e Estruturas de Fundação SA
Parque Oriente Bloco 4, EN 10, 2699-501 Bobadela LRS Portugal
Tel.: 219958000 Fax : 219958001 Mail : mail@geocontrole.pt

Ensaio de Penetração Estática

CPT Nº 2

Data	Entidade	UNIVERSIDADE DA BEIRA INTERIOR	Processo
	Obra	ENSAIOS CPT NA ZONA DA GUARDA	35511

M	P	Z	Nivel freático (m) :	Profundidade (m) :
277313.532	380633.692	714.367		4.2

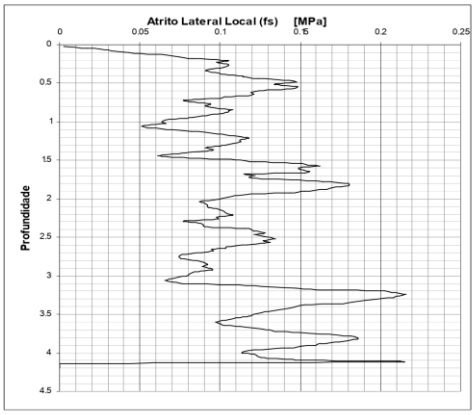

Obs. :

Geocontrole
Geotecnia e Estruturas de Fundação SA
Parque Oriente Bloco 4, EN 10, 2699-501 Bobadela LRS Portugal
Tel.: 219958000 Fax : 219958001 Mail : mail@geocontrole.pt

Ensaio de Penetração Estática

CPT Nº 2

Data	Entidade	UNIVERSIDADE DA BEIRA INTERIOR	Processo
	Obra	ENSAIOS CPT NA ZONA DA GUARDA	35511

M	P	Z	Nivel freático (m) :	Profundidade (m) :
277313.532	380633.692	714.367		4.2

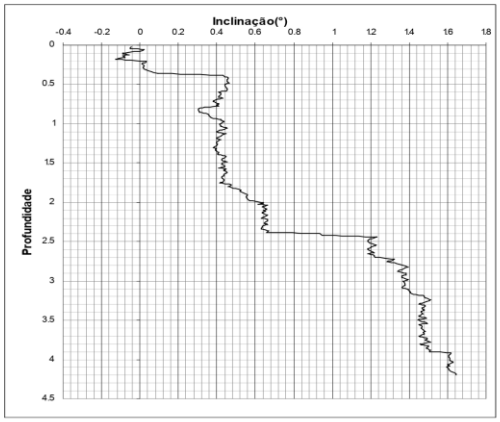

Obs. :

Geocontrole
Geotecnia e Estruturas de Fundação SA
Parque Oriente Bloco 4, EN 10, 2699-501 Bobadela LRS Portugal
Tel.: 219958000 Fax : 219958001 Mail : mail@geocontrole.pt

Ensaio de Penetração Estática

CPT Nº 2

Data	Entidade	UNIVERSIDADE DA BEIRA INTERIOR	Processo
	Obra	ENSAIOS CPT NA ZONA DA GUARDA	35511

M	P	Z	Nivel freático (m) :	Profundidade (m) :
277313.532	380633.692	714.367		4.2

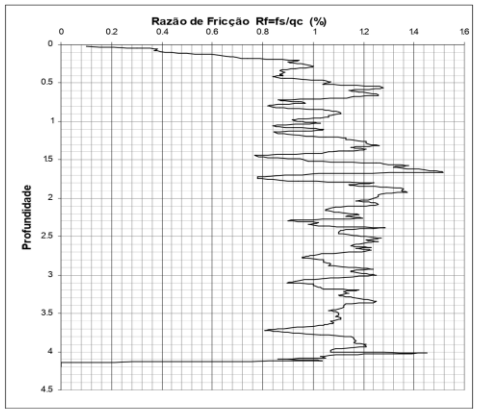

Obs. :

CPT3

Geocontrole
Geotecnia e Estruturas de Fundação SA
Parque Oriente Bloco 4, EN 10, 2699-501 Bobadela LRS Portugal
Tel.: 219958000 Fax: 219958001 Mail: mail@geocontrole.pt

Ensaio de Penetração Estática

CPT Nº 3

Data	Entidade	UNIVERSIDADE DA BEIRA INTERIOR	Processo
	Obra	ENSAIOS CPT NA ZONA DA GUARDA	35511

M	277314.414	P	380633.842	Z	714.372	Nível freático (m) :	Profundidade (m) :	4.32

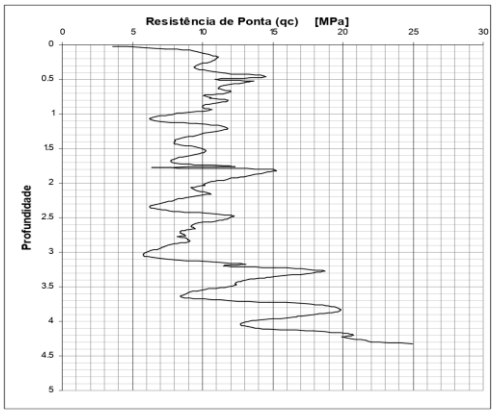

Obs. :

Geocontrole
Geotecnia e Estruturas de Fundação SA
Parque Oriente Bloco 4, EN 10, 2699-501 Bobadela LRS Portugal
Tel.: 219958000 Fax: 219958001 Mail: mail@geocontrole.pt

Ensaio de Penetração Estática

CPT Nº 3

Data	Entidade	UNIVERSIDADE DA BEIRA INTERIOR	Processo
	Obra	ENSAIOS CPT NA ZONA DA GUARDA	35511

M	277314.414	P	380633.842	Z	714.372	Nível freático (m) :	Profundidade (m) :	4.32

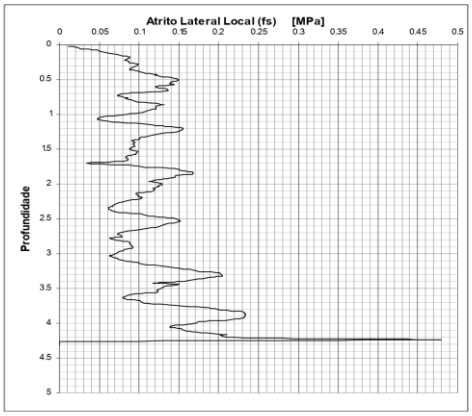

Obs. :

Geocontrole
Geotecnia e Estruturas de Fundação SA
Parque Oriente Bloco 4, EN 10, 2699-501 Bobadela LRS Portugal
Tel.: 219958000 Fax: 219958001 Mail: mail@geocontrole.pt

Ensaio de Penetração Estática

CPT Nº 3

Data	Entidade	UNIVERSIDADE DA BEIRA INTERIOR	Processo
	Obra	ENSAIOS CPT NA ZONA DA GUARDA	35511

M	277314.414	P	380633.842	Z	714.372	Nível freático (m) :	Profundidade (m) :	4.32

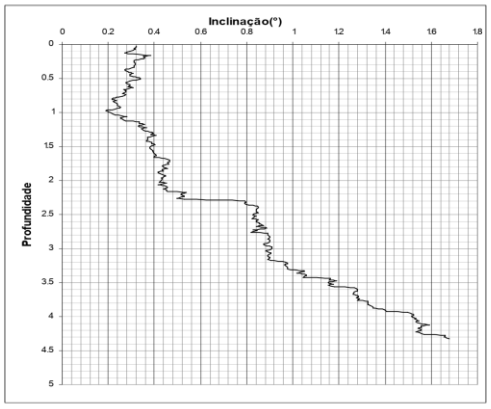

Obs. :

Geocontrole
Geotecnia e Estruturas de Fundação SA
Parque Oriente Bloco 4, EN 10, 2699-501 Bobadela LRS Portugal
Tel.: 219958000 Fax: 219958001 Mail: mail@geocontrole.pt

Ensaio de Penetração Estática

CPT Nº 3

Data	Entidade	UNIVERSIDADE DA BEIRA INTERIOR	Processo
	Obra	ENSAIOS CPT NA ZONA DA GUARDA	35511

M	277314.414	P	380633.842	Z	714.372	Nível freático (m) :	Profundidade (m) :	4.32

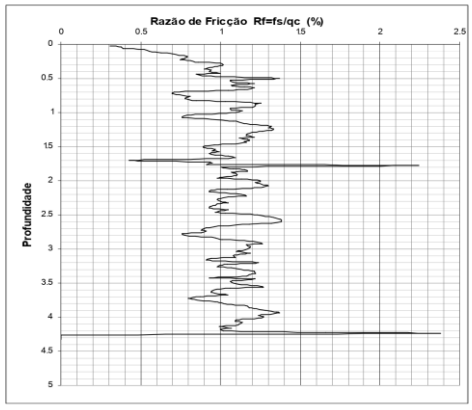

Obs. :

CPT4

Geocontrole
Geotecnia e Estruturas de Fundação SA
Parque Oriente Bloco 4, EN 10, 2699-501 Bobadela LRS Portugal
Tel.: 219958000 Fax : 219958001 Mail : mail@geocontrole.pt

Ensaio de Penetração Estática

CPT Nº 4

Data	Entidade	UNIVERSIDADE DA BEIRA INTERIOR	Processo
	Obra	ENSAIOS CPT NA ZONA DA GUARDA	35511

M 277316.150 | P : 380633.873 | Z : 714.358 | Nivel freático (m) : | Profundidade (m) : 4.24

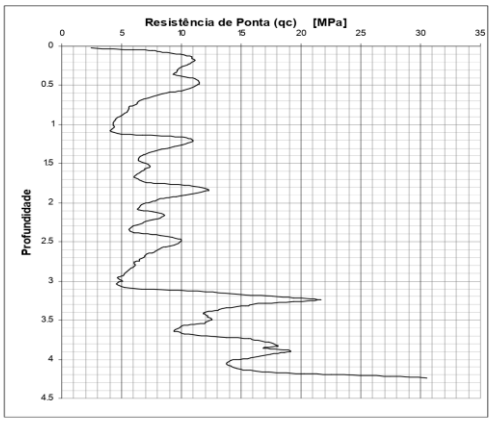

Obs. :

Geocontrole
Geotecnia e Estruturas de Fundação SA
Parque Oriente Bloco 4, EN 10, 2699-501 Bobadela LRS Portugal
Tel.: 219958000 Fax : 219958001 Mail : mail@geocontrole.pt

Ensaio de Penetração Estática

CPT Nº 4

Data	Entidade	UNIVERSIDADE DA BEIRA INTERIOR	Processo
	Obra	ENSAIOS CPT NA ZONA DA GUARDA	35511

M 277316.150 | P : 380633.873 | Z : 714.358 | Nivel freático (m) : | Profundidade (m) : 4.24

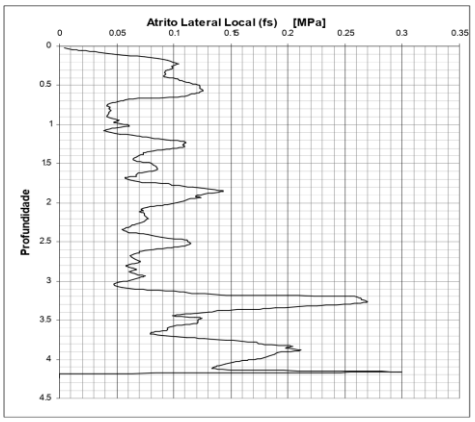

Obs. :

Geocontrole
Geotecnia e Estruturas de Fundação SA
Parque Oriente Bloco 4, EN 10, 2699-501 Bobadela LRS Portugal
Tel.: 219958000 Fax : 219958001 Mail : mail@geocontrole.pt

Ensaio de Penetração Estática

CPT Nº 4

Data	Entidade	UNIVERSIDADE DA BEIRA INTERIOR	Processo
	Obra	ENSAIOS CPT NA ZONA DA GUARDA	35511

M 277316.150 | P : 380633.873 | Z : 714.358 | Nivel freático (m) : | Profundidade (m) : 4.24

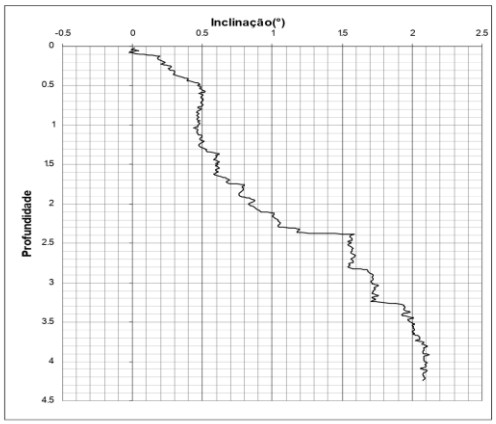

Obs. :

Geocontrole
Geotecnia e Estruturas de Fundação SA
Parque Oriente Bloco 4, EN 10, 2699-501 Bobadela LRS Portugal
Tel.: 219958000 Fax : 219958001 Mail : mail@geocontrole.pt

Ensaio de Penetração Estática

CPT Nº 4

Data	Entidade	UNIVERSIDADE DA BEIRA INTERIOR	Processo
	Obra	ENSAIOS CPT NA ZONA DA GUARDA	35511

M 277316.150 | P : 380633.873 | Z : 714.358 | Nivel freático (m) : | Profundidade (m) : 4.24

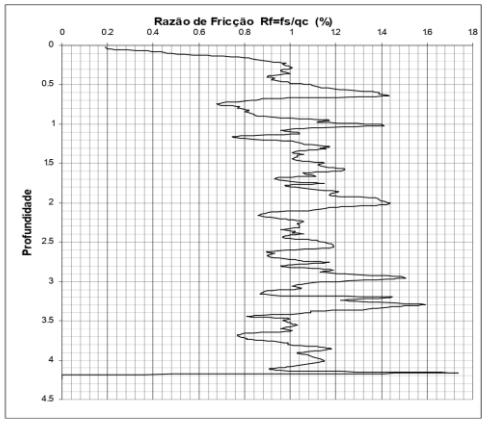

Obs. :

CPT5

Geocontrole
Geotecnia e Estruturas de Fundação SA
Parque Oriente Bloco 4, EN 10, 2699-501 Bobadela LRS Portugal
Tel.: 219958000 Fax : 219958001 Mail : mail@geocontrole.pt

Ensaio de Penetração Estática

CPT Nº 5

Data	Entidade	UNIVERSIDADE DA BEIRA INTERIOR	Processo
	Obra	ENSAIOS CPT NA ZONA DA GUARDA	35511

M 277315.321	P : 380633.843	Z : 714.355	Nivel freático (m) :	Profundidade (m) : 5.24

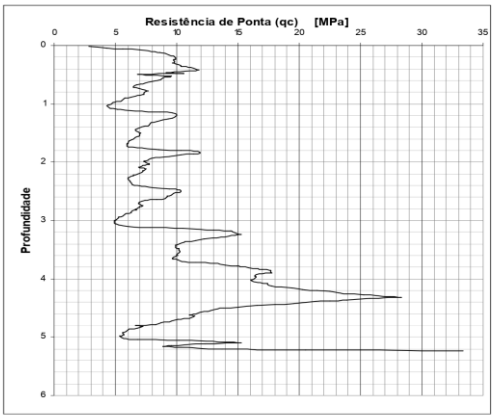

Obs. :

Geocontrole
Geotecnia e Estruturas de Fundação SA
Parque Oriente Bloco 4, EN 10, 2699-501 Bobadela LRS Portugal
Tel.: 219958000 Fax : 219958001 Mail : mail@geocontrole.pt

Ensaio de Penetração Estática

CPT Nº 5

Data	Entidade	UNIVERSIDADE DA BEIRA INTERIOR	Processo
	Obra	ENSAIOS CPT NA ZONA DA GUARDA	35511

M 277315.321	P : 380633.843	Z : 714.355	Nivel freático (m) :	Profundidade (m) : 5.24

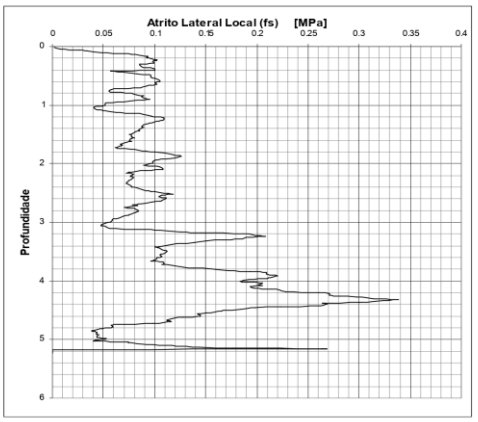

Obs. :

Geocontrole
Geotecnia e Estruturas de Fundação SA
Parque Oriente Bloco 4, EN 10, 2699-501 Bobadela LRS Portugal
Tel.: 219958000 Fax : 219958001 Mail : mail@geocontrole.pt

Ensaio de Penetração Estática

CPT Nº 5

Data	Entidade	UNIVERSIDADE DA BEIRA INTERIOR	Processo
	Obra	ENSAIOS CPT NA ZONA DA GUARDA	35511

M 277315.321	P : 380633.843	Z : 714.355	Nivel freático (m) :	Profundidade (m) : 5.24

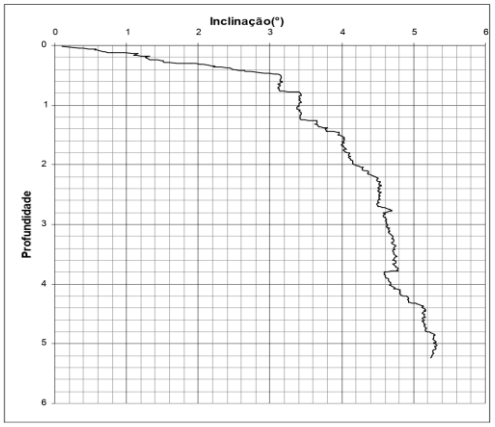

Obs. :

Geocontrole
Geotecnia e Estruturas de Fundação SA
Parque Oriente Bloco 4, EN 10, 2699-501 Bobadela LRS Portugal
Tel.: 219958000 Fax : 219958001 Mail : mail@geocontrole.pt

Ensaio de Penetração Estática

CPT Nº 5

Data	Entidade	UNIVERSIDADE DA BEIRA INTERIOR	Processo
	Obra	ENSAIOS CPT NA ZONA DA GUARDA	35511

M 277315.321	P : 380633.843	Z : 714.355	Nivel freático (m) :	Profundidade (m) : 5.24

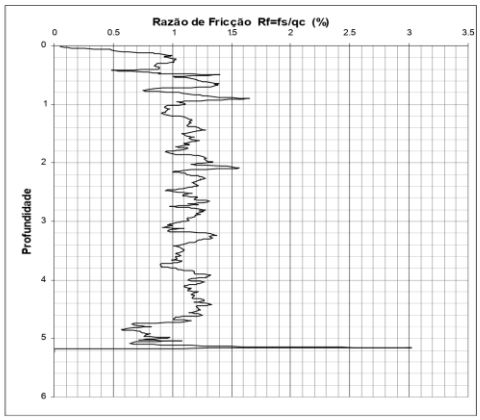

Obs. :

CPT5 – Pore Pressure

Geocontrole
Geotecnia e Estruturas de Fundação SA
Parque Oriente Bloco 4, EN 10, 2699-501 Bobadela LRS Portugal
Tel.: 219958000 Fax : 219958001 Mail : mail@geocontrole.pt

Ensaio de Penetração Estática

CPT Nº 5

Data	Entidade	UNIVERSIDADE DA BEIRA INTERIOR	Processo
	Obra	ENSAIOS CPT NA ZONA DA GUARDA	35511

M 277315.321	P : 380633.843	Z : 714.355	Nivel freático (m) :	Profundidade (m) : 5.24

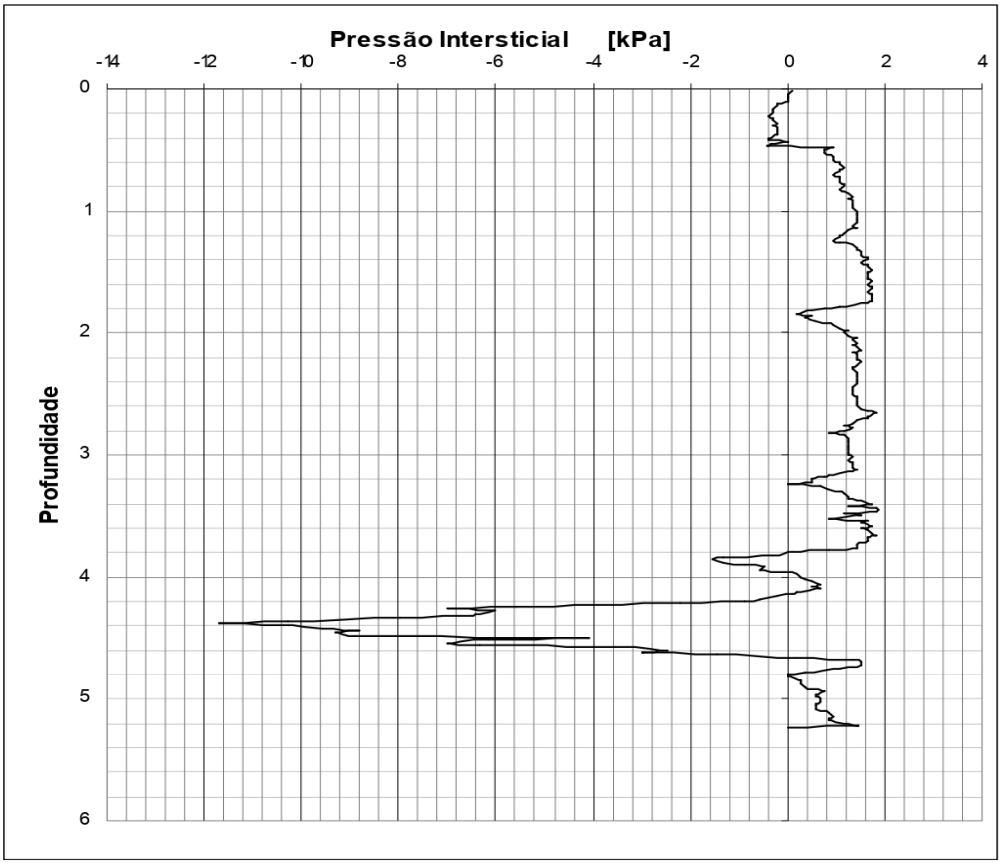

Obs. :

CPT6

Geocontrole
Geotecnia e Estruturas de Fundação SA
Parque Oriente Bloco 4, EN 10, 2699-501 Bobadela LRS Portugal
Tel.: 219958000 Fax: 219958001 Mail: mail@geocontrole.pt

Ensaio de Penetração Estática — CPT Nº 6

Data	Entidade	UNIVERSIDADE DA BEIRA INTERIOR	Processo
	Obra	ENSAIOS CPT NA ZONA DA GUARDA	35511

M: 277320.337	P: 380634.093	Z: 714.373	Nível freático (m):	Profundidade (m): 5.3

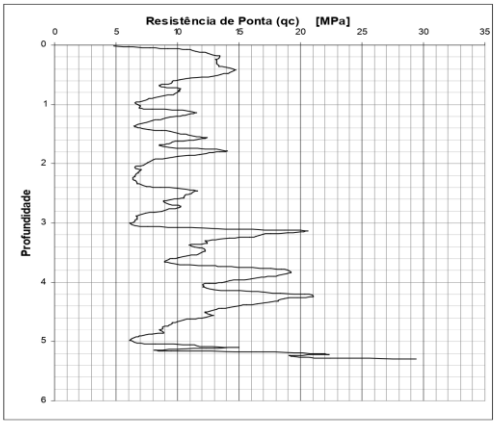

Obs.:

Geocontrole
Geotecnia e Estruturas de Fundação SA
Parque Oriente Bloco 4, EN 10, 2699-501 Bobadela LRS Portugal
Tel.: 219958000 Fax: 219958001 Mail: mail@geocontrole.pt

Ensaio de Penetração Estática — CPT Nº 6

Data	Entidade	UNIVERSIDADE DA BEIRA INTERIOR	Processo
	Obra	ENSAIOS CPT NA ZONA DA GUARDA	35511

M: 277320.337	P: 380634.093	Z: 714.373	Nível freático (m):	Profundidade (m): 5.3

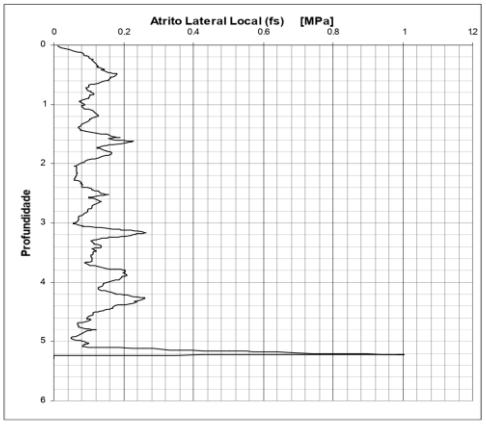

Obs.:

Geocontrole
Geotecnia e Estruturas de Fundação SA
Parque Oriente Bloco 4, EN 10, 2699-501 Bobadela LRS Portugal
Tel.: 219958000 Fax: 219958001 Mail: mail@geocontrole.pt

Ensaio de Penetração Estática — CPT Nº 6

Data	Entidade	UNIVERSIDADE DA BEIRA INTERIOR	Processo
	Obra	ENSAIOS CPT NA ZONA DA GUARDA	35511

M: 277320.337	P: 380634.093	Z: 714.373	Nível freático (m):	Profundidade (m): 5.3

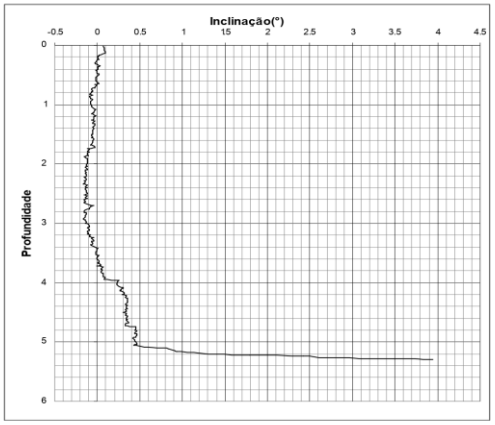

Obs.:

Geocontrole
Geotecnia e Estruturas de Fundação SA
Parque Oriente Bloco 4, EN 10, 2699-501 Bobadela LRS Portugal
Tel.: 219958000 Fax: 219958001 Mail: mail@geocontrole.pt

Ensaio de Penetração Estática — CPT Nº 6

Data	Entidade	UNIVERSIDADE DA BEIRA INTERIOR	Processo
	Obra	ENSAIOS CPT NA ZONA DA GUARDA	35511

M: 277320.337	P: 380634.093	Z: 714.373	Nível freático (m):	Profundidade (m): 5.3

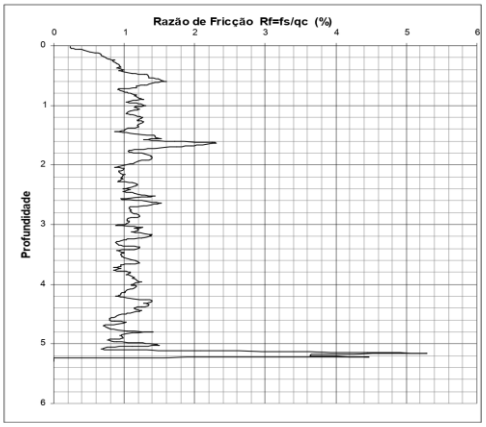

Obs.:

CPT7

Geocontrole
Geotecnia e Estruturas de Fundação SA
Parque Oriente Bloco 4, EN 10, 2699-501 Bobadela LRS Portugal
Tel.: 219958000 Fax : 219958001 Mail : mail@geocontrole.pt

Ensaio de Penetração Estática — CPT Nº 7

Data	Entidade	UNIVERSIDADE DA BEIRA INTERIOR	Processo
	Obra	ENSAIOS CPT NA ZONA DA GUARDA	35511

M	P	Z	Nível freático (m) :	Profundidade (m) :
277321.137	380634.200	714.377		4.68

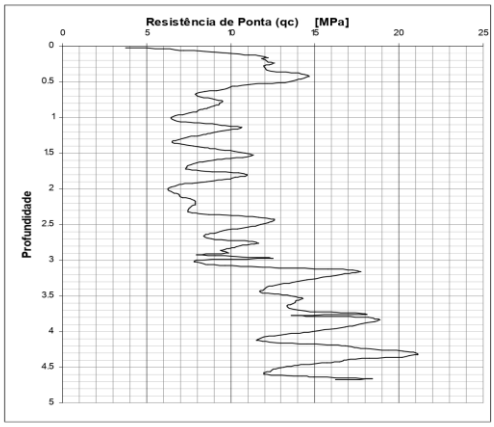

Obs. :

Geocontrole
Geotecnia e Estruturas de Fundação SA
Parque Oriente Bloco 4, EN 10, 2699-501 Bobadela LRS Portugal
Tel.: 219958000 Fax : 219958001 Mail : mail@geocontrole.pt

Ensaio de Penetração Estática — CPT Nº 7

Data	Entidade	UNIVERSIDADE DA BEIRA INTERIOR	Processo
	Obra	ENSAIOS CPT NA ZONA DA GUARDA	35511

M	P	Z	Nível freático (m) :	Profundidade (m) :
277321.137	380634.200	714.377		4.68

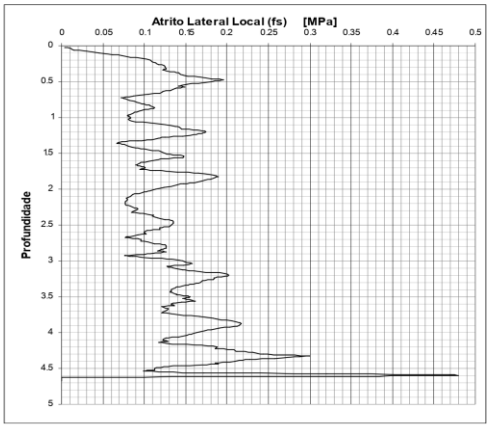

Obs. :

Geocontrole
Geotecnia e Estruturas de Fundação SA
Parque Oriente Bloco 4, EN 10, 2699-501 Bobadela LRS Portugal
Tel.: 219958000 Fax : 219958001 Mail : mail@geocontrole.pt

Ensaio de Penetração Estática — CPT Nº 7

Data	Entidade	UNIVERSIDADE DA BEIRA INTERIOR	Processo
	Obra	ENSAIOS CPT NA ZONA DA GUARDA	35511

M	P	Z	Nível freático (m) :	Profundidade (m) :
277321.137	380634.200	714.377		4.68

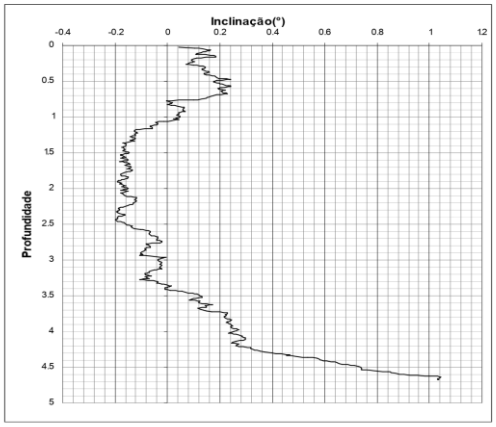

Obs. :

Geocontrole
Geotecnia e Estruturas de Fundação SA
Parque Oriente Bloco 4, EN 10, 2699-501 Bobadela LRS Portugal
Tel.: 219958000 Fax : 219958001 Mail : mail@geocontrole.pt

Ensaio de Penetração Estática — CPT Nº 7

Data	Entidade	UNIVERSIDADE DA BEIRA INTERIOR	Processo
	Obra	ENSAIOS CPT NA ZONA DA GUARDA	35511

M	P	Z	Nível freático (m) :	Profundidade (m) :
277321.137	380634.200	714.377		4.68

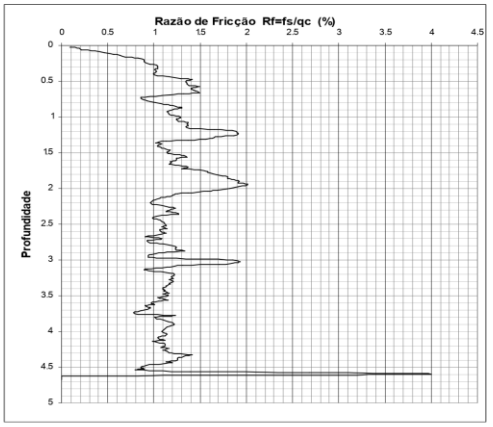

Obs. :

CPT8

Geocontrole
Geotecnia e Estruturas de Fundação SA
Parque Oriente Bloco 4, EN 10, 2699-501 Bobadela LRS Portugal
Tel.: 219958000 Fax: 219958001 Mail: mail@geocontrole.pt

Ensaio de Penetração Estática

CPT Nº 8

Data	Entidade	UNIVERSIDADE DA BEIRA INTERIOR	Processo
	Obra	ENSAIOS CPT NA ZONA DA GUARDA	35511

M 277322.158	P : 380624.155	Z : 714.375	Nivel freático (m) :	Profundidade (m) : 4.94

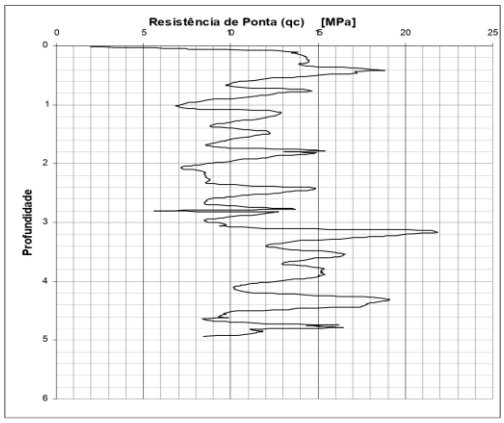

Obs. :

Geocontrole
Geotecnia e Estruturas de Fundação SA
Parque Oriente Bloco 4, EN 10, 2699-501 Bobadela LRS Portugal
Tel.: 219958000 Fax: 219958001 Mail: mail@geocontrole.pt

Ensaio de Penetração Estática

CPT Nº 8

Data	Entidade	UNIVERSIDADE DA BEIRA INTERIOR	Processo
	Obra	ENSAIOS CPT NA ZONA DA GUARDA	35511

M 277322.158	P : 380624.155	Z : 714.375	Nivel freático (m) :	Profundidade (m) : 4.94

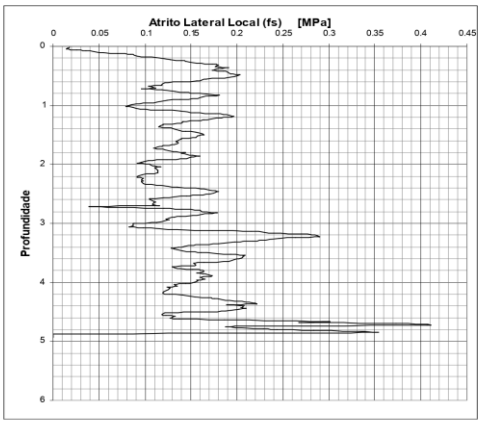

Obs. :

Geocontrole
Geotecnia e Estruturas de Fundação SA
Parque Oriente Bloco 4, EN 10, 2699-501 Bobadela LRS Portugal
Tel.: 219958000 Fax: 219958001 Mail: mail@geocontrole.pt

Ensaio de Penetração Estática

CPT Nº 8

Data	Entidade	UNIVERSIDADE DA BEIRA INTERIOR	Processo
	Obra	ENSAIOS CPT NA ZONA DA GUARDA	35511

M 277322.158	P : 380624.155	Z : 714.375	Nivel freático (m) :	Profundidade (m) : 4.94

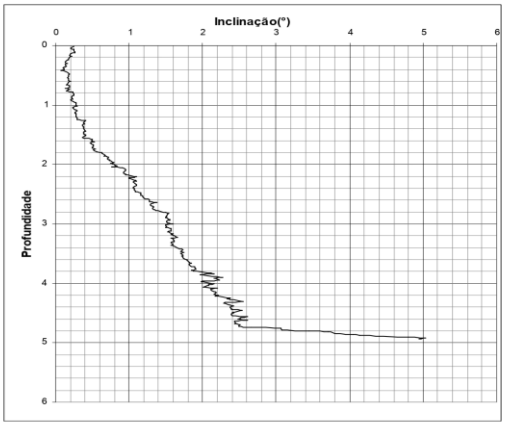

Obs. :

Geocontrole
Geotecnia e Estruturas de Fundação SA
Parque Oriente Bloco 4, EN 10, 2699-501 Bobadela LRS Portugal
Tel.: 219958000 Fax: 219958001 Mail: mail@geocontrole.pt

Ensaio de Penetração Estática

CPT Nº 8

Data	Entidade	UNIVERSIDADE DA BEIRA INTERIOR	Processo
	Obra	ENSAIOS CPT NA ZONA DA GUARDA	35511

M 277322.158	P : 380624.155	Z : 714.375	Nivel freático (m) :	Profundidade (m) : 4.94

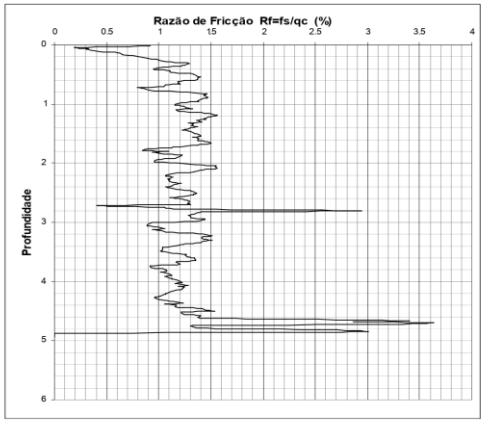

Obs. :

Appendices 2 – Plate Load Test

Load	Tension	Read (Div)			Deformation (mm)					
[kN]	[kN/m²]	1	2	3	1	2	3	Media	Acum.	Tension Acum.
0	0	0	0	0	0	0	0	0.00	0.00	0
30	153	127	155	124	1.27	1.55	1.24	1.35	1.35	153
40	204	47	63	50	0.47	0.63	0.5	0.53	1.89	204
50	255	60	70	53	0.6	0.7	0.53	0.61	2.50	255
60	306	69	72	59	0.69	0.72	0.59	0.67	3.16	306
70	357	36	37	29	0.36	0.37	0.29	0.34	3.50	357
80	407	49	51	45	0.49	0.51	0.45	0.48	3.99	407
90	458	37	41	32	0.37	0.41	0.32	0.37	4.35	458
100	509	59	64	66	0.59	0.64	0.66	0.63	4.98	509
50	255	-27	-23	-28	-0.27	-0.23	-0.28	-0.26	4.72	255
60	306	1	1	1	0.01	0.01	0.01	0.01	4.73	306
70	357	7	5	4	0.07	0.05	0.04	0.05	4.79	357
80	407	9	10	8	0.09	0.1	0.08	0.09	4.88	407
90	458	10	6	6	0.1	0.06	0.06	0.07	4.95	458
100	509	20	15	12	0.2	0.15	0.12	0.16	5.11	509
110	560	43	49	41	0.43	0.49	0.41	0.44	5.55	560
120	611	57	57	51	0.57	0.57	0.51	0.55	6.10	611
130	662	29	26	25	0.29	0.26	0.25	0.27	6.37	662
140	713	34	35	33	0.34	0.35	0.33	0.34	6.71	713
150	764	53	45	46	0.53	0.45	0.46	0.48	7.19	764
160	815	37	37	33	0.37	0.37	0.33	0.36	7.54	815
170	866	61	55	45	0.61	0.55	0.45	0.54	8.08	866
180	917	69	60	47	0.69	0.6	0.47	0.59	8.67	917
190	968	60	45	42	0.6	0.45	0.42	0.49	9.16	968
200	1019	61	38	35	0.61	0.38	0.35	0.45	9.60	1019
100	509	-38	-35	-34	-0.38	-0.35	-0.34	-0.36	9.25	509
200	1019	68	63	57	0.68	0.63	0.57	0.63	9.87	1019
220	1120	106	95	86	1.06	0.95	0.86	0.96	10.83	1120
240	1222	137	150	132	1.37	1.5	1.32	1.40	12.23	1222
250	1273	52	55	55	0.52	0.55	0.55	0.54	12.77	1273
260	1324	101	130	98	1.01	1.3	0.98	1.10	13.86	1324
280	1426	258	380	241	2.58	3.8	2.41	2.93	16.79	1426
300	1528	217	205	62	2.17	2.05	0.62	1.61	18.41	1528
200	1019	-43	-35	-23	-0.43	-0.35	-0.23	-0.34	18.07	1019
300	1528	141	135	75	1.41	1.35	0.75	1.17	19.24	1528
320	1630	167	235	-178	1.67	2.35	-1.78	0.75	19.99	1630

Appendices 3 – Specific Gravity

Água (IAPWS, 2008)	
T (°C)	Densidade (g/cm³)
0	0.99987
4	1.00000
10	0.99973
11	0.99964
12	0.99964
13	0.99941
14	0.99929
15	0.99914
16	0.99899
17	0.99882
18	0.99864
19	0.99845
20	0.99825
21	0.99804
22	0.99781
23	0.99757
24	0.99738
25	0.99710

Penalobo									
#		Unit	Gs	#			Unit	Gs	
Picnômetro + A (T1)	693.66	M3		Picnômetro + A (T1)	360.68		M3		
T1	20			T1	20				
Picnômetro + A + S (Tx)	724.52	M5		Picnômetro + A + S (Tx)	389.97		M5		
Tx	20			Tx	20				
Picnômetro + A (Tx)	693.66	M3	2.53	Picnômetro + A (Tx)	360.68		M3	2.54	
ρ(20°)/ρ(Tx)	1.00000			ρ(20°)/ρ(Tx)	1.00000				
S	51.04	M4		S	48.34		M4		
#	T	T + S		#	T		T + S		
METAL1	493.19	544.23		T5+T6	279.87		328.21		
#		Unit	Gs	#			Unit	Gs	
Picnômetro + A (T1)	281.39	M3		Picnômetro + A (T1)	280.02		M3		
T1	13			T1	13				
Picnômetro + A + S (Tx)	297.62	M5		Picnômetro + A + S (Tx)	293.28		M5		
Tx	13			Tx	13				
Picnômetro + A (Tx)	281.39	M3	2.55	Picnômetro + A (Tx)	280.02		M3	2.60	
ρ(20°)/ρ(Tx)	1.00116			ρ(20°)/ρ(Tx)	1.00116				
S	26.69	M4		S	21.58		M4		
#	T	T + S		#	T		T + S		
R1	72.07	98.76		R2	72		93.58		
#		Unit	Gs	#			Unit	Gs	
Picnômetro + A (T1)	280.82	M3		Picnômetro + A (T1)	361.42		M3		
T1	13			T1	13				
Picnômetro + A + S (Tx)	301.48	M5		Picnômetro + A + S (Tx)	379.68		M5		
Tx	13			Tx	13				
Picnômetro + A (Tx)	280.82	M3	2.54	Picnômetro + A (Tx)	361.42		M3	2.47	
ρ(20°)/ρ(Tx)	1.00116			ρ(20°)/ρ(Tx)	1.00116				
S	34.11	M4		S	30.69		M4		
#	T	T + S		#	T		T + S		
LETA1	188.45	222.56		LETA2	191.11		221.8		

Appendices 4 – Free Expansibility

Penalobo				
t (min)	read (-)	ΔH (mm)	S (%)	criteria (99%)
0	18	0	0.00%	-
10	54	0.36	2.40%	-
30	76	0.58	3.87%	62.07%
60	86	0.68	4.53%	85.29%
120	95	0.77	5.13%	88.31%
180	100	0.82	5.47%	93.90%
240	106	0.88	5.87%	93.18%
300	106	0.88	5.87%	100.00%
		S,max (%)		
		6.0		

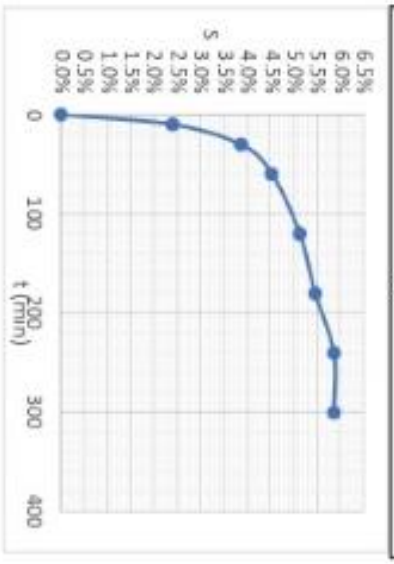

Penalobo				
t (min)	read (-)	ΔH (mm)	S (%)	criteria (99%)
0	644	0	0.00%	-
10	698	0.54	3.60%	-
30	724	0.8	5.33%	67.50%
60	734	0.9	6.00%	88.89%
120	742	0.98	6.53%	91.84%
180	745	1.01	6.73%	97.03%
240	746	1.02	6.80%	99.02%
300	747	1.03	6.87%	99.03%
		S,max (%)		
		7.5		

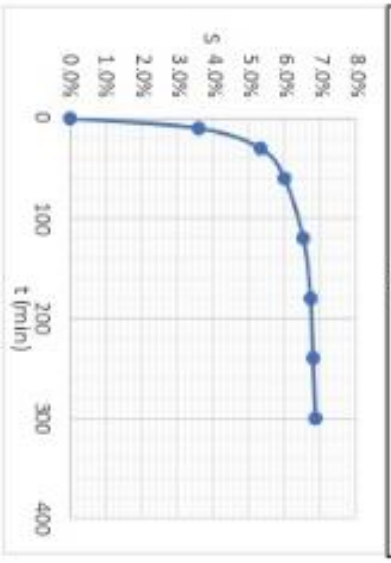

Penalobo				
t (min)	read (-)	ΔH (mm)	S (%)	criteria (99%)
0	117	0	0.00%	-
10	182	0.65	4.33%	-
30	202	0.85	5.67%	76.47%
60	214	0.97	6.47%	87.63%
120	221	1.04	6.93%	93.27%
180	228	1.11	7.40%	93.69%
240	229	1.12	7.47%	99.11%
300	230	1.13	7.53%	99.12%
		S,max (%)		
		8.0		

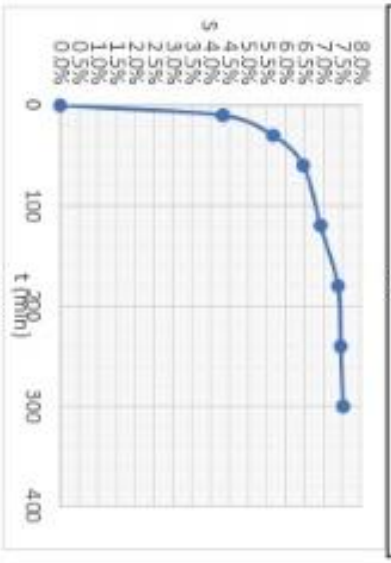

Appendices 5 – Plasticity Index

LIQUID					PLASTIC				
#	113	126	109	Unit	#	1	2	3	Unit
T	12.1	13.1	12.4	g	T	-	-	-	g
T+S+W	25.9	22.5	24.3	g	T+S+W	-	-	-	g
T+S	22.86	20.46	21.68	g	T+S	-	-	-	g
S	10.76	7.36	9.28	g	S	#VALUE!	#VALUE!	#VALUE!	g
w	28.25%	27.72%	28.23%	%	W	#VALUE!	#VALUE!	#VALUE!	g
N° Golpes	18	38	28		w	#VALUE!	#VALUE!	#VALUE!	%

LL	LP
27.99%	NP

Graphic	
18	28.25%
38	27.72%
28	28.00%

PI
NP

Appendices 6 – Normal Proctor

Normal Proctor											
REF(%)	T,Proctor (g)	M,total (g)	M,h (g)	ρ,h (g/cm³)	w (%)	ρ,d (g/cm³)	γ,d (KN/m³)	e (%)	Sr=100	SR95 (g/cm³)	SR90 (g/cm³)
12%	2126.17	4093.01	1966.84	2.09	13.65%	1.84	18.02	0.39	1.891710534	1.87	1.84
14%	2126.17	4100.38	1974.21	2.10	14.69%	1.83	17.93	0.40	1.85501324	1.83	1.80
14%	2126.19	4081.68	1955.49	2.08	15.56%	1.80	17.62	0.42	1.825721446	1.80	1.77
13%	2126.19	4128.6	2002.41	2.13	14.18%	1.86	18.26	0.37	1.872710209	1.85	1.82
12%	2126.19	4078.56	1952.37	2.07	12.87%	1.84	18.01	0.39	1.919836485	1.90	1.87
Plot											
12%	2126.19	4078.56	1952.37	2.07	12.87%	1.81	18.01	0.39	1.92	1.90	1.87
12%	2126.17	4093.01	1966.84	2.09	13.65%	1.84	18.02	0.39	1.89	1.87	1.84
13%	2126.19	4128.60	2002.41	2.13	14.18%	1.86	18.26	0.37	1.87	1.85	1.82
14%	2126.17	4100.38	1974.21	2.10	14.69%	1.83	17.93	0.40	1.86	1.83	1.80
14%	2126.19	4081.68	1955.49	2.08	15.56%	1.80	17.62	0.42	1.83	1.80	1.77

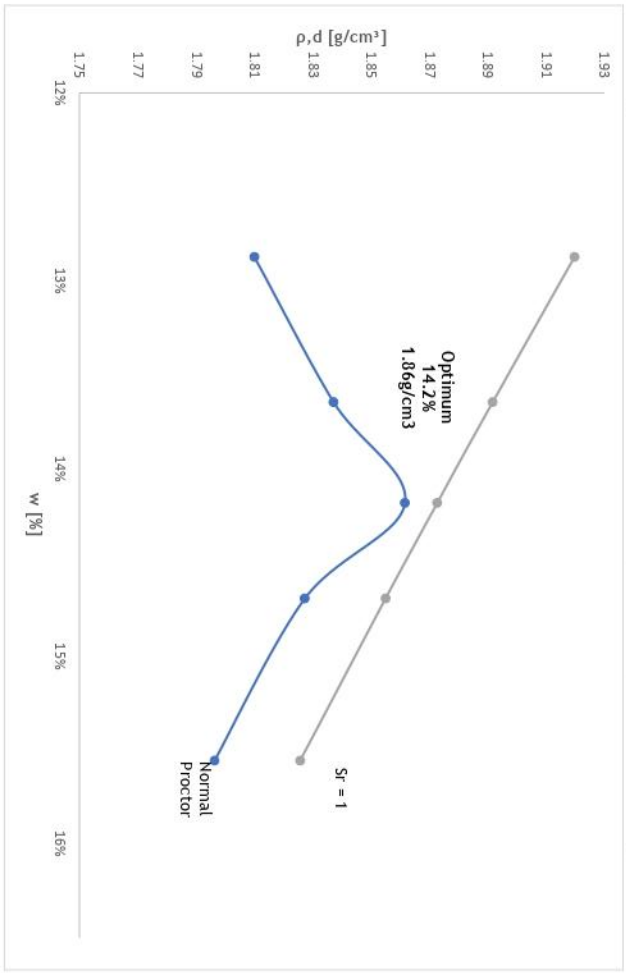

PROCTOR	
V(cm³)	942
Gs	2.55
w,opt (%)	14.0%
ρ,d,opt (g/cm³)	1.86

W					
REF	#	T	T+S+W	T+S	w
12%	273	47.32	135.63	125.01	13.67%
	276	46.66	114.05	105.97	13.62%
14%	265	47.03	165.27	150.67	14.09%
	278	48.18	140.66	128.39	15.30%
14%	204	48.8	119.34	110.04	15.19%
	178	47.75	130.43	119.07	15.93%
13%	189	48.55	150.74	138.01	14.23%
	282	47.48	124.75	115.18	14.14%
12%	104	47.44	134.05	123.88	13.30%
	2001	50.84	125.32	117.08	12.44%

Appendices 7 – Hydraulic Conductivity